THE LONG-TERM EFFECTS OF ADOLESCENT AND POSTNATAL ETHANOL EXPOSURE ON THE ADULT MOUSE BRAIN: A MULTIDISCIPLINARY APPROACH

Leon Garland Coleman, Jr.

A dissertation submitted to the faculty of the University of North Carolina at Chapel Hill in partial fulfillment of the requirements for the degree of Doctor of Philosophy in the Curriculum of Neurobiology

Chapel Hill
2010

Approved By:

Fulton T. Crews, PhD

Weili Lin, PhD

Sheryl Moy, PhD

Ben Philpot, PhD

Kathleen Sulik, PhD

ABSTRACT

LEON GARLAND COLEMAN JR: The long-term effects of adolescent and postnatal ethanol exposure on the adult mouse brain: A multidisciplinary approach
(Under the direction of Fulton T. Crews, PhD)

Studies on the effects of alcohol on adolescent and fetal development find developing tissues are particularly sensitive to alcohol toxicity. Since, during adolescence, brain regions associated with cognitive function, decision making, and intelligence mature to adulthood, ethanol exposure during adolescence and early postnatal life may have persistent effects. Long-term effects of alcohol exposure (P7 or P28-37) on the adult brain (P60-P110) were examined using magnetic resonance imaging (MRI), immunohistochemistry (IHC), and behavior. On postnatal day seven (P7), the effects of ethanol (2.5 g/kg s.c., two hours apart) which blocks NMDA receptors, was compared to dizocilpine, another NMDA antagonist. Mice receiving P7 ethanol treatment and studied at P82, had a 4% reduction in adult brain volume, reduced numbers of parvalbumin (PV) immunoreactive (IR) cells in the frontal cortex (18-31%), as well as a reduction in cux1 IR layer II pyramidal neurons. Dizocilpine (MK801) administered on P7 also reduced frontal cortical PV interneurons (50%) and layer V pyramidal neurons (42%) in adulthood. Interestingly, P7 ethanol treatment resulted in a 52% increase in adult hippocampal neurogenesis in males, but not in females.

Two models of underage drinking were employed: adolescent continuous ethanol (ACE) and adolescent intermittent ethanol (AIE). Both showed changes in adult behaviors, regional brain volumes, and cellular architecture. Mice treated with ACE (5g/kg/day, i.g.,

P28-37) showed adult deficits including: altered neurotransmitter gene expression, a reversal learning deficit in the Morris water maze, olfactory bulb and basal forebrain volume reductions (7.8% and 4.6% respectively), and a 7.5% reduction in numbers of choline-acetyltransferase (ChAT) IR cholinergic neurons in the basal forebrain. AIE (5g/kg, i.g., P28-37, 2 days on-2 days off) also caused an adulthood deficit in reversal learning in a different test, the Barnes Maze. AIE also resulted in increased anxiety-like behavior in adults, evidenced by a 43% reduction in time spent in the center of the open field. There were no significant adult regional brain volume reductions at P110 as a result of this treatment. The orbitofrontal cortex, a region critical for reversal learning, showed increased volume. Thus, alcohol exposure during adolescent or postnatal life can cause persistent changes in adult brain.

DEDICATIONS

To my Father

ACKNOWLEDGEMENTS

I thank Dr. Crews for his true mentorship the past three years. I am so appreciative to have been able to study under Dr. Crews. It really has been an honor, as well as a great time. Dr. Crews has been a great mentor as well as an advisor. He has made a lot of sacrifices for me and others, and I really appreciate having worked under his tutelage. I would also like to thank Fred Jarskog for advising me my first two years, and taking me on as his first graduate student. I would like to thank Sheryl Moy, Swarooparani Vadlamudi, Weili Lin, Martin Styner, Ipek Oguz, Yu Cai, Hongyu An, Shriya Soora and Randal Nonneman for their experimental expertise. I would also like to thank Liya Qin, Jian Zhou, and Olivera for setting a good example for me on a day to day basis. I thank Tonya Hurst for her friendship and help with the day to day tasks. I would also like to thank my thesis committee for their guidance and oversight. I would also like to thank the Curriculum in Neurobiology for their program support. I would like to thank Eugene Orringer, David Siderovski, Liz Garman, Alison Reagan, and Susan Herion in the MD/PhD program for the constant support and counsel over these past few years. Thank you, Dr. O for your guidance, support, and patience. Finally, I would like to sincerely thank the NIAAA (R01 AA06069, 5P60-AA011605, F30-AA018051) and the UNC-Bowles Center for Alcohol Studies for their financial support.

TABLE OF CONTENTS

LIST OF TABLES

LIST OF FIGURES

LIST OF ABBREVIATIONS

ACE - adolescent continuous ethanol

Ache - acetylcholine esterase

AIE - adolescent intermittent ethanol

ANOVA - analysis of variance

AMYG - amygdala

APAF-1 – Apoptotic protease activating factor 1

AUD - alcohol use disorder

BRIC - UNC Biomedical Research Imaging Center

BSF - basal forebrain

C57BL/6 – C57 black 6

CCK - cholecystokinin

Cg1, Cg2 - cingulate gyrus divisions 1 and 2

ChAT - choline acetyltransferase

COMT - Catechol-O-methyltransferase

D4DR - dopamine receptor D4

DAB - diaminobenzidine

DCX - doublecortin

DTI - Diffusion Tensor Imaging

FAS - fetal alcohol syndrome

FASD - fetal alcohol spectrum disorders

FDR - false discovery rate

GABA - γ-amino butyric acid

GAD67 - glutamic acidic decarboxylase

GFAP - glial fibrillary acidic protein

GRPR - gastrin releasing peptide receptor

HIPP - hippocampus

IHC - immunohistochemistry

IR - immunoreactivity

MK801 - dizocilpine

mPFC - Medial prefrontal cortex

MRI - Magnetic Resonance Imaging

NIRAL - UNC Neuro Image Research and Analysis Laboratory

NMDA - *N*-methyl D-aspartate

OFC - orbitofrontal cortex

PBS - phosphate buffered saline

PV - parvalbumin

PCP - phencyclidine

PCD - physiological cell death

PFC - prefrontal cortex

PPI - prepulse inhibition

SAMSA - Substance Abuse and Mental Health Services Administration

TUNEL - TdT-mediated dUTP nick end-labeling

YFP- yellow fluorescent protein

Introduction

The Long-Term Effects of Adolescent and Postnatal Ethanol Exposure on the Adult Mouse Brain: A Multidisciplinary Approach

Human and Rodent Brain Development

In both humans and rodents, brain development begins *in utero* and continues into the early stages of adulthood. There are differences between the gestation and lifespan of humans and rodents that can make comparisons challenging. For instance, the mouse gestational period ranges from 18-21 days, while human pregnancy usually lasts between 37 and 42 weeks. The lifespan for humans extends for several decades, whereas the lifespan of C57Bl/6 mice is between 2-3 years (Blackwell et al., 1995). However, since similar developmental milestones occur in both humans and rodents, cross-species developmental comparisons can be made (Figure I.1). *In utero* comparisons across species have been made primarily by comparing appearance of embryonic structures and the rates of neurogenesis in developing brain nuclei (Finlay and Darlington, 1995). At the time of birth in humans, and during the first two weeks of life in rodents, the relative brain size (expressed as the % of total body weight) reaches its peak (Dobbing and Sands, 1979). This developmental milestone has been established as a point of inter-species comparison between humans and rodents. This period of life is a dynamic period involving marked cortical growth (Lyck et

al., 2007), synaptogenesis (Dobbing and Sands, 1979), and physiological cell death (PCD) (Ishimaru et al., 1997; Ishimaru et al., 1999).

Adolescence, the transition from childhood to adulthood, is a developmental period characterized by puberty and common behaviors. In both humans and rodents adolescence can be defined primarily by behavioral measures. Human adolescents (roughly 12-24 years old) have characteristic behaviors that are common to rodents and other species (Spear, 2000). Adolescent behaviors include increased social and play behavior, novelty seeking and risk taking. By these criteria, cross-species comparisons define adolescence in mice as ages P28-P42 (Spear, 2000).

Working memory also improves across adolescence (Luna et al., 2004). This may be related to the reorganization of learning brain networks from being dominated by parietal cortices to the prefrontal cortex during adolescence (Schweinsburg et al., 2005). Response inhibition, or the ability to refrain from a learned behavior, is a critical component of reversal learning (Pierrot-Deseilligny et al., 1991) and is also refined during childhood and early adolescence reaching adult functioning levels by age 14 (Luna et al., 2004). Adolescence is an important window for maturation of several structures, including the frontal cortex (Blakemore, 2008; Crews et al., 2007a; Lewis, 1997; Sowell et al., 1999) and the basal forebrain (Bentivoglio et al., 1994; Dinopoulos et al., 1997; Dori et al., 1998).

Human imaging studies have found that cortical gray matter volume and thickness follow an inverted U-shaped curve, with an increase during childhood, and a peak during late childhood/early adolescence in most cortical regions (Giedd, 2004; Giedd et al., 1999; Gogtay et al., 2004; Lenroot and Giedd, 2006; Shaw et al., 2006). Interestingly, white matter volume continues to increase linearly into the early twenties, though the rate of myelination

is less than during prenatal and early postnatal life (Giedd, 2004; Toga et al., 2006). Gogtay et al demonstrated that the dorsolateral prefrontal cortex, which includes the orbitofrontal cortex (OFC), declined in volume to reach adult volume during adolescence between ages 16-20 (Gogtay et al., 2004). The orbitofrontal cortex regulates response inhibition (Pierrot-Deseilligny et al., 1991) and reversal learning (Dias et al., 1996; McAlonan and Brown, 2003; Schoenbaum et al., 2007). Brain regional volume changes may be related to cognitive function. For example, individuals with a more narrow U-shaped curve (from age 7 to 19) and a later peak cortical thickness in the right superior frontal and superior/medial prefrontal regions, performed better on several measures of intelligence (Shaw et al., 2006). Thus, the age of peak cortical thickness was found to be associated with increased IQ. Therefore, an insult or experience that alters either final volume or the trajectory of volume changes could potentially have persistent effects on cognitive function.

Figure I1: Human and Rodent Brain Development

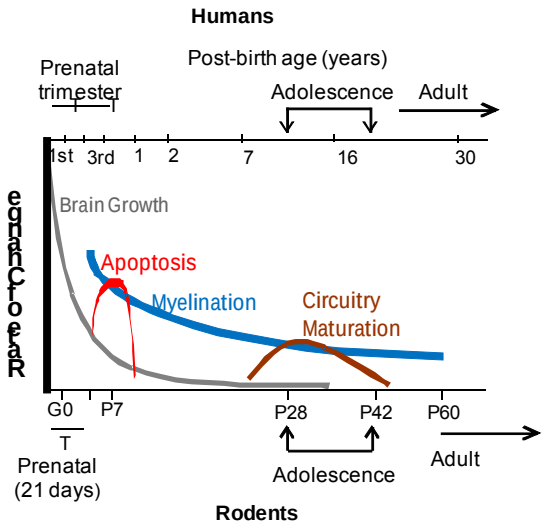

neurons in C57BL/6 mice increases from 2.2 x 10^6 at postnatal day zero P0 to peak on P16 (8.5 x 10^6) and declines during adolescence to 6.7 x 10^6 by P50 (Lyck et al., 2007). Markham et al have also found in rats that the number of neurons in the ventral medial prefrontal cortex declines across adolescence (Markham et al., 2007). Cholinergic neuron number in the basal forebrain Ch4 region also declines during adolescence in C57BL/6 mice (Bentivoglio et al., 1994). Thus rodent studies find major changes in regional brain volumes and cellular architecture during adolescence.

Rodent studies have revealed changes in transmitter neurochemistry during adolescence. Several neurotransmitter systems are maturing during this time. D1, D2 and D4 receptors as well as dopamine varicosity size reach adult levels in the medial and dorsal PFC between ages P28 and P45 (Benes et al., 2000; Tarazi and Baldessarini, 2000; Tarazi et al., 1998). NMDA receptor binding declines during adolescence to reach adult levels by P60 (Insel et al., 1990). Serotonin synapses in the basal forebrain are also undergoing functional maturation during adolescence (Dinopoulos et al., 1997; Dori et al., 1998).

Effects of Ethanol on Neurodevelopment

The most profound effects of ethanol on neurodevelopment occur via transplacental ethanol exposure *in utero* resulting in a syndrome of craniofacial malformations and behavioral disturbances termed Fetal Alcohol Syndrome (FAS). This syndrome has been observed in both humans and rodents (Jones and Smith, 1975; Jones et al., 1973; Sulik et al., 1981). The entire group of conditions that can occur as a consequence of maternal ethanol consumption is termed fetal alcohol spectrum disorders (FASD) (Center for Disease Control 2010). The observations from these conditions indicate that ethanol has its most potent

teratogenic effects on brain structures that are actively undergoing development. Consistent with this concept, P7 ethanol treatment, a model of 3rd trimester alcohol exposure, has been shown to enhance PCD, which is occurring at that developmental age (Ikonomidou et al., 2000; Olney et al., 2002b). However, the persistent effects of P7 ethanol exposure on the adult brain are not known. We hypothesized that P7 ethanol would cause changes in adult brain structure. Maternal drinking may occur during the third trimester; however, perhaps a greater public health concern is adolescent alcohol abuse. Alcohol abuse during adolescence is common with the rate of binge drinking peaking during adolescence (Masten et al., 2008). Since the brain is also actively developing during adolescence, we hypothesized that adolescent alcohol exposure would cause persistent brain deficits.

Human studies find that adolescent alcohol use is associated with altered cognitive function and brain structure. Adolescent drinkers perform worse on verbal and nonverbal retrieval tests (Brown et al., 2000). Adolescents with a history of alcohol dependence in the past year had reduced visuospatial block design ability as measured by the Wechsler Adult Intelligence Scale (Sher et al., 1997). Adolescents with histories of alcohol use have reductions in hippocampal, thalamic, and cerebellar volumes (De Bellis et al., 2005; Nagel et al., 2005). Interestingly, adolescent male binge drinkers have been shown to have an increased volume of the ventral lateral prefrontal cortex, which includes the OFC (Medina et al., 2008). Thus, human adolescents that abuse alcohol show differences in brain structure and cognitive ability. However, it is not known if these deficits are pre-existing or if they are caused by alcohol use. Further, it is not known if adolescent alcohol abuse can alter adult brain structure and function.

Human epidemiological studies suggest that drinking during adolescence might have long-term behavioral effects. The prevalence of both alcohol abuse and alcohol dependence in adulthood is related to the age of onset of regular drinking during adolescence (Grant and Dawson, 1997). Also, alcohol problem use (i.e., associated with adverse consequences) during late adolescence (ages 16 & 18), is a predictor of major depressive disorder in young adulthood (age 22) (Mason et al., 2008). However, a fundamental limitation of human studies is that they do not enable investigators to identify whether deficits were induced by alcohol use, or if they were pre-existing. Therefore, we employed an animal model to investigate the effects of adolescent ethanol exposure on adult learning and memory.

Adolescent rodents respond differently to alcohol than adults. Young rats are more resistant to the sedative effects of alcohol (Silveri and Spear, 1998) and more sensitive to the acute impairment of spatial learning acquisition by ethanol (Markwiese et al., 1998). Adolescent rodents are more sensitive to alcohol induced neurotoxicity in a 4 day binge model (9-10 g/kg/day ethanol) with developing frontal regions showing enhanced toxicity (Crews et al., 2000b). However, the long-term effects of adolescent ethanol exposure on the adult brain are not known. Therefore, we have investigated the persistent effects of models of adolescent binge ethanol exposure on adult brain structure and behavior.

Deficits in adult prefrontal cortex neurons and behavior following early postnatal NMDA antagonist treatment.

Leon G. Coleman Jr, L. Fredrik Jarskog, Sheryl S. Moy, Fulton T. Crews. Pharmacology, biochemistry, and behavior. 2009 Sep; 93(3):322-30. PMID: 19409920

Abstract

The prefrontal cortex (PFC) is associated with higher cognitive functions including attention and working memory and has been implicated in the regulation of impulsivity as well as the pathology of complex mental illnesses. *N*-methyl D-aspartate (NMDA) antagonist treatment with dizocilpine induces cell death which is greatest in the frontal cortex on postnatal day seven (P7), however the long-term structural and behavioral effects of this treatment are unknown. This study investigates both the acute neurotoxicity of P7 dizocilpine treatment of mice and the persistent effects of this treatment on pyramidal cells and parvalbumin interneurons in the adult PFC, a brain region involved in the regulation of impulsivity.

Dizocilpine treatment on P7 increased cleaved caspase-3 immunoreactivity (IR) in the PFC on P8. In adult mice (P82), P7 dizocilpine treatment resulted in 50% fewer parvalbumin-positive interneurons ($p<0.01$) and 42% fewer layer V pyramidal neurons ($p<0.01$) in the PFC. Double immunohistochemistry revealed cleaved caspase-3 IR in both GAD67, a GABA marker, IR and GAD67 (-) neurons. Following dizocilpine treatment at P7, adults during locomotor activity assessment, showed reduced time in the center of the open field suggesting increased anxiety-like behavior. These findings suggest that early

brain insults affecting PFC lead to persistent changes in adult brain and may contribute to impulsivity and cognitive dysfunction.

Introduction

The prefrontal cortex (PFC) is a critical brain region involved in executive functioning, decision making and behavioral planning. The PFC controls attention and integrates information from the limbic and other regions to appropriately manage the subject's impulsive and compulsive responses. Dysfunctional control of impulsivity and deficits in executive function, such as in schizophrenia and addiction, could be secondary to damage to the PFC. PFC in humans and rodents is primarily defined by reciprocal projections with the medial dorsal nucleus of the thalamus (Kuroda et al., 1998; Rotaru et al., 2005; Uylings et al., 2003). PFC also receives input from substantia nigra, amygdala, olfactory cortex, ventral pallidum, and other regions (Fuster, 1997). Both human and rodent medial PFC includes anterior cingulate and infralimbic regions. Similar to humans, medial regions of the rodent prefrontal cortex are involved in regulating cognition and impulsivity through modulating the attentional aspects of decision making (Birrell and Brown, 2000; Muir et al., 1996). The PFC is a multilayer cortical structure in rodents and humans that contains varied glutamatergic and γ-amino butyric acid (GABA)ergic neurons in varied morphology and layers. PFC cortical layers, glutamatergic excitatory pyramidal cells and inhibitory GABAergic interneurons develop over an extended prenatal and postnatal period that likely correspond with development of executive functions of the PFC.

Developmental damage to the PFC may result in altered cellular structure and connectivity that causes dysfunction in adults. In rodents the early postnatal period is known

to be particularly sensitive to insults. For example, a comparison of dizocilpine, a non-competitive NMDA antagonist and ethanol across postnatal days 3-21 (P3-P21) found marked toxicity that declined on P21 with postnatal day 7 being the peak time point for neurotoxicity in PFC (Ikonomidou et al., 2000). Later studies using 2 doses of dizocilpine on P7 and investigating P60 brain found significant hippocampal neuronal loss and damage to thalamic regions, but PFC was not studied (Harris et al., 2003). Recently, studies treating rats with PCP, an NMDA antagonist, on P7 and investigating adult brain (P56) found a selective loss of a subtype of GABAergic interneurons in superficial cortical layers II-IV of primary somatosensory, motor and retrospenial cortex. (Wang et al., 2008). There were no changes found in striatum or hippocampus, but PFC anterior cingulate and infralimbic regions were not investigated. PFC dysfunction is suspected in impulsivity and addiction (For review see Crews and Boettiger 2009, current issue) and has been implicated in schizophrenia (Powell and Miyakawa, 2006). Stefani and Moghaddam (Stefani and Moghaddam, 2005), in an effort to model schizophrenia, treated rats with PCP, for 4 days (P7-P10) and found persistent deficits in adult cognitive set shifting ability, presumably a PFC function, but they did not investigate anatomy. Interestingly, adult rats treated with the NMDA antagonist CPP directly into the PFC display increased impulsive behavior as measured by anticipatory responses in the 5-Choice Serial Reaction Time task (5-CSRT) (Baviera et al., 2008; Mirjana et al., 2004). Therefore, both disruption of PFC signaling in adulthood and developmental damage to the PFC during early postnatal life can induce impulsive behavior and cognitive dysfunction respectively. Though some adult behavior effects of early postnatal NMDA antagonism have been observed, adult PFC neuroanatomy has not been studied.

We hypothesized that early postnatal NMDA antagonists will induce cell death in PFC resulting in a persistent change in PFC structure in adulthood (P82). The cortex contains VI (6) layers with important neuronal densities of GABAergic interneurons and glutamatergic pyramidal cells. PFC layer V pyramidal neurons project to several brain regions, including reciprocal connections with the medial dorsal thalamic nucleus (Kuroda et al., 1998; Molnar and Cheung, 2006). PFC has at least 3 types of GABAergic interneurons characterized by expression of different calcium binding proteins, e.g. parvalbumin (PV), calretinin (CR), or calbindin (CB) (Baimbridge et al., 1992; Gabbott et al., 1997) which can be distinguished immunohistochemically in adults. Many early postnatal GABAergic interneurons do not show the mature calcium binding protein phenotype, since PV and CB expression increase substantially from P7 to P21 (Lema Tome et al., 2006). Using glutamic acid decarboxylase-67 (GAD67), a marker of GABAergic neurons (Tamamaki et al., 2003), and cleaved caspase 3 immunohistochemistry, a marker of cell death (Krajewska et al., 1997), we were able to assess which neuronal phenotypes were insulted. We found both GABAergic and non-GABAergic neurons were insulted. Previous studies have found that PCP treatment of P7 rats selectively reduces adult somatosensory and motor cortical PV interneurons (Wang et al., 2008), similar to the loss of PV interneurons in human schizophrenic PFC (Beasley and Reynolds, 1997). Since, neither CB nor CR GABAergic interneurons were found to be decreased in these brain regions in young adulthood (P56) following P7 PCP treatment (Wang et al., 2008), cortical PV interneurons, rather than other GABAergic interneuron subtypes, are likely more vulnerable to this type of insult. We focused on PV interneurons and layer V glutamatergic pyramidal cells in the medial region of the PFC in adult

animals. Pyramidal neurons were quantified in adults using a mouse that expresses a YFP transgene in cortical layer V pyramidal neurons (Feng et al., 2000). Interneurons in adults were quantified using PV immunohistochemistry. We report here for the first time that P7 treatment of mice with dizocilpine results in a persistent loss of adult (P82) PFC pyramidal neurons and PV GABAergic interneurons. These neuronal deficits were associated with decreased center time in open field behavior in adults, suggesting increased anxiety, with no changes in pre-pulse inhibition. Future studies will investigate if the persistent loss of PFC neurons disrupts executive functions and alters impulsivity.

Methods

Subjects.

Transgenic mice expressing Thy1/yellow fluorescent protein (YFP) line H mice on a C57BL/6 background, were bred in the University of North Carolina at Chapel Hill (UNC-CH) animal facility (Feng et al., 2000). Layer V pyramidal neurons express the YFP transgene in cerebral cortex of these mice. Transgene expression was confirmed by PCR. Genomic DNA was extracted from tail biopsies of mice no later than postnatal day five, and analyzed by PCR using PCR primers (5' to 3') specific for Thy1F1 (TCTGAGTGG CAAAGGACC TTAGG) and EYFPR1 (CCGTCGCCGATGGGGGTGTT). Heterozygous males were mated with homozygous negative females. For long-term studies, only pups that were homozygous for the transgene were used. Approximately 40% of pups bred from heterozygous parents were homozygous for YFP. Other than the YFP expression, animals appeared normal. Animals were maintained in Association for Assessment and Accreditation of Laboratory Animal Care (AAALAC) accredited facilities and experiments were approved

by the UNC-CH Institutional Animal Care and Use Committee in accordance with the Congressional Animal Welfare Act.

Experimental design and P7 dizocilpine treatment.

Mice were treated on P7 with either saline (N=10) or dizocilpine (N=10) (1mg/kg, i.p.) every eight hours (t = 0, 8, 16 hours) as described previously (Ikonomidou et al., 1999). There were no significant differences in weight between treatment groups during the treatment period or prior to observation in adulthood (not shown). Half of the animals (group 1) were sacrificed eight hours after the last injection to assess the acute effects of dizocilpine on cleaved caspase-3 immunoreactivity (IR). Mice from group 1 were sacrificed by decapitation on P8, and the brain was removed. The whole brain was submerged in 4% paraformaldehyde (PFA) for 24 hours at 4°C. Coronal sections were prepared using a vibratome at a thickness of 40 μm. The second group of animals (group 2) matured under normal housing conditions and underwent behavioral assessment on P80, followed by sacrifice at P82 for immunohistochemical analysis. On P82, mice in group 2 were first mildly anesthetized using vaporized isoflurane, followed by intra-peritoneal pentobarbital injection. Animals were then perfused transcardially with 0.1M phosphate buffered saline (PBS) followed by 4% PFA. Brains were incubated in 4% PFA for 24 hours at 4°C. Coronal sections were prepared on a vibratome at a thickness of 100 μm in order to optimize visualization of YFP.

Cleaved caspase-3 immunohistochemistry on P8.

Caspase-3 cleavage was assessed via cleaved (19 kD) caspase-3 immunoreactivity (IR) using established methods (Jarskog et al., 2007; Lema Tome et al., 2006). Briefly, every fourth section from animals in group 1 was mounted on Superfrost plus® slides, washed in PBS, and incubated in 0.3% hydrogen peroxide for 30 minutes. This resulted in 3-4 sections per animal that contained the PFC. Following subsequent washes in PBS, sections were blocked in 5% goat serum in 0.3% Triton X-100 for 1 hour followed by overnight incubation with primary antibody for cleaved caspase-3 (1:200, Cell Signaling) at 4°C in a humidification chamber. After washing, the sections were incubated 1 hour with anti-rabbit secondary antibody (1:200, Vector Labs) at room temperature in 5% goat serum. Immunostaining was performed using the avidin-biotin (ABC) method (Vectastain Elite Kit, Vector Labs) with diaminobenzidine (DAB)/Nickel enhancement for 10 minutes. Nissl counterstaining was performed to visualize the cortical layers. Sections were then dehydrated in a series of ethanol dilutions, immersed in xylene and cover-slipped.

Cleaved caspase-3 and GAD67 co-labeling on P8, double immunohistochemistry

Free-floating sections from mice in group 1 (P8) were prepared for immunoflourescent double labeling as described (Nixon and Crews, 2002). Briefly, sections were washed in PBS followed by 30 min incubation in 0.1% hydrogen peroxide to reduce endogenous fluorescence. Sections were then incubated with cleaved caspase-3 antibody with an Alexa-Fluor 488 conjugate (1:10, Cell Signaling) and an anti-GAD67 antibody (1:100, Santa Cruz) overnight at 4°C in a blocking solution containing 0.1% Triton X-100 and 3% rabbit serum. The following day sections were washed in PBS and

incubated in Alex-Fluor 594 rabbit anti-goat secondary (1:1000) for 1 hour at room temperature.

Parvalbumin and YFP immunohistochemistry in adulthood (P82).

The same procedure was performed as above with the following modifications. Free-floating sections from adult mice (group 2) were washed three times in (PBS), followed by incubation in 0.1% hydrogen peroxide (He and Crews, 2006). This thickness was chosen in order to optimize visualization of YFP fluorescent neurons. However, since quantification of fluorescence was unreliable, sections were visualized using the ABC-DAB method as described above. Floating sections were incubated overnight in either anti-parvalbumin (1:2000, Sigma) or anti-EGFP/EYFP [6AT316] (1:1000, ABCAM/fisher) at 4°C followed by washing and appropriate secondary antibody incubation the following day. Following ABC and DAB exposure, sections were mounted, allowed to air dry over night at room temperature and cover-slipped.

Anatomical boundaries of the PFC

The medial regions of the PFC (anterior cingulate (Cg), pre-limbic, and infra-limbic cortices) were investigated. Since it was difficult to clearly distinguish between the pre-limbic and infra-limbic regions, they were combined and analyzed as the limbic region (LI). The boundaries of the anterior cingulate and the limbic cortices (Figure 1.1A) were as guided by the mouse atlas (Franklin and Paxinos, 2001) as well as guidelines in a previous immunohistochemical study (Grobin et al., 2003). Coronal sections were identified by comparison with the mouse atlas between bregma 1.98, the appearance of the forceps minor

corpus callosum (fmi), and bregma 1.10, the genu of the corpus callosum being the antero-posterior boundaries. The dorsal boundary of the anterior cingulate was defined as the diagonal parallel to the dorso-lateral curvature of the fmi, beginning at the medial peak of the fmi to the medial pial surface. The ventral boundary of the anterior cingulate cortex was defined as a diagonal parallel to the dorsal boundary, beginning one fourth of the maximum length of the fmi ventral from the peak of the fmi to the medial pial surface. The limbic region of the medial PFC was defined as previously from the medial pial surface laterally to the fmi, ventral to the anterior cingulate cortex.

Quantification of immunopositive cells.

Immunopositive cells were visualized with a CCD camera connected to an Olympus microscope. The PFC was traced and the area traced measured using the Bioquant Image Analysis system as previously described (He et al., 2005). Labeled cells were counted within the region of interest, divided by the area of the section, expressed as cells/mm^2. For each animal, PFC cell counts in were made in 3-4 sections coursing the PFC (bregma +1.98 to +1.1). Counts were determined for each hemisphere individually, and then an average value for each section was calculated. Next the average value across all sections for each animal was determined. Lastly, the average density for each treatment group (i.e., control or dizocilpine) was calculated and compared statistically. We have previously shown that this profile counting method and stereological estimations show identical results in percentage change (Crews et al., 2004; Nixon and Crews, 2002; Nixon and Crews, 2004).

Open field exploration in adulthood (P80).

Reduced exploratory behavior is an index of anxiety-like behavior (Crawley, 1999). We evaluated exploratory behavior of adult mice (P80) in a novel environment following P7 saline or dizocilpine treatment. Mice were placed in an open field chamber crossed by a grid of photobeams (VersaMax system, AccuScan Instruments) for two hours as described (Mohn et al., 1999). Both total distance traveled and time spent in the center were evaluated. Values were collected every five minutes.

Inhibition of the acoustic startle response (PPI) in adulthood (P80).

The acoustic startle response is a measure of the whole-body flinch reflex following a sudden noise. PPI occurs when a low pre-stimulus leads to a reduced startle in response to a subsequent louder noise. Adult mice (P80) treated on P7 with either saline or dizocilpine were tested in a San Diego Instruments SR-Lab system, as described previously (Moy et al., 2006; Paylor and Crawley, 1997). Briefly, a softer pre-pulse stimulus (74, 78, 82, 86, or 90 dB) was given 100 ms prior to the startle stimulus (120 dB). The peak startle response during the 65-msec period following the startle stimulus was recorded. The PPI for each mouse was calculated using the following equation: (100 - [(response amplitude for pre-pulse stimulus and startle stimulus together / response amplitude for startle stimulus alone) x 100]).

All behavioral tests were performed at the Mouse Neurodevelopmental Research Behavioral Measurement Core facility at UNC. Both pre-pulse inhibition (PPI) and locomotor testing were performed on the same day.

Statistical Analysis

For the immunohistochemistry studies, the average number of immunopositive cells per area for treatment and control groups (calculation described above) was compared using Student's *t*-test. Behavioral tests were analyzed using repeated measures ANOVA, with the variable treatment (vehicle or drug) and the repeated measure (five-minute interval in the activity test and pre-pulse sound level in the acoustic startle test). Significance level was set at $p < 0.05$.

Results

Cleaved caspase-3 immunoreactivity and double immunohistochemistry with GAD67 on P8.

Treatment with dizocilpine on P7 increased caspase-3+IR in PFC on P8 (Figure 1.1B). Caspase-3+IR in anterior cingulate cortex was increased over 4 fold (4 ± 1 to 17 ± 4 caspase-3+IR cells/mm^2 in control and dizocilpine respectively, mean ± standard error $p<0.03$, $n = 5$ per group) and in the limbic cortex 7 fold (5 ± 1 to 34 ± 11 caspase-3+IR cells/mm^2 in control and dizocilpine respectively, $p<0.03$, $n = 5$ per group) (Figure 1.2). Thus, dizocilpine treatment causes a significant increase in PFC caspase-3+IR, which is evidence of an acute increase in apoptotic cell death.

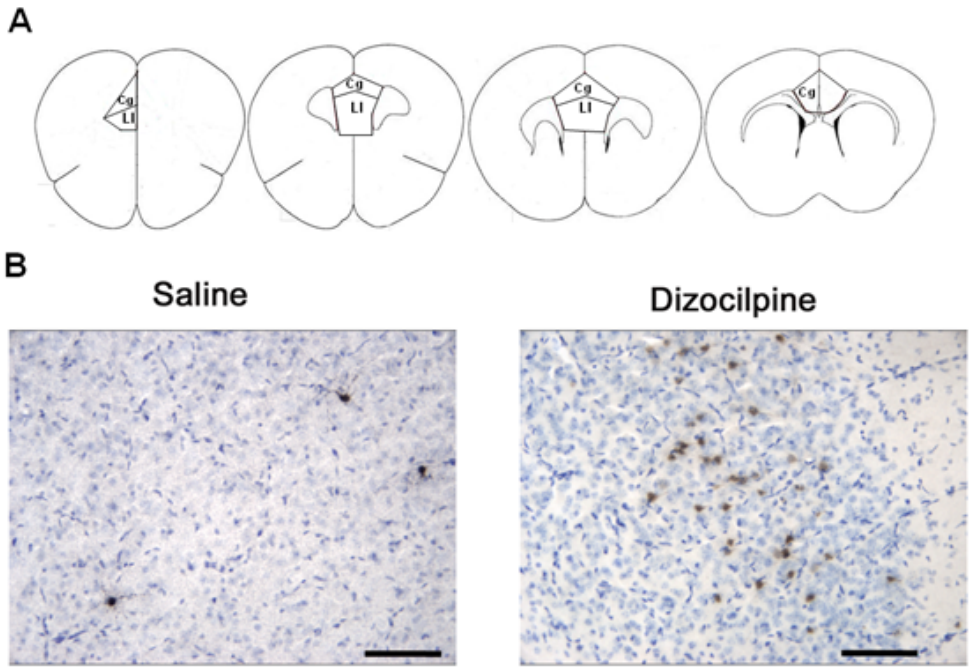

Figure 1.1 P7 Dizocilpine Increases Caspase-3 Cleavage. (A.) Diagrams of coronal brain sections between bregma +1.98 to bregma +1.10 that identify the areas of mouse PFC quantified for cleaved caspase-3 immunohistochemistry (Franklin and Paxinos, 2001). Briefly, the dorsal boundary of the anterior cingulate was defined as the diagonal parallel to the dorso-lateral curvature of the fmi (arrows), beginning at the medial peak of the fmi to the medial pial surface. The ventral boundary of the anterior cingulate cortex was defined as a diagonal parallel to the dorsal boundary, beginning one fourth of the total medial length of the fmi, ventral from the peak of the fmi, across to the medial pial surface. (B.) Cleaved Caspase-3+IR. Mice were treated on postnatal day 7 with either saline or dizocilpine (1 mg/kg, 3x24h, i.p.) and assessed for cleaved caspase-3 immunoreactivity (IR) in the prefrontal cortex (PFC) 24 hours after the initial injection. Representative images of cleaved caspase-3 staining with Nissl counterstain (blue) in PFC following either saline or dizocilpine. Note dizocilpine treatment caused an increase in multiple+IR brown cellular profiles indicating cleaved caspase-3+IR. Arrows denote cleaved caspase-3 + IR. Scale bar denotes 50 microns.

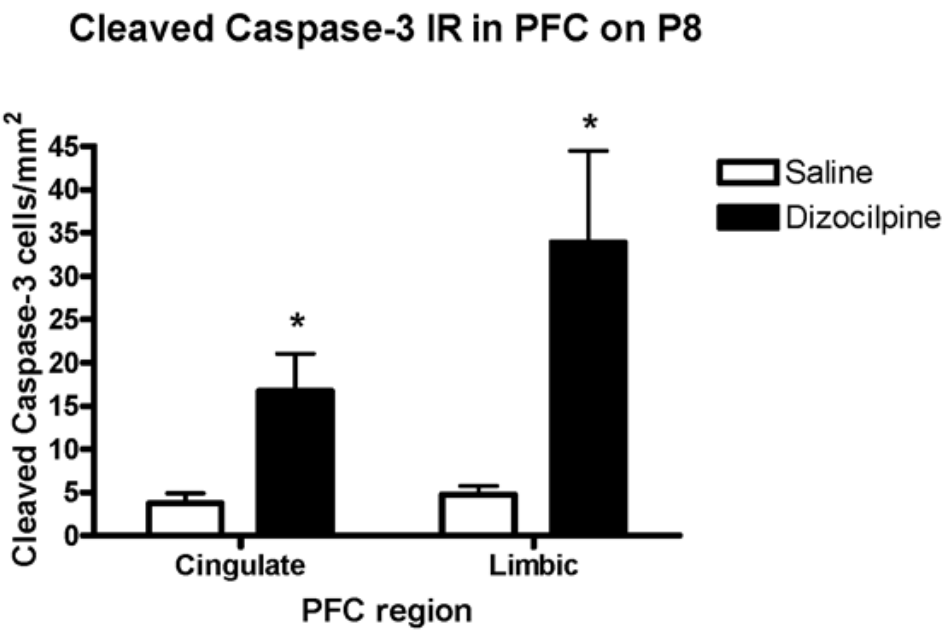

Figure 1.2 Quantification of Cleaved Caspase-3 Immunohistochemistry. The number of cleaved caspase-3 + immunoreactive (IR) neurons was counted per unit of cortical area as described in the methods. Data shown has been divided into PFC cingulated and PFC limbic as shown in Fig. 1A and described in the methods. Overall PFC cleaved caspase-3+IR cells were increased about 4-7 fold. Within subregions of PFC the anterior cingulate cortex (Cg) increased 4-5 fold and the limbic cortex (LI) increased 6-7 fold (Mean ± standard error, *p<0.03, t-test). Number of mice per treatment group: Saline, n = 5; Dizocilpine, n = 5.

Using double immunohistochemistry and confocal microscopy on P8 following dizocilpine treatment, we found caspase-3+IR was detected in both GAD67 immunopositive and GAD67 immunonegative cells (Figure 1.3). A pictured neuron that is positive for both cleaved caspase-3 and GAD67 displays nuclear swelling and cytoplasmic shrinkage, suggesting ongoing cell death (Figure 1.3C, arrow) (Obernier et al., 2002a). Thus, caspase-3 cleavage associated with P7 dizocilpine treatment occurs in both GABAergic and non-GABAergic neurons in frontal cortex.

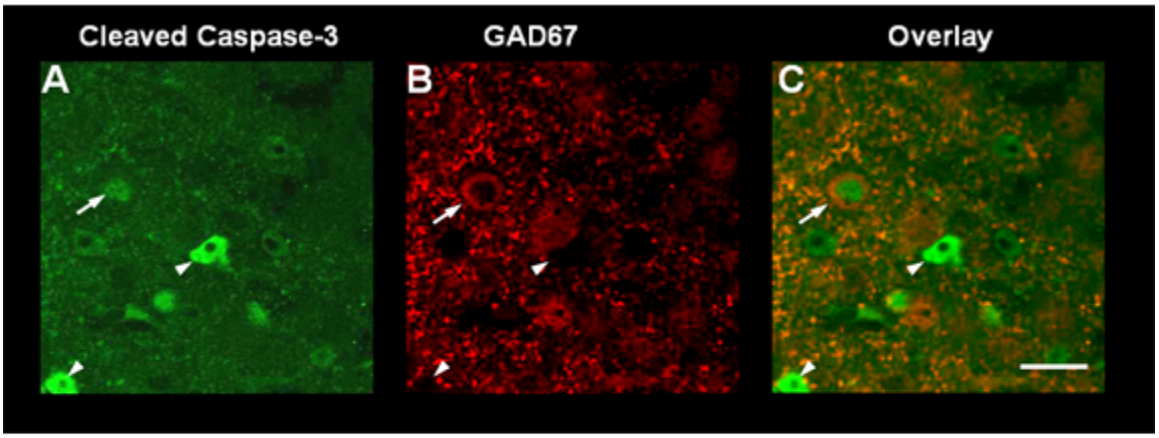

Figure 1.3 Cleaved Caspase-3 and GAD67 Immunoflourescent+ IR. Shown are images of PFC from double immunohistochemistry for cleaved caspase-3 (A, green), for the GABAergic enzyme GAD-67 (B, red) and for the merged images (C). Mice were treated on postnatal day 7 with dizocilpine and assessed for colocalization of cleaved (19 kD) caspase-3 + IF and GAD67 + IR in PFC. on P8. Since parvalbumin is not yet expressed on P8, GAD67 was chosen to identify GABA interneurons. Arrow denotes a swollen nuclear form in a cleaved caspase-3+IR cell (A) that is also GAD67+IR (B) and merges to show the same figure has both +IR. Swollen nuclei often identify dying cells (Obernier et al., 2002). Arrowheads denote caspase-3 positive cells that do not show GAD67+IR and are therefore not GABAergic neurons. Scale bar denotes 20 microns.

P7 dizocilpine reduces PFC PV interneurons in adults (P82).

The number of GABAergic PV+ IR cells in adults (P82) was assessed following P7 dizocilpine demonstrating visibly fewer PV+IR in PFC (Figure 1.4). Saline treated animals had nearly twice as many PV + IR neurons (106 ± 19 PV positive cells/mm^2) compared to dizocilpine (58 ± 10 PV+IR cells/mm^2) across the medial regions of the PFC, $p = 0.05$, *t*-test (Figure 1.5). More detailed analysis of cortical subregions, found a 54% loss of PV cells in anterior cingulate cortex (saline, 113 ± 14 PV + IR cells/mm^2 $n = 4$; dizocilpine, 64 ± 9; $n = 5$, $p<0.02$), and a 51% decrease limbic cortex (saline, 98 ± 29; dizocilpine, 50 ± 10; $p=0.13$) which in limbic cortex was not statistically significant. These studies indicate that GABAergic neurons are insulted on P7 resulting in about a 50% loss of PFC PV GABAergic interneurons in adulthood.

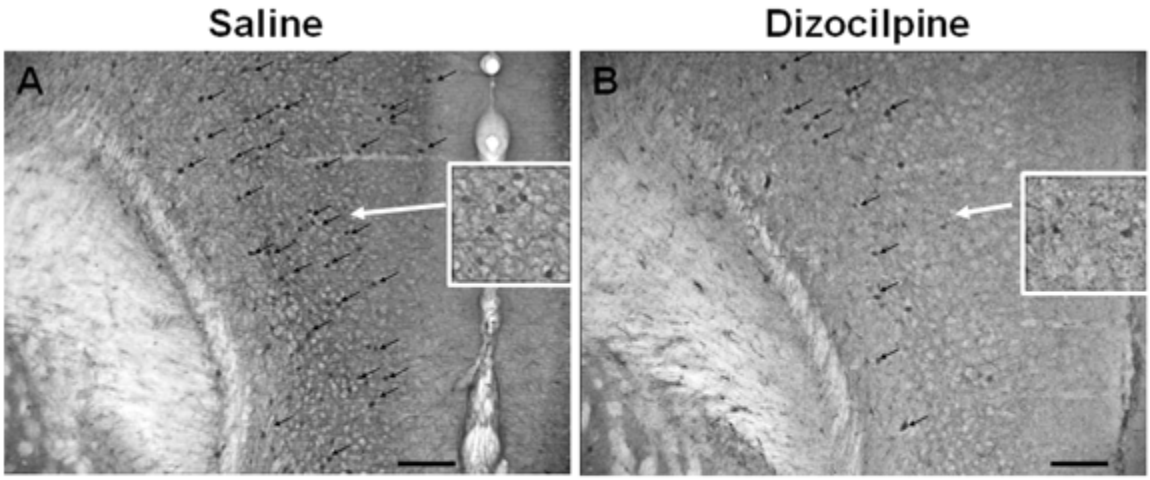

Figure 1.4 P7 Dizocilpine Reduces Parvalbumin (PV) Immunoreactivity in Adults. Shown are sections of PFC from mice treated on postnatal day 7 (P7) with either saline or dizocilpine and assessed for PV + immunoreactivity in adulthood (P82). Dizocilpine treatment results in reduced PV + immunoreactive (IR) neurons in the prefrontal cortex (PFC) of adult animals (P82). Representative images (10X) of parvalbumin + IR. Black arrows denote parvalbumin positive immunoreactive neurons. Inserts show higher magnification of PV + IR neurons. Scale bar denotes 100microns.

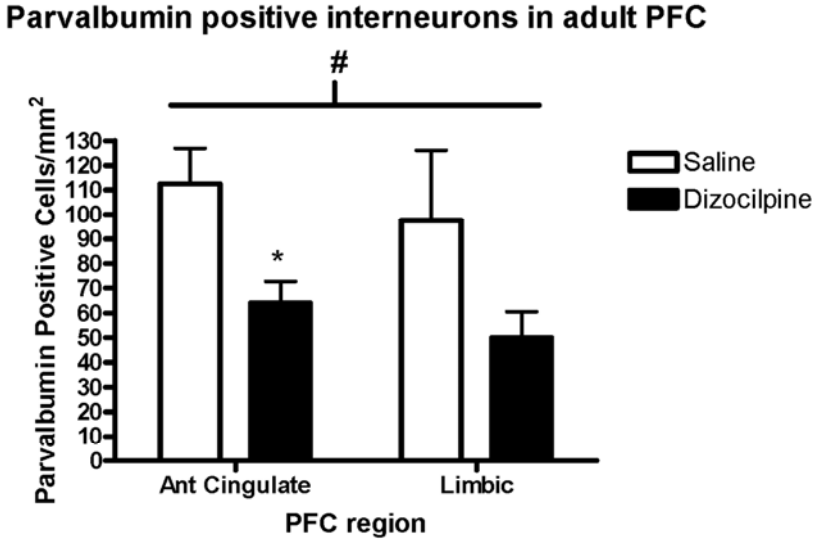

Figure 1.5 Quantification of Parvalbumin (PV) Immunohistochemistry. The number of PV + immunoreactive (IR) neurons in the prefrontal cortex (PFC) per unit of cortical area was determined in adult mice on postnatal day 82 (P82) as described in the methods. In the entire PFC dizocilpine treatment on P7 caused a 45% reduction in the number of adult PFC (P82) PV + immunoreactive (IR) (# $p=0.05$). Dividing PFC into subregions indicated that the anterior cingulate cortex lost about 50% of PV+IR cells (*$p<0.02$), and the limbic cortex lost about 50% which did not reach statistical significance. (Saline, 98 ± 29; Dizocilpine, 50 ± 10, $p=0.13$). Mean ± standard error. Number of mice per treatment group: Saline, n = 4; Dizocilpine, n = 5.

An examination of potential microglial activation using the microglial marker Iba-1+IR showed no apparent differences in PFC microglia following P7 dizocilpine (not shown). Thus, P7 dizocilpine results in the loss of PV+ GABAergic interneurons without affecting adult microglia numbers in the adult PFC.

P7 dizocilpine results in reduced layer V pyramidal neurons in adults

To investigate PFC pyramidal neurons we used immunohistochemistry staining for YFP in transgenic mice expressing YFP in layer V pyramidal neurons. We used immunohistochemistry for YFP, since it provided clearer and more sustained visualization than native fluorescence. Differences in the number of YFP positive pyramidal neurons between P7 saline treated and dizocilpine treated animals were readily observable (Figure 1.6). Quantification revealed that dizocilpine treatment on P7 resulted in a 43% reduction of YFP positive layer V pyramidal neurons across the entire PFC (saline, 446 ± 82 YFP + IR neurons/mm^2; dizocilpine, 254 ± 20, $p<0.05$, n=3 per group) (Figure 1.7). Thus, both PV GABAergic interneurons and layer V glutamatergic pyramidal neurons are reduced in adult PFC following P7 dizocilpine.

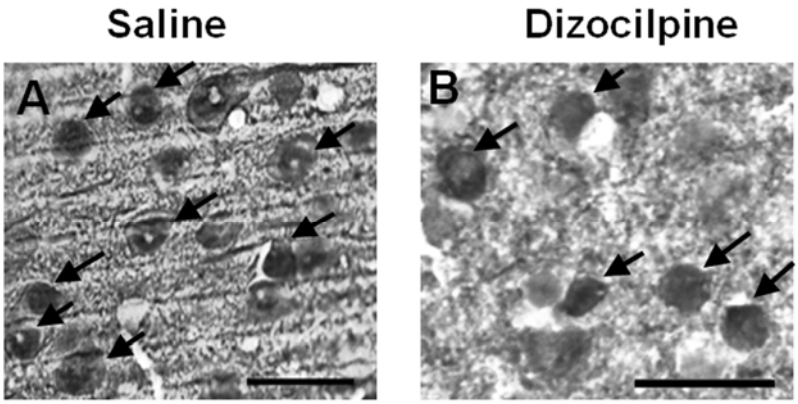

Figure 1.6 P7 Dizocilpine Reduces Layer V Pyramidal Neurons in Adults. Shown are representative images of YFP+IR. As described in the methods, the C57BL/6 mice studied express YFP in layer V pyramidal neurons. Arrows highlight YFP+IR in layer V pyramidal neurons. Dizocilpine treatment on P7 reduced YFP + IR layer V pyramidal neurons in adult mice (P82). Representative images of YFP + IR in adult PFC (40X), following (A) P7 saline or (B) P7 dizocilpine treatment. Scale bar denotes 20 microns.

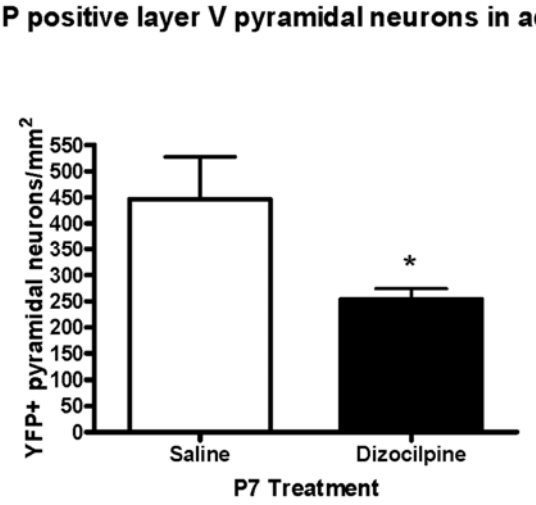

Figure 1.7 Quantification of Layer V Pyramidal Neuron Immunohistochemistry. The number of YFP + immunoreactive (IR) layer V pyramidal neurons per cortical area in the PFC was determined as described in the methods. Dizocilpine treatment on P7 caused a significant 43% reduction of layer V pyramidal neurons at P82 across the PFC (*$p<0.05$). Mean ± standard error. Number of mice per treatment group: Saline, n = 3; Dizocilpine, n = 3.

P7 dizocilpine alters open field behavior in adults (P80) without disrupting PPI

Center time in the open field, overall locomotor activity, and PPI of acoustic startle

responses were evaluated in mice at P80. PPI is an index of sensorimotor gaiting and open field activity is a global measure of motor activity, exploration and overall locomotion. There were no significant effects of the early exposure to dizocilpine on overall locomotor activity (Figure 1.8A, main effect of treatment, $F_{1,7}$=0.20, p = 0.67), or on the time course for habituation i.e., the reduced activity with time in the open field (treatment x time interaction, $F_{23,161}$=1.19, p = 0.26). Additional information is obtained from open field activity by assessing time in the center of the open field. Comparisons of total center time showed controls spent about twice as much time in the center during the first 50 minutes of the test, prior to habituation (Figure 1.8B). Controls spent an average of 36± 7 seconds/5 min observation period, whereas dizocilpine treated mice spend an average of 19± 3 seconds/ 5min (2-way ANOVA with repeated measures: $F_{1,7}$= 5.81, * p < 0.05)in the center of the open field. The tendency to avoid the center open field, or thigmotaxis, has been used as a standard measure of anxiety-like behavior (Crawley, 1999), that is enhanced by anxiogenic drugs and reduced by anxiolytic drugs (Simon et al., 1994; Treit and Fundytus, 1988). Treatment with dizocilpine on P7 did not lead to changes in PPI in adult (P80) animals (Figure 1.9, repeated measures ANOVA, main effect of treatment, $F_{1,7}$=1.64, p = 0.24; treatment x decibel level interaction, $F_{4,28}$=1.16, p = 0.35). Thus, P7 dizocilpine significantly reduced time spent in the center region of the chamber, without altering overall locomotor activity or pre-pulse inhibition.

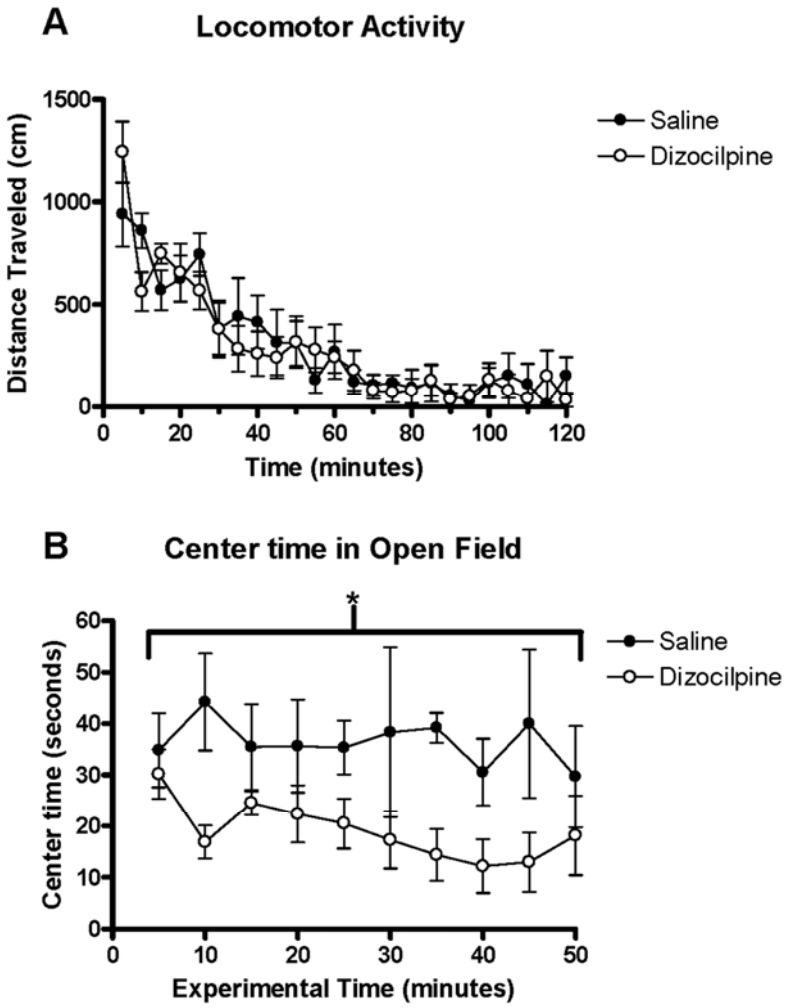

Figure 1.8 Open Field Activity of P80 Adult Mice With or Without P7 Dizocilpine. Mice were placed in an open field chamber and activity automatically recorded when light beams were broken. (A) Overall Open Field Locomotor activity (5 minute periods). Note high exploratory activity at early time points that declines over time as the animal habituates to the novelty of the new environment. Saline and dizocilpine mice displayed no differences in their overall locomotor activity ($F_{1,7}= 0.2$, $p = 0.67$) . Mice habituated to the test chamber during the first 50 minutes. There was no difference in the time course for habituation between groups (Treatment x time interaction $F_{23,161}= 1.19$, $p = 0.26$). (B) Center time open field activity. Note mice treated on P7 with dizocilpine show less center time during most 5 minute periods during the 50 minute exploratory phase. In general dizocilpine treated mice spent about half as much time exploring the center of the open field as mice treated with saline on P7 over the first 50 minutes, prior to habituation. Saline, n = 4; Dizocilpine, n = 5.

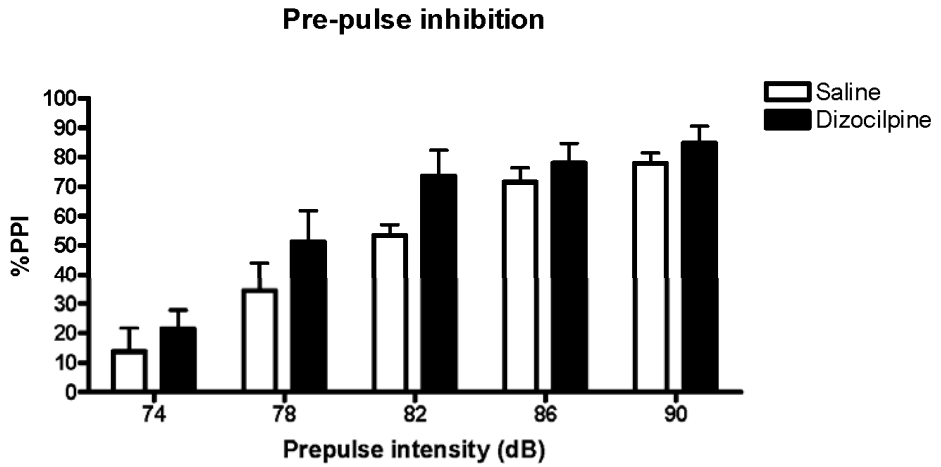

Figure 1.9 P7 Dizocilpine Does Not Change Adult Pre-Pulse Inhibition. Mice were treated with either saline or dizocilpine on P7 and PPI was measured on P80. PPI, a measure of sensorimotor gating, was not changed by dizocilpine (repeated measures 2-way ANOVA (main effect of treatment $F_{1,7} = 1.64$, $p<0.24$; treatment x decibel level interaction, $F_{4,28}=1.163$, $p = 0.35$). Number of mice per treatment group: Saline, n = 4; Dizocilpine, n = 5.

Discussion

We found that postnatal day 7 NMDA antagonism increases cleaved caspase-3 IR in the PFC in both GABAergic and non GABAergic cells. Our observation of a 4-7 fold increase in the density of cleaved caspase-3 IR cells in the PFC (Figure 1.2) is consistent with previous studies that show NMDA antagonist induced cell death in other brain regions (Harris et al., 2003; Ikonomidou et al., 1999; Lema Tome et al., 2006; Wang and Johnson, 2007). In their groundbreaking work, Ikonomidou et al demonstrated by TUNEL staining that P7 dizocilpine (0.5-1.0mg/kg, i.p., 1 injection every 8 hours, 3 total injections) robustly increases the number of degenerating neurons in thalamic, hypothalamic, hippocampal,

parietal, retrosplenial, cingulate, and frontal layers II and IV, with 2-22 fold increase in the number degenerating neurons in frontal and cingulate regions (Ikonomidou et al., 1999). This study, however, did not differentiate between different frontal cortical regions. Lema Tome et al identified this observation in the somatosensory cortex, with one subcutaneous injection of dizocilpine (1mg/kg) on P7 increasing the number of cleaved caspase-3 IR cells by 20 fold, 16 hours after the injection (Lema Tome et al., 2006). Cleaved caspase-3 IR is a putative marker for dying cells (Krajewska et al., 1997). Olney et al found that the pattern of cleaved caspase-3 IR closely corresponds to the pattern of argyrophilic neurodegeneration following P7 dizocilpine treatment in rodents (Olney et al., 2002b). Wang et al showed that following 1 injection of the NMDA antagonist PCP (1, 3, or 10 mg/kg), cleaved caspase-3 IR was found to co-localize with TUNEL positive neurons up to nine hours after the injection (Wang and Johnson, 2007). Broad inhibition of caspases reduces dizocilpine-induced cell death in neuronal cultures by 60-80% (Yoon et al., 2003). Thus, cleaved caspase-3 likely identifies cells undergoing cell death in this paradigm.

Though it is clear that many neurons are dying following P7 NMDA antagonism, it was previously unknown which neurons are vulnerable. We have extended our studies into this area, and show that some of the PFC neurons expressing cleaved caspase-3 also express GAD67 (Figure 1.3), a marker for GABAergic interneurons. GAD67 is expressed prior to P7 (Kiser et al., 1998; Tamamaki et al., 2003), and neurons expressing GAD67 on P7 mature into various GABAergic interneurons e.g. PV, CR, and somatostatin (Tamamaki et al., 2003). Interestingly, Wang et al found almost no co-localization of the cell death markers cleaved caspase-3 or TUNEL with GABAergic interneuron markers CB or CR in dorsal subiculum, retrosplenial cortex, motor cortex, cingulate, hippocampus, or somatosensory

cortex 16 hours after injection on P7 with PCP (10 mg/kg) (Wang et al., 2008). In this study they did not study parvalbumin co-localization with cleaved caspase-3 due to its low expression on P7. Likewise, Lema Tome et al found very little co-localization of cleaved caspase-3 with PV, CB, or CR in different brain regions following P7 dizocilpine (Lema Tome et al., 2006). In fact, developmental calcium binding protein expression coincided with a decline in dizocilpine induced caspase-3 cleavage and the number of cortical neurons expressing CB and PV increased substantially from P7 to P21 (10 fold and 60 fold respectively). Therefore, GAD67 is probably a better marker for identifying dying GABAergic interneurons during early postnatal life. We demonstrate for the first time that P7 dizocilpine treatment causes a robust increase in cleaved caspase-3 IR in the PFC, including some that are GABAergic interneurons.

In adult animals we found a striking, persistent reduction in PV GABAergic interneurons and layer V pyramidal neurons in PFC following P7 treatment with dizocilpine. The density of adult PV interneurons and layer V pyramidal neurons was reduced by 45% and 43% respectively (Figure 1.5). Wang et al showed persistent reductions in PV interneurons in the somatosensory (63%), motor (36%), and retrosplenial (21%) cortices, with no measureable reductions in the striatum, hippocampus, or cingulate in young adult rats (P56) following one P7 injection of PCP (10 mg/kg) (Wang et al., 2008). Our studies, however, show a robust (43%) reduction in PV interneurons in the anterior cingulate (Figure 1.5). A possible reason for this difference is that Wang et al used saggittal sections so that their investigation spanned the entire antero-posterior length of the cingulate (i.e., bregma +3.7 to -1.4 in the rat). In our studies, however, we used coronal sections and only measured PV neurons in the anterior cingulate region associated with the PFC (i.e., bregma +1.98 to

+1.10 in the mouse). Previous studies have not investigated the effect of P7 NMDA antagonism on layer V pyramidal neuron numbers. The use of the YFP mouse allowed us to investigate these important neurons and we found a 45% reduction in adult PFC. In the rodent PFC parvalbumin identifies wide arbor basket and chandelier interneurons (Conde et al., 1994; Gabbott and Bacon, 1996) which converge onto pyramidal neurons in both layers III and V modulate their activity patterns. Layer V pyramidal neurons represent the major glutamatergic projections from the PFC to contralateral cortex, striatum, subcortical structures and posteromedial thalamus (Hattox and Nelson, 2007; Molnar and Cheung, 2006). Layer V pyramidal neurons also send reciprocal projections to the medial dorsal thalamus (though layer III pyramidal neurons receive the majority of medial dorsal thalamic input) (Kuroda et al., 1998). Thus, the reduction of these neurons that we observed could result in dysregulation of PFC functions including cognition and the control of impulsivity.

The findings of persistent reductions in PV interneurons and layer V pyramidal neurons in PFC may also be pertinent for human cognitive disorders. Deficits in PV interneurons in the prefrontal cortex have been found in postmortem tissue in patients with schizophrenia (Beasley and Reynolds, 1997) and major depressive disorder (Rajkowska et al., 2007). A recent study has shown a reduction in the density of layer III and V calmodulin (+) pyramidal neurons in the postmortem human schizophrenic PFC (Broadbelt and Jones, 2008). Thus, the persistent reduction in PV interneurons and layer V pyramidal neurons we observed in adults following P7 dizocilpine treatment reflects the neuropathology found in some mental diseases.

Consistent with this line of reasoning, we observed persistent behavioral changes in adults as seen by reduced exploration of the center in the open field test following P7

dizocilpine. Reduced center time in the open field, or thigmotaxis, is a standard index of non-conditioned anxiety-like behavior, as high anxiety animals spend less time in the center (Belzung and Griebel, 2001; Crawley, 1999; Heisler et al., 1998). This anxiety-like behavior is reversed by anti-anxiety drugs that do not impair overall locomotor activity (Hoplight et al., 2005; Simon et al., 1994; Treit and Fundytus, 1988). We observed that mice treated with dizocilpine on P7 spent about half the time in the center of the open field apparatus as compared to control animals (Figure 1.8). This is similar to the reduced center time reported for high-anxiety transgenic mice lacking functional serotonin-1A receptors (Heisler et al., 1998). Thus, our findings suggest that early postnatal NMDA antagonists induce persistent adult anxiety.

Anxiety is a complex behavioral phenotype, but, given clinical and animal observations, anxiety is probably related to impulsivity. Heightened anxiety is a common comorbid feature of several psychiatric conditions displayed reduced impulsive control such as attention deficit hyperactivity disorder (ADHD) (Bowen et al., 2008; Schatz and Rostain, 2006), schizophrenia (Braga et al., 2005), and alcohol dependence (Brady and Lydiard, 1993). Rodent studies also suggest an association between anxiety and impulsivity. Thiebot demonstrated that serotonin uptake inhibitors, modern anxiolytic drugs, reduce the choice of rats for a small reward rather than a larger delayed reward by nearly 40% (i.e., they reduce impulsivity) (Thiebot et al., 1985), while benzodiazepines had the opposite effect. More recent studies showed that 5-HT_{1A} agonism and 5-HT_{2A} antagonism, which are modern anxiolytic approaches, reduce anticipatory and perseverative responses in the 5-CSRT (i.e., reduced impulsivity) to control levels following enhancement of impulsive behavior by acute NMDA antagonism directly into the PFC of adults (Carli et al., 2006; Mirjana et al., 2004).

These studies suggest that anxiety and impulsivity might be directly related. Further, it has been theorized that impulsive behavior may be in part due to an imbalance between the impulsive drive from the amygdala and the inhibitory response from the PFC (Bechara, 2005). The PFC is also considered to counteract "pro-anxiety" drives coming from the amygdala by promoting swift recovery from negative emotional stimuli and inhibiting output from the amygdala (Davidson, 2002). Thus anxiety and impulsivity may both prove to be parallel features of imbalanced PFC-amygdala interactions. Therefore, our observation of heightened anxiety-like behavior in adults pretreated with dizocilpine on P7 suggests that this treatment might also increase impulsive behaviors.

Though other studies have not looked at anxiety-like behavior in adults following early postnatal NMDA antagonism, other behaviors associated with PFC function have been found to be investigated. For example, Stefani and Moghaddam found that young adult rats (P60) treated postnatally with dizocilpine for four days (P7-P10) made fewer correct choices in a four arm maze following a change in the cue associated with the reward from brightness to texture (Stefani and Moghaddam, 2005). This ability to respond to a shift in the perceptual dimension of a cue associated with a reward (such as brightness to texture) has been shown to require proper function of medial regions of the PFC in rats (Birrell and Brown, 2000). To demonstrate this, adult rats were first trained to find a reward hidden in a bowl by associating a defined odor with the correct bowl. Once they had learned successfully, the cue associated with the correct bowl was changed from odor to texture. Rats with medial PFC lesions learned the first association (i.e., with an odor) equally as well as controls, and they also performed equally as well when the quality of the odor was changed. However, lesioned rats required 40% more trials to successfully reach criterion once the cue associated with the

reward was changed from odor to texture. In studies investigating the role of PFC in impulsivity, adult rats treated with the NMDA antagonist CPP (50ng/μl) administered directly into the adult PFC made 4 times as many anticipatory responses and three times as many perseverative responses in the 5-Choice Serial Reaction Time task (5-CSRT) than controls, signifying increased impulsive behavior (Baviera et al., 2008; Mirjana et al., 2004). Thus, NMDA antagonism both during postnatal life as well as adulthood can alter PFC behaviors associated with cognitive function and impulsivity.

We found no disruption in PPI in adult animals following P7 dizocilpine (Figure 1.9). Pre-pulse inhibition is a measure of sensorimotor gating, which is primarily a pontine reflex, and modulated by several brain regions e.g. PFC, hippocampus, thalamus and others (Caine et al., 1992; Davis et al., 1982; Fendt et al., 2001; Schwabe and Koch, 2004). A similar inability of PCP on P7 to produce later deficits in PPI in animals (P25) has been shown previously (Anastasio and Johnson, 2008). Harris et al showed that two injections of dizocilpine (0.5 mg/ml) on P7 caused a disruption in PPI in adult female rats only (55%), while males were unaffected. Since PPI is primarily a brain stem reflex, the absence of a disruption of PPI in our study may be due to insufficient damage to either brain stem nuclei or other regions as a result of this insult (Wang et al., 2008). This idea is supported by the fact that repeated NMDA antagonist treatment regimens do disrupt PPI in older animals (e.g. PCP (10 mg/kg) on P7, P9, and P11 causes a 55% reduction in PPI on P25 (Wang et al., 2001) and CGP on P1, P3, P6, P9, P12, P15, P18, and P21causes a 74% reduction in PPI on P60 (Wedzony et al., 2008)). Thus, the inability of one day of dizocilpine treatment on P7 to disrupt PPI in adults may be due to the lack of damage to the pontine nucleus accompanied by sufficient accommodation from other brain regions to account for the damage to the PFC.

This study is the first to show that NMDA antagonism with dizocilpine on P7 causes cleavage of caspase-3 in both GABAergic and non GABAergic neurons in the PFC. This is associated with persistent reductions of approximately 45% PV GABAergic interneurons and layer V pyramidal neurons in PFC as well as a 50% reduction in center exploration in the open field test. The PFC cellular losses and anxiety-like behavior suggest that this early postnatal insult might result in increased impulsivity in adulthood. Future studies will directly investigate the effects of the loss of these PFC neurons on impulsive behavioral phenotypes.

Persistent effects of P7 ethanol treatment on adult mouse brain: reduced brain volume, frontal cortical neuron reductions and altered adult hippocampal neurogenesis.

Abstract

Ethanol treatment on postnatal day seven (P7) causes a robust enhancement of physiological cell death in multiple brain regions. This is considered a model of fetal alcohol spectrum disorders (FASD), since P7 in rodents is comparable to the late third trimester in humans. In order to investigate the long-term effects of P7 ethanol treatment on adult brain, mice received two doses of ethanol on P7 (2.5g/kg, s.c., 2 hours apart) and were assessed as adults (P82) for brain volume (using postmortem MRI) and cellular architecture (using immunohistochemistry). Adult mice that received P7 ethanol had reduced total brain volume (4%) with several brain regions being effected in both males and females. Reductions in frontal cortical parvalbumin (PV) interneurons (18-33%) and cux1+ layer II pyramidal neurons (15%) were observed in both sexes using immunohistochemistry. Interestingly, differences in adult hippocampal neurogenesis were observed between genders. Males were found to have increased doublecortin and Ki67 expression (52 and 57% respectively) in the dentate gyrus, consistent with increased neurogenesis. These findings suggest that P7 ethanol treatment causes reductions in adult brain volume and frontal cortical neuron numbers. These findings also suggest that there may be differences in adult neurogenesis between males and females that received P7 ethanol. Thus, P7 ethanol causes deficits that persist into adulthood.

Introduction

Fetal alcohol spectrum disorders (FASD) is a group of conditions in which *in utero* ethanol exposure causes persistent cognitive and behavioral disturbances with or without craniofacial abnormalities (Barr and Streissguth, 2001; Mattson et al., 1997). Brain dysfunction can include IQ reductions, hyperactivity, learning deficits and epilepsy and seizures (Bell et al., ; Kodituwakku, 2007; Mattson and Riley, 1998). FASD is common, with one study estimating that the prevalence of FASD in the US may be as high as 2-5% (May et al., 2009). Since the prevalence of this disorder is high, and the complications can be severe, it is important to understand the neurostructural deficits associated with FASD. Postnatal day 7 in rodents is analogous to the late third trimester or birth in humans. Thus, ethanol treatment on this age is a model of FASD.

Ethanol causes cell death similar to that of MK801 on P7, enhancing PCD (Ikonomidou et al., 2000). We treated mice on P7 as described previously (2 injections of 2.5 g/kg ethanol two hours apart) (Ikonomidou et al., 2000). This treatment regimen produces blood alcohol levels that are above 200 mg/dl, which is a threshold to produce pronounced cell death on P7 (Ikonomidou et al., 2000). It is not known whether *in utero* ethanol treatment has differential long-term effects on males and females. Estrogens are generally considered to be neuroprotective (Gibbs, 1999; Levi and Brimble, 2004), though, repeated injections of estradiol can cause reductions in adult neurogenesis (Barker and Galea, 2008). Thus, it is possible that there are gender-specific differences in the effect of P7 ethanol on the adult brain. Ikonomidou et al investigated the acute effects of ethanol after P7 treatment, which is prior to gonadal maturation. We investigated the effects of P7 ethanol on

the adult brain in both males and females which provided information about the effects of ethanol on the specific genders.

P7 ethanol treatment was found to cause a persistent reduction in adult brain volume. This was associated with a reduction in frontal cortical parvalbumin interneurons and layer II medial prefrontal pyramidal neurons. P7 ethanol treatment resulted in reduced hippocampal volume in adult females, but not males. Interestingly, adult males that received P7 ethanol showed increased adult hippocampal neurogenesis, evidenced by increased doublecortin immunoreactivity and Ki67 immunolabeled cells in the dentate gyrus. This shows clearly that P7 ethanol treatment results in deficits that persist into adulthood. These findings suggest that maternal ethanol consumption during the third trimester may have long-term effects on brain volume and cellular architecture.

Methods

Animal Treatment

Pregnant C57BL/6 mothers were ordered from Charles River (Raleigh, NC). Offspring were treated as shown in Figure 2.1. Pups were given two injections of ethanol (2.5g/kg, i.p.) two hours apart on P7.

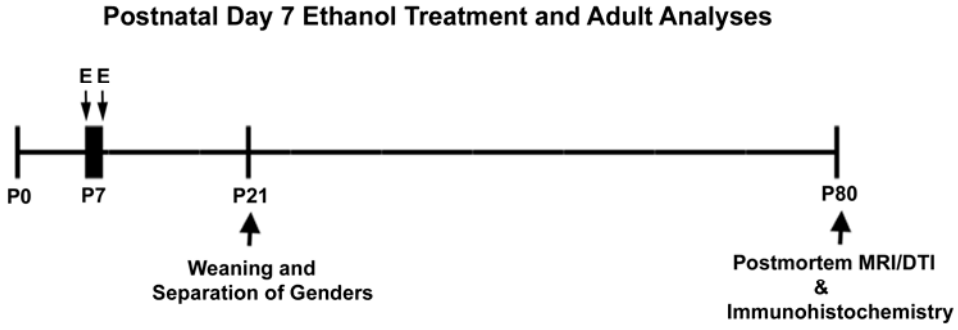

Figure 2.1 P7 ethanol treatment with adult (P80) investigation. Mice were treated with 2 ethanol treatments (2.5g/kg, i.p.) two hours apart on P7. Postmortem brain imaging and immunohistochemistry were performed in adulthood (P80).

This did not cause a statistically significant difference in weight through P22 (not shown). Mice were weaned and separated by gender on P21. Mice were sacrificed by perfusion with 4% paraformaldehyde as adults on P80 for postmortem brain imaging and immunohistochemistry as described previously (Coleman et al., 2009; Qin et al., 2007).

Adult postmortem MRI brain imaging

Postmortem brain DTI was performed as described previously (Coleman Jr et al., 2009). Whole mouse skulls were scanned at the UNC Biomedical Research Imaging Center (BRIC). DTI images (0.12mm x 0.12mm x 0.12mm) were acquired using the following diffusion weighted 3D RARE sequence: TR=0.7s, TE_{eff} =23.662ms, Rare Factor = 3, RARE echo spacing = 11.3067ms, diffusion gradient time δ=6ms, diffusion gradient separation Δ = 12.422, b value – 1000s/mm^2, matrix size = 200x125x80, FOV=24.0mm x 15mm x 9.6mm. Mean diffusivity images were computed from reconstructed diffusion tensor data and were segmented for volumetric, fractional anisotropic, and mean diffusivity analyses. Brain regions were segmented automatically using a previously established method (Lee et al., 2009a). Segmentation errors were corrected manually by blinded investigators. Brain regional boundaries were determined using the Brookhaven National Library 3-D MRI Digital Atlas Database of the adult C57BL/6 mouse (www.bnl.gov/medical/RCIBI/mouse).

Immunohistochemistry

Immunohistochemical analysis was performed as described previously (Coleman et al., 2009; Crews et al., 2004). Up to six sections (40μm) per mouse were incubated with 0.6% H_2O_2 for 30 minutes to remove endogenous peroxidase activity. After washes, sections

were incubated with one of the following primary antibodies: Parvalbumin (1:1000, overnight, Sigma), Doublecortin (1:400, 48hr, Santa Cruz Biotechnology), Ki67 (1:200, 48hr, Vector Labs). Immunoreactive neurons or pixels per area were counted using Bioquant Image Analysis Software as described (Coleman et al., 2009; Crews et al., 2004).

MRI brain structural volume statistics: For brain structural volume data, Student *t*-tests were performed on whole brain volume comparisons. For brain regional assessments, *t*-tests followed by a false discovery rate (FDR) analysis were employed to ascertain statistical significance while accounting for type II errors that may be generated during multiple comparisons. The FDR method reports a *q*-value, which is used to calculate the number of false positives expected. The *q* values were calculated using the *Q-value* module in the *R for Windows Software* © R Development Core Team 1995-2009. The following formula was then used to determine the chance of detecting a false positives: likelihood of a false positive = q_{target} x (# of regions with $q_{calculated} \leq q_{target}$)/number of tests. The threshold for significance was set such that the likelihood of detecting a false positive would be less than 0.025. For this data set, this corresponded to a *q*-value < 0.032.

Immunohistochemistry statistics: A Student's *t*-test or 2-way ANOVA was employed to determine statistical significance. A *p*-value less than 0.05 was considered significant.

Results

P7 Ethanol treatment results in global reductions in adult brain volume

Ethanol treatment on P7 is known to cause cell death in multiple brain regions (Ikonomidou et al., 2000). We assessed the persistent effects of this treatment on total brain volume using structural DTI brain images. Adult mice (P80) that received P7 ethanol treatment showed approximately a 5% reduction in total brain volume when compared to litter-matched controls (Figure 2.2B). This reduction in total brain volume was seen in both males and females (4.4%, $p<0.007$ and 5.95%, $p< 0.0001$ respectively; data not shown). Since there were no significant differences in total brain volume between males and females, both sexes were grouped in Figure 2.2.

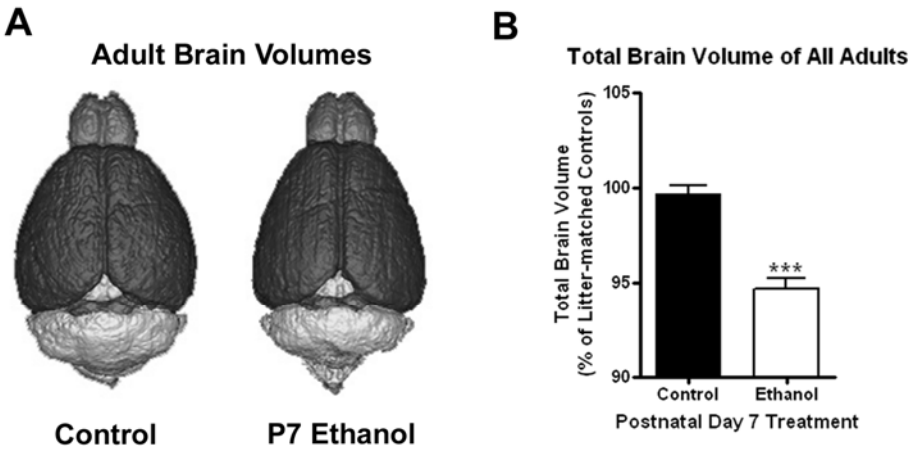

Figure 2.2 Reduction in adult total brain volume following P7 ethanol. (A) 3D Renderings of adult subjects that received either control or ethanol on P7. Note the global reductions in brain volume. (B) Adult brain volumes of all subjects. Adult mice that received P7 ethanol treatment showed approximately a 5% reduction in total brain volume when compared to litter-matched controls (***p<0.0001).

This reduction in adult brain volume caused by P7 ethanol treatment occurred in several specific brain regions. Brain volumes were normalized to the average volume of litter-matched control groups to account for variation across litters. When volumes from all

subjects were pooled (i.e., both males and females), all brain regions assessed showed statistically significant reductions, except for the inferior colliculi (Table 2.1). Fourteen of these regions showed significant volume reductions ranging from 4.09% to 6.92% (*p<0.05, **p<0.01, ***p<0.001 by t-test and †q<0.03, FDR). Though the volumes of several brain regions were reduced, the percentage of the total volume of each region was unchanged by P7 ethanol treatment (Tables 2.2 and 2.3), suggesting global changes in volume due to ethanol treatment.

Table 2.1: Regional brain volumes assessment (all subjects)

Region	% Difference	p-value (t-test)	q-value (FDR)
Neocortex	- 6.37	0.0003***	0.001†
Hypothalamus	- 6.92	0.0003***	0.001†
Amygdala	- 6.33	0.0005***	0.001†
Hippocampus	- 4.75	0.0010**	0.001†
Caudate & Putamen	- 4.40	0.0010**	0.001†
Basal Fore Brain & Septum	- 6.62	0.0011**	0.001†
Thalamus	- 4.28	0.0019**	0.002†
Internal capsule	- 5.63	0.0023**	0.002†
GP	- 4.30	0.0026**	0.002†
Central Gray	- 4.09	0.0035**	0.002†
Rest of Midbrain	- 4.44	0.0052**	0.003†
Superior Colliculi	- 4.17	0.0074**	0.004†
Corpus Callosum/Ext Capsule	- 4.40	0.0078**	0.004†
Fimbria	- 4.82	0.0116*	0.006†
Brain Stem	- 5.95	0.0300*	0.015
Cerebellum	- 3.85	0.0589	0.028
Olfactory Bulb	- 4.98	0.2260	0.100
Inferior colliculi	+0.26	0.9486	0.396

Post-hoc analyses revealed that the variances in the volumes of some regions were different between males and females. For instance, the internal capsule was smaller in ethanol treated males (Table 2.2; p<0.0036) but not in females (Table 2.3, p=0.09). Seven brain regions showed strong significant reductions in females but not males. However, the magnitudes of the volume changes were similar in both sexes (Tables 2.2 and 2.3). This may be due to differences in the sample sizes between males (N=4 control, 6 ethanol) and females (N=7

control, 9 ethanol). However, it is still possible that certain regions, such as the hippocampus, may have been differentially affected between males and females. A power analysis revealed that in order for males to reach the same level of statistical significance as the females for the hippocampus, (which had N=7 control and 9 ethanol), a sample size of 21 control and 21 ethanol treated male animals would be needed. This suggests that the volume of the adult hippocampus could truly be more affected in females than males. However, more animals would be needed in order to confirm this possibility.

Table 2.2 Regional brain volume changes in males

Region	Control V (mm^3)	% total	Ethanol V(mm^3)	%total
Hippocampus	24.3	5.5	23.6	5.6
CC & External capsule	12.9	2.9	12.5	2.9
Caudate & Putamen	24.8	5.6	24.3	5.7
AC	1.2	0.3	1.2	0.3
GP	3.0	0.7	3.0	0.7
Internal capsule	2.2	0.5	2.1 **	0.5
Thalamus	24.7	5.6	24.3	5.7
Cerebellum	54.0	12.2	52.3 **	12.3
Superior Colliculi	7.9	1.8	7.7	1.8
Ventricle	1.5	0.3	1.4	0.3
Hypothalamus	11.9	2.7	11.3 **	2.7
Inferior colliculi	5.4	1.2	5.3	1.2
Central Gray	4.2	0.9	4.2	1.0
Neocortex	144.7	32.7	140.5 0.053	33.2
Amygdala	12.8	2.9	12.1 **	2.8
Olfactory Bulb	27.0	6.1	24.0	5.7
Brain Stem	49.7	11.2	48.1	11.4
Rest of Midbrain	12.2	2.8	11.9	2.8
Basal Fore Brain & Septum	12.6	2.9	12.1	2.9
Fimbria	2.2	0.5	2.1	0.5

Table 2.3 Regional brain volume changes in females				
Region	Control V (mm^3)	% total	Ethanol V (mm^3)	%total
Hippocampus	25.4	5.6	23.8 **	5.6
CC & External capsule	13.5	3.0	12.8	3.0
Caudate & Putamen	26.1	5.8	24.6 **	5.8
AC	1.2	0.3	1.2	0.3
GP	3.2	0.7	3.0 **	0.7
Internal capsule	2.3	0.5	2.1	0.5
Thalamus	26.0	5.8	24.4 **	5.7
Cerebellum	55.3	12.3	53.3	12.5
Superior Colliculi	8.4	1.9	8.0 **	1.9
Ventricle	1.6	0.3	1.5	0.3
Hypothalamus	12.6	2.8	11.5 **	2.7
Inferior colliculi	5.3	1.2	5.4	1.3
Central Gray	4.4	1.0	4.2 **	1.0
Neocortex	147.9	32.8	135.9 **	31.9
Amygdala	13.1	2.9	12.2 **	2.9
Olfactory Bulb	26.9	6.0	26.7	6.3
Brain Stem	52.2	11.6	48.2	11.3
Rest of Midbrain	12.9	2.9	12.1 **	2.9
Basal Fore Brain & Septum	13.1	2.9	12.1 **	2.8
Fimbria	2.3	0.5	2.1	0.5

P7 Ethanol treatment results in a reduction in the number of parvalbumin positive interneurons and layer II pyramidal neurons in the adult frontal cortex.

It is known that postnatal ethanol (between P2 and P21) causes robust cell death throughout the brain with the damage to the frontal cortex peaking on P7 (Ikonomidou et al., 2000). We have found previously that P7 dizocilpine treatment, which mimics P7 ethanol neurotoxicity, resulted in persistent reductions in adult parvalbumin interneurons in the frontal cortex (Coleman et al., 2009). Also, we found that P7 ethanol caused a reduction in the volume of the neocortex in adulthood. Therefore, we investigated whether P7 ethanol treatment results in a persistent reduction in cortical parvalbumin interneurons focusing within the frontal cortex. Immunohistochemical staining showed visible reductions of PV+IR neurons in the frontal cortex (Figure 2.3A). Parvalbumin interneuron staining was

reduced in both M2 frontal motor cortex (Figure 2.3B, 31%, ***p<0.001) and the medial prefrontal cortex (Figure 2.3C, 19%, *p<0.02 2-way ANOVA).

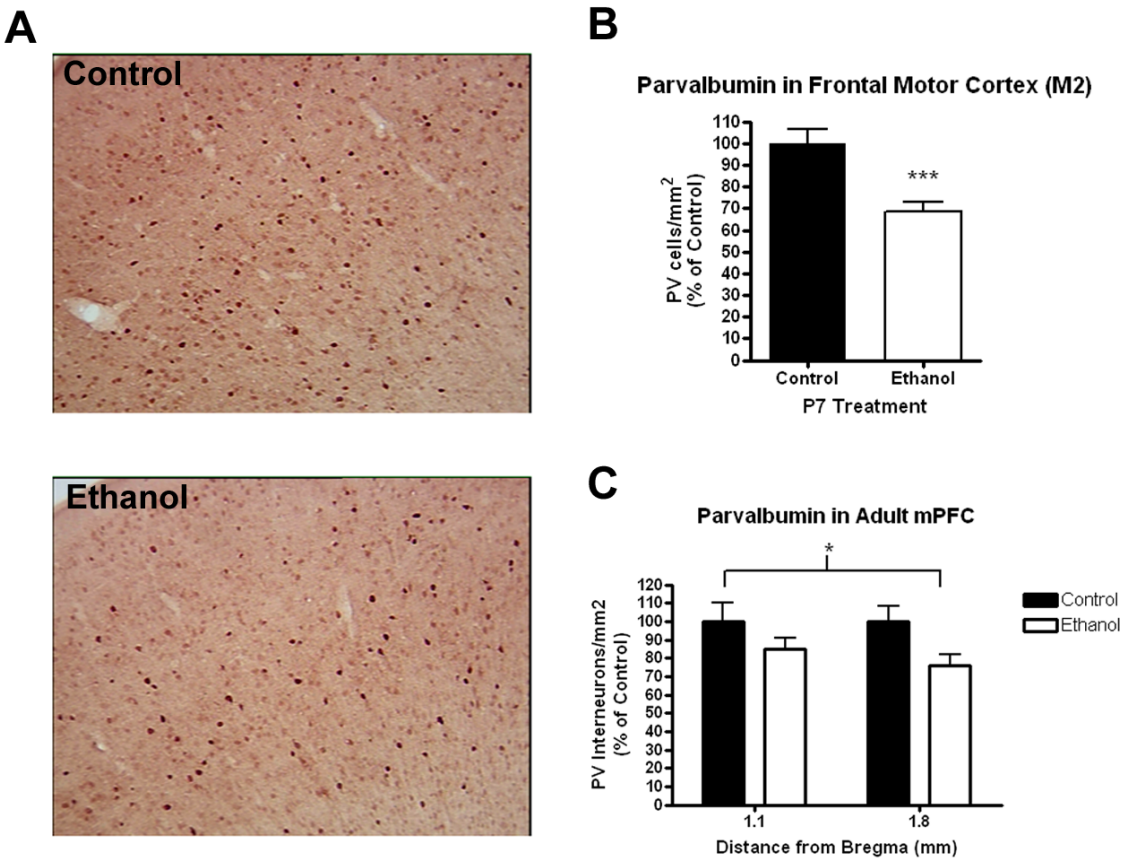

Figure 2.3: Reduction of parvalbumin interneurons in the adult frontal cortex following P7 ethanol treatment. Mice were given either saline or ethanol (2.5g/kg, i.p.) two times, two hours apart on P7. Both sexes were pooled. (A) Representative images of PV+IR staining in the M2 region of the frontal cortex. Visible reductions in PV+IR are seen. (B) Significant reduction in PV+IR neuron density in the frontal M2 motor cortex (31%, ***p<0.001). (C) Significant reduction in PV+IR neuron density in the medial prefrontal cortex 19% *p<0.02, 2-way ANOVA.

MRI volume investigation revealed that P7 ethanol caused a reduction in the corpus callosum in adults (Table 2.1). Therefore, we examined whether layer II callosal projection neurons were persistently reduced as a result of P7 ethanol treatment. We performed cux1 immunohistochemistry, to identify layer II pyramidal neurons. There was a visible reduction in cux1 immunoreactive cells in the medial prefrontal cortex (Figure 2.4A). Quantification revealed approximately a 15% reduction in the density of cux1 cells (Figure 2.4B). Both

male and female adults showed similar reductions. Interestingly, there were no reductions in cux1 pyramidal neurons seen in the M2 frontal motor cortex (p=0.98, data not shown). This suggests that mPFC layer II pyramidal neurons are vulnerable to ethanol neurotoxicity on P7.

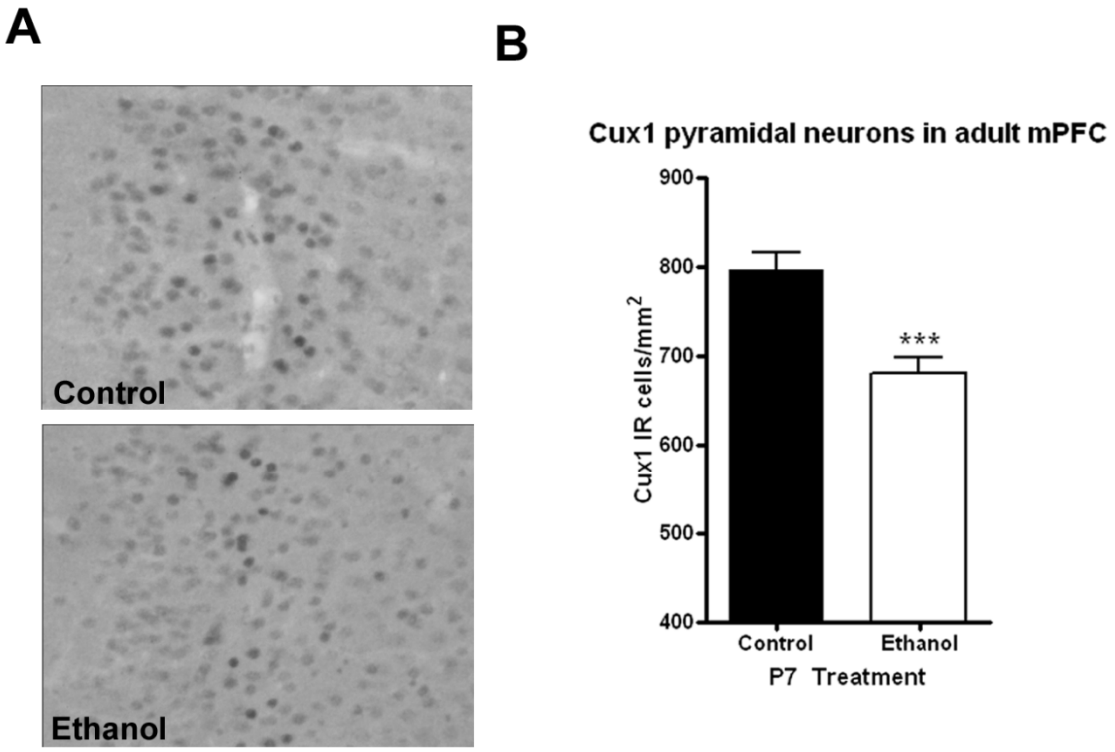

Figure 2.4 P7 ethanol reduces cux1 labeled layer II pyramidal neurons in the medial prefrontal cortex (mPFC). Adult mice that received ethanol (2.5g/kg, i.p. twice, two hours apart) showed fewer cux1 immunopositive neurons in the mPFC (A) Images showing fewer cux1 layer II pyramidal neurons in the mPFC (B) Quantification of cux1 layer II pyramidal neurons in the mPFC showed approximately a 15% significant reduction in adult mice that received P7 ethanol (***p<0.001, N=8 control, 9 ethanol).

P7 Ethanol results in increased neurogenesis in males but not females

We have found previously that alcohol can alter neurogenesis in adult males causing an initial reduction in neurogenesis followed by a compensatory increase in neurogenesis up to 14 days after the end of alcohol treatment (Nixon and Crews, 2004). Using doublecortin (DCX) immunohistochemistry, we investigated whether P7 ethanol altered adult neurogenesis. DCX+IR was visibly increased in adult mice that received P7 ethanol (Figure 2.5A). There was an increase in adult doublecortin immunoreactivity in mice that received

P7 ethanol (30% increase) when values from both sexes were combined ($p<0.04$, data not shown). However, when the data from the sexes was separated, it became clear that this robust increase in adult neurogenesis following P7 ethanol only occurred in males.

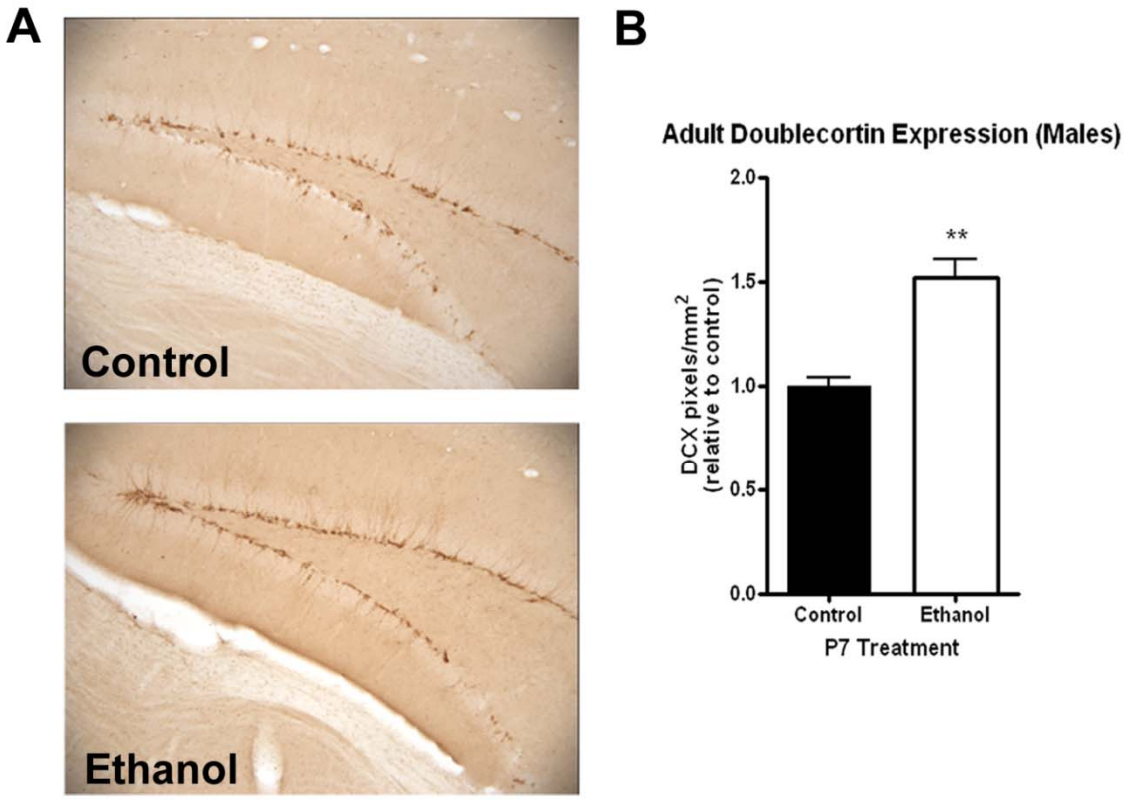

Figure 2.5 P7 ethanol alters neurogenesis in adult males. Males that received ethanol (2.5g/kg, i.p. twice, two hours apart) showed an increase doublecortin (DCX) expression in the dentate gyrus. (A) Representative images showing increased DCX expression (B) Quantification of DCX-IR pixels shows a 52% increase in dentate gyrus DCX expression (**p<0.004). N=4 control, 6 ethanol

When quantified, a 52% increase in DCX expression per area in male adult mice that received P7 ethanol was found (Figure 2.5B). There was no difference in the area of dentate gyrus assessed (p=0.22, not shown). In order to gain insight into whether this difference was a result of increased cell proliferation, we performed immunohistochemical staining for Ki67, a marker of cell proliferation. An increase in Ki67+cells was observed (Figure 2.6A).

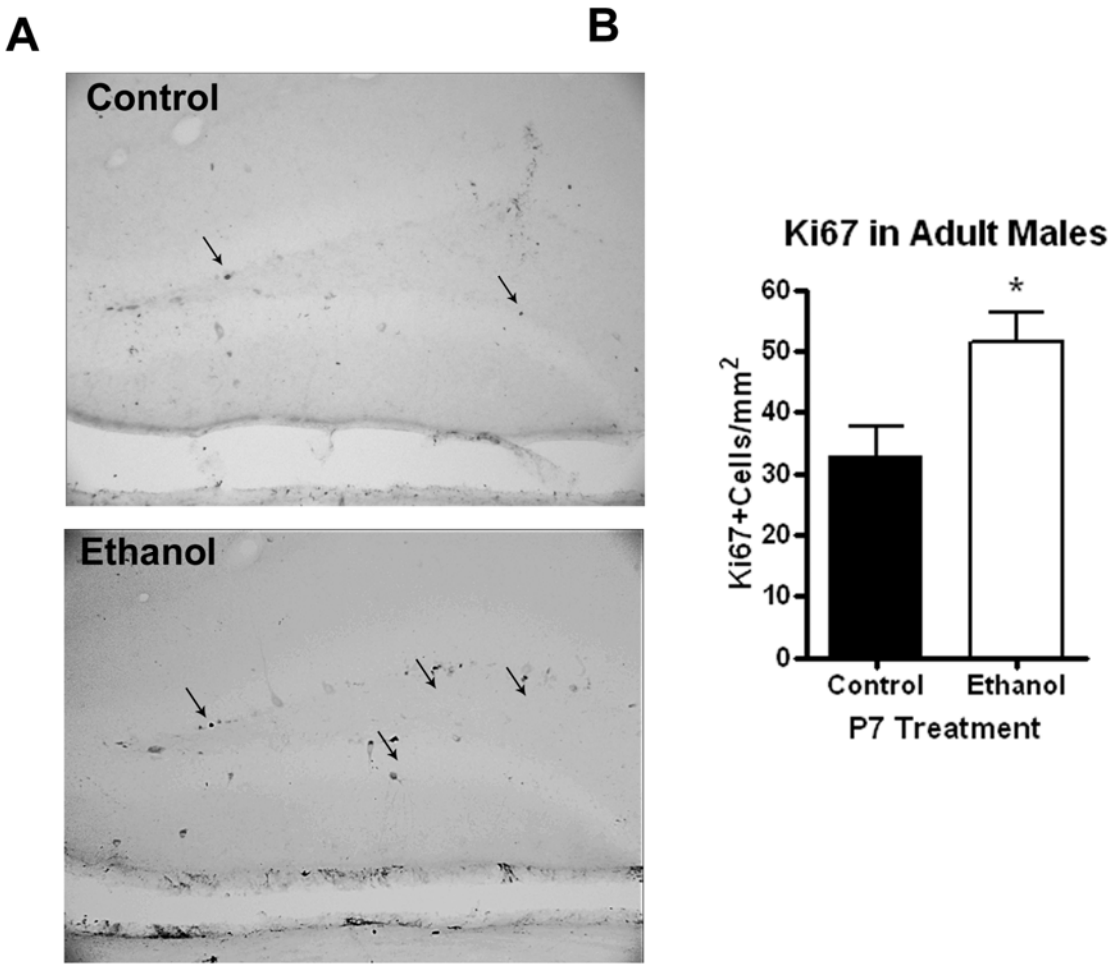

Figure 2.6 P7 ethanol alters cell proliferation in adult males. Males that received ethanol (2.5g/kg, i.p. twice, two hours apart) showed an increase Ki67 expression in the dentate gyrus. (A) Representative images showing increased ki67 expression. Arrows highlight Ki67+cells (B) Quantification of ki67 cells per area showed a 57% increase in dentate gyrus Ki67 expression (**p<0.004). N=4 control, 6 ethanol

Quantification of Ki67+IR revealed that adult males that were given ethanol on P7 showed a 57% increase in Ki67+cells per area (Figure 2.6B). This increase in cell proliferation is consistent with the observed increase in DCX+IR immature neurons in the dentate gyrus. Interestingly, there was no difference in DCX staining in adult female groups.

Postnatal day 7 ethanol treatment did not result in a change in DCX expression in the dentate gyrus of adult females (Figure 2.7). There was no difference in the dentate areas

measured between both groups (not shown). This is clearly different than our observations in adult males that received ethanol treatment on P7.

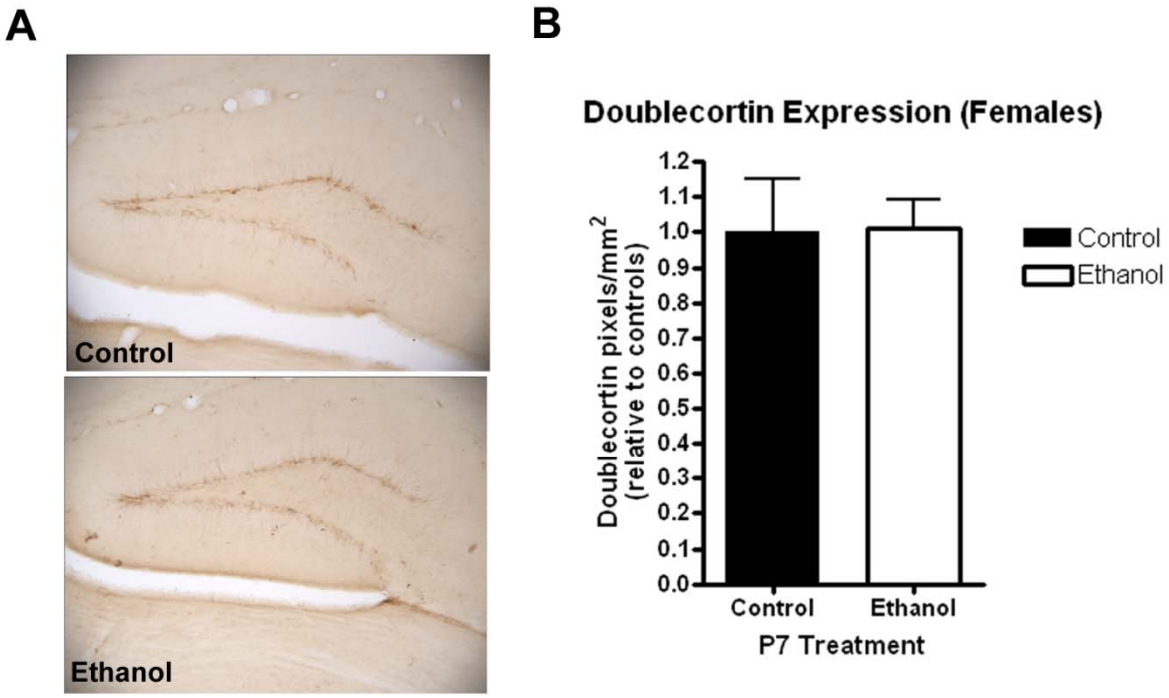

Figure 2.7 P7 ethanol does not alter neurogenesis in adult females. Females that received ethanol (2.5g/kg, i.p. twice, two hours apart) showed no change in doublecortin (DCX) expression in the dentate gyrus. (A) Representative images showing similiar DCX expression (B) Quantification of DCX-IR pixels no change in dentate gyrus DCX expression ($p<0.95$). N=6 control, 6 ethanol.

Ki67 expression was visualized in the dentate gyrus using immunohistochemistry (Figure 2.8A). Consistent with DCX measurements in adult females, there were no changes in Ki67 expression in adult females regardless of P7 ethanol treatment. Quantification revealed similar numbers of Ki67+ neurons in both adult females groups (Figure 2.8B).

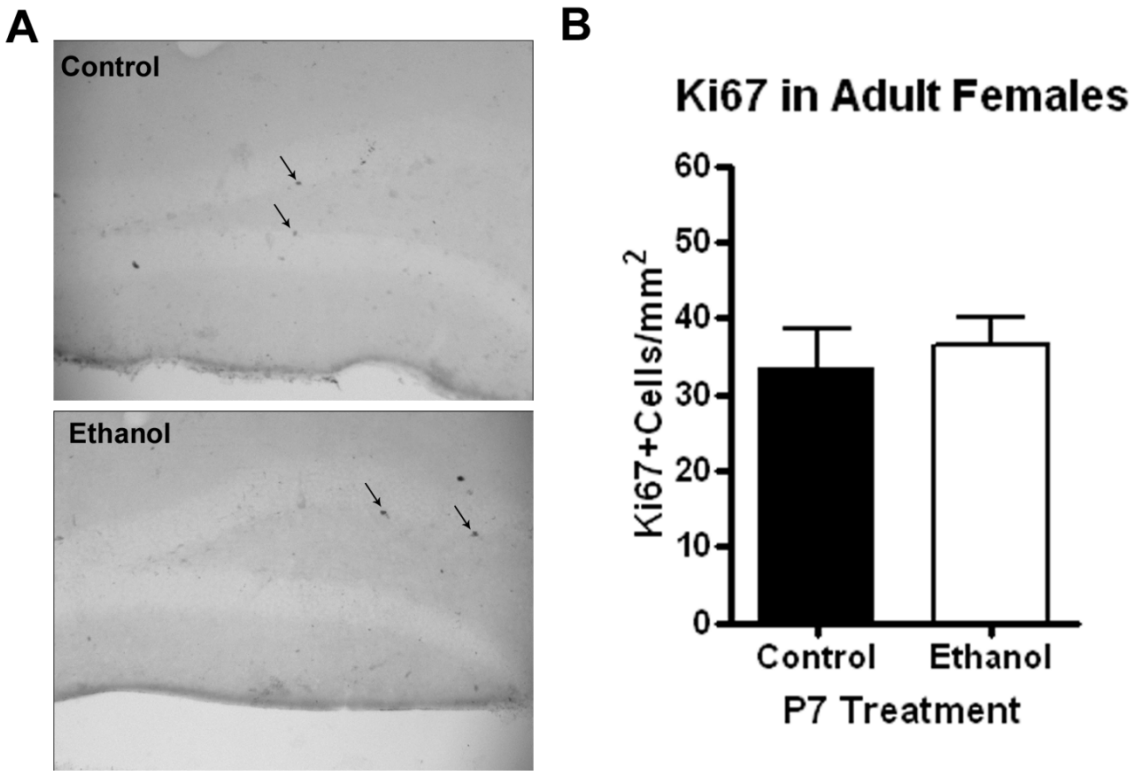

Figure 2.8 P7 ethanol does not alter cell proliferation in adult females. Females that received ethanol (2.5g/kg, i.p. twice, two hours apart) showed no change in Ki67 expression in the dentate gyrus. (A) Representative images showing similiar Ki67 expression in both groups (B) Quantification of ki67 cells per area showed a similiar density of Ki67 cells in both treatment groups. N=5 control, 6 ethanol

Discussion

The developing brain is sensitive to ethanol neurotoxicity during the early postnatal period. We found a reduction in total brain volume in adult mice that received P7 ethanol. This reduction involved several brain regions in both sexes. Human brain imaging studies have found reductions in total brain volume as well as specific brain regional volume reductions in humans with FASD (for review see (Norman et al., 2009)). In humans, several brain regions including the cortex, corpus callosum, caudate, cerebellum and hippocampus

have been found to have volume reductions. Therefore, our observations in mice using structural brain imaging are consistent with observations in human imaging studies.

Several studies have demonstrated neuron death acutely after this alcohol treatment (Ikonomidou et al., 2000; Olney et al., 2005; Olney et al., 2002a). This study now demonstrates that the neurotoxicity associated with ethanol administration on P7 (2.5mg/kg, 2 hours apart) causes deficits in brain volume and frontal cortical parvalbumin interneurons and layer II pyramidal neurons that persist into adulthood (P82). This is consistent with our previous work using the NMDA antagonist MK801 on P7 (Coleman et al., 2009). Layer II cortical projection pyramidal neurons were reduced in the medial prefrontal cortex, but not in the M2 motor region. This suggests that the mPFC, a region associated with attention and other executive functions, may be more vulnerable to ethanol toxicity. Attentional deficits are observed in FASD and may be related to prefrontal cortical damage. The loss of layer II projection neurons is likely a cause of the volume reduction of the corpus callosum. P7 ethanol might also damage axons directly or alter myelination. Since deficits in fractional anisotropy and mean diffusivity are seen in humans with FAS, the potential effects of P7 ethanol on myelin should be investigated in the mouse model.

Interestingly, we also observed changes in adult neurogenesis. Male mice that received P7 ethanol had an increase in neurogenesis evidenced by both increased doublecortin staining and Ki67 expression. We have shown previously in adult male rats, following a 4-day ethanol binge an immediate impairment in neurogenesis followed by a wave of enhanced neurogenesis up to two weeks after treatment (Nixon and Crews, 2004). This may represent a compensatory response to damage following ethanol administration. This observation might potentially conflict with observations by Ieraci and Herrera who found reduced

doublecortin staining on P147 of adulthood following P7 ethanol (5mg/kg) (Ieraci and Herrera, 2007). The high concentration of ethanol given in one administration (5mg/kg) may be considerably more toxic than two separate administrations of 2.5mg/kg, a limitation that the authors noted. Also, their observations were made more than 2 months later than ours (P147 vs P82). Since neurogenesis is known to diminish with age, differences may disappear at later ages (He and Crews, 2006). Interestingly, Dong et al found increased adult (P60) after P7 kainate treatment (Dong et al., 2003). Both P7 ethanol (GABA agonist and NMDA antagonist) and kainate (NMDA agonist) cause neuronal cell death in the hippocampus. Increased neurogenesis during early adulthood (P60-P80) could be a compensatory mechanism that occurs in response to various early post-natal insults. The exact outcome may depend on the level of alcohol and the age investigated.

In summary, FASD can be modeled in rodents using early postnatal ethanol treatment. We found that P7 ethanol causes deficits in adult brain volumes and frontal cortical parvalbumin interneurons and layer II projection pyramidal neurons. Adult males had an increase in hippocampal neurogenesis following P7 ethanol treatment, while females did not. Future studies should investigate potential therapies to either reduce the immediate neurotoxic effects of ethanol or to reverse ethanol-induced neuropathology.

Adolescent binge drinking alters adult brain neurotransmitter gene expression, behavior, brain regional volumes and neurochemistry in mice

Leon G. Coleman Jr. B.S[1,2], Jun He, MD, PhD[2], Joohwi Lee, B.S.[3], Martin Styner, Phd[3], and Fulton T. Crews, Phd[1,2]

[1]Curriculum in Neurobiology, University of North Carolina at Chapel Hill, Chapel Hill, NC 27599-7178, United States.
[2]Bowles Center for Alcohol Studies, University of North Carolina at Chapel Hill CB# 7178, Chapel Hill, NC 27599-7178, United States.
[3]Department of Psychiatry and Computer Science, University of North Carolina at Chapel Hill Chapel Hill CB# 7160, Chapel Hill, NC 27599-7178, United States.

Abstract

Binge drinking is common in human adolescents. Recent findings indicate ongoing brain structural maturation and unique sensitivity of developing neurotransmitter and neuroprogenitor stem cells to alcohol toxicity during adolescent development. To determine if adolescent binge drinking alters adult brain structure and behavior a model was employed in which male C57BL/6 mice received either water or ethanol (5g/kg/day i.g.) during adolescent postnatal days 28-37 (P28-37). An array of 84 neurotransmitter-specific genes, behavioral testing (P60-72), (reversal learning, prepulse inhibition, and open field) and postmortem brain structure using MRI and immunohistochemistry (P79), were used to assess persistent alterations in adult brain. At P38, 24 hours after adolescent ethanol treatment, dopamine receptor type 4 mRNA was reduced by 70% and frontal cortical IHC was reduced by 44%. Neurotransmitter-specific gene expression declined an average of 56% between P38 and P88. At P88, neurotransmitter-specific mRNA in adolescent ethanol mice decreased an average of 73% vs P38 controls. Adolescent ethanol did not alter adult Morris water maze spatial learning, but did induce adult reversal learning deficits. Adolescent ethanol reduced adult olfactory bulb and basal forebrain volume as measured by structural MRI, reduced

histochemical basal forebrain area, and decreased basal forebrain cholinergic neuron density. Adolescent ethanol-induced alterations in adult neurotransmitter gene expression or acetylcholinergic neurons could alter neurocircuitry important for reversal learning. These findings indicate adolescent binge drinking can cause persistent changes in behavior and brain structure that are relevant to alcohol use disorders and cognitive function in adults.

Introduction

Adolescence is best defined by characteristic behaviors including high social interaction and play behavior, high levels of risk-taking, high activity and exploration, impulsivity, and novelty and sensation seeking (Ernst et al., 2009; Spear, 2000). Adolescent behaviors are shared across many species, from humans (12 to 20–25 years of age) to mice (postnatal days 28 to 42) and others (Spear, 2000). Recent studies indicate that adolescent brain structural development coincides with consolidation of adult abilities (Blakemore and Choudhury, 2006), including intelligence (Shaw et al., 2006) and behavioral control of executive functions (Ernst et al., 2009). In humans, changing social interactions and gonadal maturation also contribute to brain maturation (Windle et al., 2008). Adolescent brain maturation involves peaks in specific cortical volumes and synapses that stabilize to adult levels. Cholinergic, dopaminergic, and serotoninergic inputs to frontal cortex, as well as cortical width peak during adolescence and then decline to stable adult levels (Giedd, 2004; Giedd et al., 2008; Gould et al., 1991; Kalsbeek et al., 1988; Kostovic, 1990; Rosenberg and Lewis, 1994; Spear, 2000). Developing systems are sensitive to ethanol neurotoxicity. Rat models of adolescent binge drinking find significant frontal neurodegeneration (Crews et al., 2000a) and loss of neurogenesis (Crews et al., 2006), suggesting that the adolescent brain is uniquely sensitive to ethanol neurotoxicity (Crews et al., 2007b).

Current statistics indicate alcohol consumption during adolescence is common, with approximately 12% of 8th graders, 22% of 10th graders and 28% of 12th grade seniors reporting heavy episodic drinking (more than 5 drinks in a row) within the past 2 weeks of survey (Johnston et al., 2004; Masten et al., 2008). Heavy drinking increases among college students, 44% report binge drinking every 2 weeks and 19% report more than 3 binge drinking episodes per week (O'Malley et al., 1998; Wechsler et al., 1995). Adolescents have low sedative responses to alcohol that contribute to risky drinking to high blood alcohol levels (Silveri and Spear, 1998). The lifetime prevalence of past-year alcohol dependence peaks at 12% between the ages of 18 and 20, and declines across adulthood (Masten et al., 2008). The numerous changes in brain structure coupled with the high levels of alcohol consumption provide a strong rationale to conduct basic studies to understand the cumulative impact of underage drinking over the lifespan**.**

We utilized a mouse model of adolescent binge drinking to better understand adolescent brain development and the impact of binge drinking. C57BL/6 mice were evaluated both just after ethanol treatment towards the end of adolescence (P38) and weeks after treatment during young adulthood. The most common subtype of alcohol dependence is adolescent alcohol dependence that is often developmentally limited, similar to our adolescent binge treatment and young adult abstinence (Jacob et al., 2005; Moss et al., 2008). We found that the young adult brain following adolescent binge treatment had altered neurotransmitter gene expression, reduced olfactory bulb volume, decreased forebrain cholinergic neurons, reduced forebrain histological area and MRI volume, and deficits in reversal, but not spatial learning.

Materials and Methods:

Animal treatment

Male C57BL/6 mice were used ordered from Charles River Labs (Raleigh, NC), and were allowed to acclimate to the animal facilities for seven days in our animal facility prior to treatment. Adolescent mice were requested with the stipulation that all mice were the same weight, in order to reduce potential variability in brain size. Mice were orally administered either water or ethanol (5g/kg, i.g. 25% ethanol w/v) during adolescence (P28-37; Figure 3.1A, C) and during adulthood (P88-97, Figure 3.1B) once per day for 10 days. Adolescent ethanol treatment resulted in an average blood alcohol level of 287.7 mg/dL ± 36.8 (mean±SEM) measured 1 hour after the last ethanol administration. Mice treated identically in our lab during young adulthood (P56-65) have blood alcohol levels of 316 mg/dL ± 11 (Qin et al., 2008).

For gene array studies, mice were sacrificed by saline perfusion either 24 hours or 50 days following the adolescent alcohol binge treatment (Figure 3.1A). A group of young adult mice (P88) underwent the same treatment (P88-97) and were assessed either 24 hours or 50 days after binge ethanol. A third group of mice that received adolescent binge ethanol (Figure 3.1C) underwent behavioral testing in adulthood (P60-72). One week after behavioral testing, mice were sacrificed for postmortem brain magnetic resonance imaging (MRI) and immunohistochemistry (IHC). All protocols were approved by the University of North Carolina Institutional Animal Care and Use Committee and were in accordance with the Congressional Animal Welfare Act.

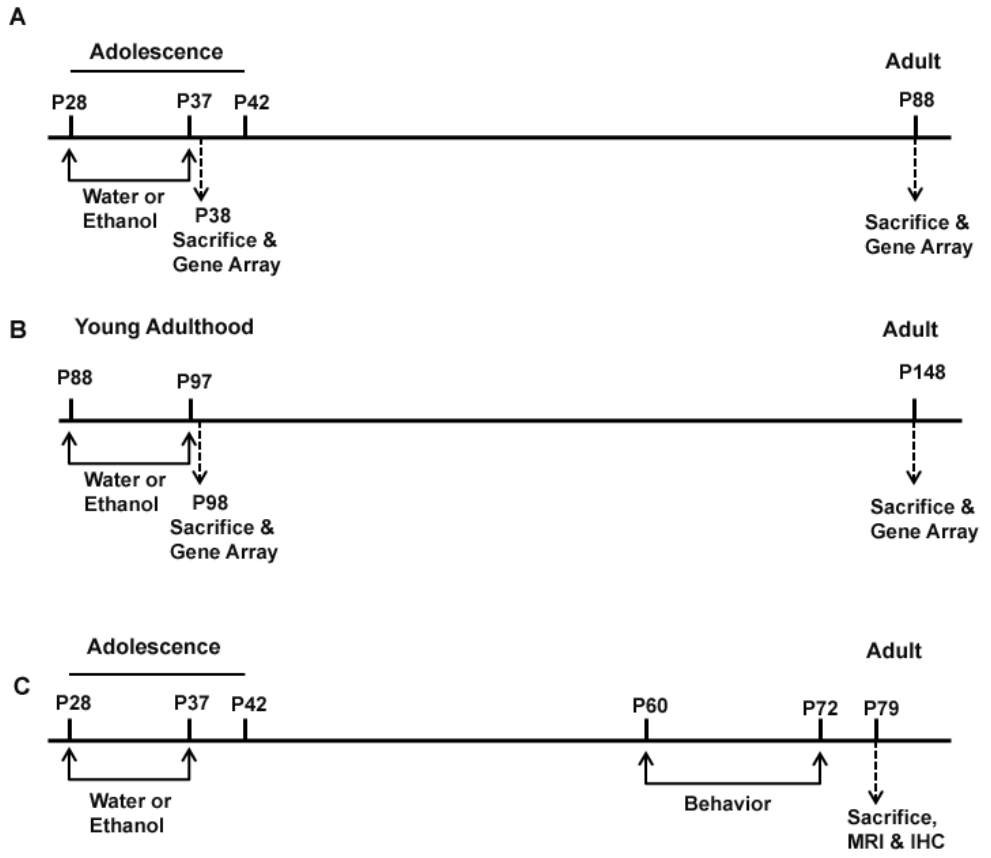

Figure 3.1: Experimental Design. (A) Gene Expression: Adolescent mice (P28) received either water or ethanol (5g/kg i.g.) once daily for ten days during adolescence (P28-37) and were assessed for neurotransmitter receptor and regulator gene expression. The Neurotransmitter Receptor and Regulator Gene SuperarrayTM was used to measure gene expression both during adolescence 24 hours after treatment (P38) and during adulthood 50 days after treatment (P88) (B) Gene Expression: Adult mice (P88) received either water or ethanol (5g/kg i.g.) once daily for ten days (P88-97). Mice were sacrificed either 24 hours (P98; N=6 control, 6 ethanol) or 50 days later (P148) by perfusion with saline for gene Superarray. (C) Behavior, Magnetic Resonance Imaging (MRI) and Immunohistochemistry (IHC): Adolescent mice received either water or ethanol as above, (P28-37) and were left without further intervention until early adulthood. Behavioral testing was performed from P60-P72. Mice were sacrificed by perfusion with 4% paraformaldehyde one week after the end of behavioral testing (P79) and underwent postmortem MRI, followed by sectioning for IHC experiments.

Perfusion and brain tissue preparation for MRI and IHC:

Mice were sacrificed by perfusion as described previously (Coleman et al., 2009; Crews et al., 2004). Briefly, mice were perfused with 0.1M phosphate buffered saline (PBS) followed by 4% PFA with a 48 post-fixation in 4% PFA at 4°C. Mouse skulls with the brains intact were stored in a 1% PFA/PBS solution at 4°C until MRI. To ensure that time between imaging did not alter brain volume; four postmortem adult mice were scanned twice, with

each scan being three months apart. Importantly, there was no significant difference in total brain volume across this 3 month time period in these mice (*t*-test, p=0.62). Neither did we observe a correlation between brain volume and scan date (R= -0.0017, *p*=0.994).

Neurotransmitter receptor and regulator gene quantitative real-time PCR array

Mice were treated either during adolescence or adulthood as described (Figure 3.1A, B). Messenger RNA was extracted from whole brain using Trizol reagent, followed by purification with RNeasy column (Qiagen, Valencia, CA). The total RNA was converted into first stranded-cDNA using an RT first strand kit (SAB Bioscience Corporation, Frederick, MD). The Mouse Neurotransmitter Receptors and Regulators RT^2 Profiler^{TM} PCR Array, which assesses 84 genes was used to perform the reaction (SABioscience Corporation; PAMM-060) using the Sybr green DNA Real-Time PCR Mix. A total of 40 PCR cycles were performed.

Adult Behavior

Behavioral testing was performed in the UNC Neurodevelopmental Disorders Research Center Mouse Behavioral Phenotyping Core using previously published methods (Moy et al., 2007).

Morris water maze spatial and reversal learning: The Morris water maze task was used to test spatial learning and memory as well as the ability to reverse a learned response as described previously (Moy et al., 2007). Briefly, the water maze was filled with water at 24-26^{o}C. Water in the maze was tinted white with nontoxic poster paint so the escape platform was not visible. Each mouse was placed in the pool at one of four possible randomly ordered locations, and then given 60 seconds to find the platform. The room had numerous visual

cues. An automated tracking system acquired the measures (Noldus Ethovision). Criterion for acquisition of learning was set at a 15-second average latency of all the mice to find the platform. Mice were given four trials per day until the group-wide criterion was achieved. Mice that displayed significant floating behavior (average swimming velocity of <10cm/s) were removed from the analysis.

Visual Cue: Mice were first tested for their ability to find the visible platform having a tall cylinder as the visual cue to ensure mice had no visual or motor deficits that could prohibit them from learning the hidden platform tasks. *Initial Learning Acquisition:* The platform was submerged in Quadrant 1. Once the 15 second criterion was reached for the entire group, mice were given a one-minute probe trial in the pool without the platform in place as an additional index of learning. *Reversal Learning:* Mice were tested for their ability to 'unlearn' the previous location of the platform and to learn its new location. The location of the hidden platform was moved to the opposite quadrant of the water maze (Quadrant 3). After reaching the 15-second group-wide criterion, mice underwent a second probe trial to assess retention after reversal.

Elevated Plus Maze: Mice underwent one five-minute trial. Analysis was performed as described (Moy et al., 2007).

Locomotor activity: Mice spent one hour in the open field chamber (40 cm x 40 cm x 30 cm, VersaMax system, AccuScan Instruments) (Moy et al., 2007).

Prepulse inhibition: Mice were evaluated using a San Diego Instruments SR-Lab system as described previously (Coleman et al., 2009; Moy et al., 2006). Briefly, a low pre-stimulus of

varying intensity (74, 78, 82, 86, and 90 dB) was given 100ms prior to a louder startle stimulus (120 dB). The peak startle amplitude within 65-msec of the startle stimulus was measured.

Postmortem MRI Volume Analysis

Whole mouse skulls with brain intact were scanned individually at the UNC Biomedical Research Imaging Center (BRIC) on a 9.4 Tesla Bruker BioSpec spectrometer (Bruker Biospin Inc., Billerica, MA). Total scan time was 15 hours per animal. MRI images (0.12mm x 0.12mm x 0.12mm) were acquired using the following diffusion weighted 3D RARE sequence: TR=0.7s, TE_{eff} =23.662ms, Rare Factor = 3, RARE echo spacing = 11.3067ms, diffusion gradient time δ =6ms, diffusion gradient separation Δ = 12.422, b value – 1000s/mm^2, matrix size = 200x125x80, FOV=24.0mm x 15mm x 9.6mm. Mean diffusivity images, computed from the reconstructed diffusion tensor data, were aligned and brain structures were segmented using an automatic segmentation protocol developed at the UNC Neuro Image Research and Analysis Laboratory (NIRAL) (Lee et al., 2009b). Following automatic segmentation, blinded investigators manually segmented selected regions of interest identified from the automatic segmentation, as well as measuring region volume using ITK-SNAP^{TM} software version 1.8. Brain region boundaries were determined using the Brookhaven National Library 3-D MRI Digital Atlas Database of the adult C57BL/6 mouse (www.bnl.gov/medical/RCIBI/mouse).

Immunohistochemistry and Image Analysis

Immunohistochemistry was performed as described previously (Coleman et al., 2009; Crews et al., 2004). Briefly, three to six sections (40μm) were incubated with 0.6% H_2O_2 to remove endogenous peroxidase activity. Primary antibody incubation was performed overnight at 4°C (choline acetyl transferase 1:500, Millipore; dopamine receptor D4 1:50, Santa Cruz). Secondary antibody (1 hr, 1:200), ABC incubation (1hr) and DAB activation were performed at room temperature on the following day. The Bioquant Nova Advanced Image Analysis System™ was used to assess histological area and neuron density as described previously (Coleman et al., 2009; Crews et al., 2004). We have shown previously that this method results in nearly identical percent changes between treatment and control groups as other unbiased stereological techniques (Crews et al., 2004). In order to confirm MRI volume findings, area measurements of the basal forebrain were taken using Bioquant on sections labeled for parvalbumin. Parvalbumin interneurons filled the nuclei of the basal forebrain, making landmarks and boundaries easily identifiable. Up to six sections in three different regions, defined by distance from bregma, were assessed. Anatomical landmarks were identified using the mouse atlas (Franklin and Paxinos, 2001).

Gene array statistics: mRNA expression level was calculated using the ΔCt method with the Data Analysis Template Excel file provided by SABioscience Corporation (Lee et al., 2008). Values for ΔCt were normalized to the average of five housekeeping genes: glucuronidase β, hypoxanthine guanine phosphoribosyl tranferase1, heat shock protein 90kDa α class b member 1, glyceraldehydes-3-phosphate dehydrogenase, and β actin. As recommended by SABioscience, a 2-Way ANOVA (using average ΔCt values) with Bonferroni post-tests was used to detect gene changes while accounting for multiple comparisons to reduce the probability of type II errors. To gain additional insight, simple *t*-tests of normalized ΔCt

values were also performed in order to identify genes that may not reach statistical significance following the stricter Bonferroni method. The *t*-test analyses may result in type II errors resulting in false positives due to the multiple comparisons, but these statistics are presented in order to more completely identify candidate genes.

Structural MRI Image statistics: For the automatic segmentation volume data, simple *t*-tests were performed to identify candidate regions for further manual segmentation ($p<0.05$). Following manual correction, *t*-tests corrected for multiple comparisons using the Bonferroni method using the following formula: $p<0.05/4$ new comparisons. Therefore a $p<0.0125$ was required to be considered statistically significant.

Behavioral and Immunohistochemistry statistics: A Student's *t*-test or two-Way ANOVA were used for most behavioral and immunohistochemical comparisons ($p<0.05$ for significance). For prepulse inhibition and locomotor activity, a

Table 3.1: RT PCR Neurotransmitter Receptor and Regulator Gene Superarray Genes. Genes that were not measured due to low yield are emboldened in italics.

Symbol	Description
Ache	Acetylcholinesterase
Anxa9	Annexin A9
Brs3	Bombesin-like receptor 3
Cckar	Cholecystokinin A receptor
Cckbr	Cholecystokinin B receptor
Chat	Choline acetyltransferase
Chrm1	Cholinergic receptor, muscarinic 1, CNS
Chrm2	Cholinergic receptor, muscarinic 2, cardiac
Chrm3	Cholinergic receptor, muscarinic 3, cardiac
Chrm4	Cholinergic receptor, muscarinic 4
Chrm5	Cholinergic receptor, muscarinic 5
Chrna1	Cholinergic receptor, nicotinic, α1 (muscle)
Chrna2	Cholinergic receptor, nicotinic, α2 (neuronal)
Chrna3	Cholinergic receptor, nicotinic, α3
Chrna4	Cholinergic receptor, nicotinic, α4
Chrna5	Cholinergic receptor, nicotinic, α5
Chrna6	Cholinergic receptor, nicotinic, α6
Chrna7	Cholinergic receptor, nicotinic, α7
Chrnb1	Cholinergic receptor, nicotinic, β1 (muscle)
Chrnb2	Cholinergic receptor, nicotinic, β2 (neuronal)
Chrnb3	Cholinergic receptor, nicotinic, β3
Chrnb4	Cholinergic receptor, nicotinic, β4
Chrnd	***Cholinergic receptor, nicotinic, δ***
Chrne	Cholinergic receptor, nicotinic, ε
Chrng	***Cholinergic receptor, nicotinic, γ***
Comt	Catechol-O-methyltransferase
Drd1a	Dopamine receptor D1A
Drd2	Dopamine receptor 2
Drd3	Dopamine receptor 3
Drd4	Dopamine receptor 4
Drd5	Dopamine receptor 5
Gabra1	GABA-A receptor, α1
Gabra2	GABA-A receptor, α2
Gabra3	GABA-A receptor, α3
Gabra4	GABA-A receptor, α4
Gabra5	GABA-A receptor, α5
Gabra6	***GABA-A receptor, α6***
Gabrb2	GABA-A receptor, subunit β2
Gabrb3	GABA-A receptor, subunit β3
Gabrd	GABA-A receptor, subunit δ
Gabrg1	GABA-A receptor, subunit γ1
Gabrg2	GABA-A receptor, subunit γ2
Gabrp	***GABA-A receptor, π***
Gabrq	GABA-A receptor, θ
Gabrr1	GABA-A receptor, ρ1
Gabrr2	GABA-A receptor, ρ2
Gad1	Glutamic acid decarboxylase 1
Galr1	Galanin receptor 1
Galr2	Galanin receptor 2
Galr3	Galanin receptor 3
Glra1	Glycine receptor, α1
Glra2	Glycine receptor, α2
Glra3	Glycine receptor, α3
Glra4	Glycine receptor, α4
Glrb	Glycine receptor, β
Gpr103	G protein-coupled receptor 103
Npffr1	Neuropeptide FF receptor 1
Prokr1	Prokineticin receptor 1
Prokr2	Prokineticin receptor 2
Npffr2	Neuropeptide FF receptor 2
Gpr83	G protein-coupled receptor 83
Grpr	Gastrin releasing peptide receptor
Htr3a	5-hydroxytryptamine (serotonin) receptor 3A
Maoa	Monoamine oxidase A
Mc2r	***Melanocortin 2 receptor***
Nmur1	Neuromedin U receptor 1
Nmur2	Neuromedin U receptor 2
Npy1r	Neuropeptide Y receptor Y1
Npy2r	Neuropeptide Y receptor Y2
Npy5r	Neuropeptide Y receptor Y5
Npy6r	***Neuropeptide Y receptor Y6***
Ntsr1	Neurotensin receptor 1
Pgr15l	***G protein-coupled receptor 15-like***
Ppyr1	***Pancreatic polypeptide receptor 1***
Prlhr	***Prolactin releasing hormone receptor***
Slc5a7	Solute carrier family 5 (choline transporter), member 7
Sstr1	Somatostatin receptor 1
Sstr2	Somatostatin receptor 2
Sstr3	Somatostatin receptor 3
Sstr4	Somatostatin receptor 4
Sstr5	***Somatostatin receptor 5***
Tacr1	Tachykinin receptor 1
Tacr2	***Tachykinin receptor 2***
Tacr3	Tachykinin receptor 3

repeated measures 2-way ANOVA was used.

Results:

Decreased Neurotransmitter-Specific Gene Expression During Adolescent Brain Maturation and Binge Ethanol Treatment.

Synaptic connections increase during brain development, reaching a developmental peak associated with high levels of plasticity that mature to lower stable adults levels. To investigate broad changes in neurotransmitter gene expression during adolescent brain maturation to young adulthood (P38 - P88), we used an RT-PCR Superarray^{TM} of 84 neurotransmitter-specific mRNA. Eleven genes were removed from the analysis due to insufficient yield (Table 3.1).

Interestingly, there was a dramatic change in the expression of neurotransmitter receptor and regulator genes across development from P38 to P88 (Figure 3.2A, Table 3.2; average reduction of 56%, 2-Way ANOVA: $p<0.0001$, F=275.9). The expression of thirty-five mRNA was lower in P88 young adults as compared to P38 adolescents (Table 3.2; $*p<0.05$, *t*-test of normalized ΔCt values). Only six of the 73 neurotransmitter-specific mRNA did not decline between P38 and P88 (See Figure 3.2A). Adolescent brain maturation showed large decreases in peptide, γ-amino-butyric acid (GABA), cholinergic and dopaminergic gene expression (Fig. 3.3, Fig. 3.4 and Table 3.2). Examples include peptides such as NPY and somatostatin receptors, which decreased 70-80% across receptor subtypes (Table 3.2). These peptides are often found in inhibitory GABAergic interneurons. Between P38 and P88, $GABA_A$ receptor subunit mRNA and the GABA synthetic enzyme, glutamate decarboxylase, decreased 70-80%. Also, acetylcholine receptor mRNA, both

muscarinic and nicotinic, and the acetylcholine synthetic enzyme ChAT decreased approximately 60-80% during adolescent brain maturation (Table 3.2, Fig. 3.4A), although acetylcholinesterase (Ache), the acetylcholine inactivating enzyme, maintained a constant level of expression during adolescent brain development (Fig. 3.2A). A reduction in neurotransmitter mRNA expression between adolescence and young adulthood is consistent with maturation of neurocircuitry.

To compare maturation changes in gene expression across adolescent to young adulthood (P38-P88) to a similar period, e.g. 50 days, across young adulthood, we also investigated neurotransmitter gene changes between P98 to P148. There was a significant main effect of developmental age between P98 and P148 (Figure 3.2B; average reduction of 33%, 2-Way

Table 3.2 The effect of adolescent binge ethanol on neurotransmitter receptor and regulator gene expression.

Symbol	Description	P38 Ethanol	P88 Control	P88 Ethanol
	Peptide receptors			
Brs3	Bombesin-like receptor 3	66*	45*	25**
Cckar	Cholecystokinin A receptor	64	43*	15**†§
Cckbr	Cholecystokinin B receptor	55	45*	18**†§
Galr1	Galanin receptor 1	50	28	15*§
Grpr	Gastrin releasing peptide receptor	83	102	55*†
Gpr103	G protein-coupled receptor 103	39	26*	17*
Npffr1	Neuropeptide FF receptor 1	36	20*	12**§
Npffr2	Neuropeptide FF receptor 2	37	13 §	10**§
Nmur1	Neuromedin U receptor 1	36	36*	23*
Nmur2	Neuromedin U receptor 2	24*	18**§	16**§
Npy1r	Neuropeptide Y receptor Y1	44	32	30*
Npy2r	Neuropeptide Y receptor Y2	35	19*	16**§
Npy5r	Neuropeptide Y receptor Y5	40	21*	21**
Ntsr1	Neurotensin receptor 1	48	25	19*§
Prokr1	Prokineticin receptor 1	45	20*	20**
Prokr2	Prokineticin receptor 2	40	19*§	12**§
Sstr2	Somatostatin receptor 2	48	36*	26*
Sstr4	Somatostatin receptor 4	33	19**	14**§
Tacr1	Tachykinin receptor 1	41	22*	24*
Tacr3	Tachykinin receptor 3	40	23	15*§
	Cholinergic receptors			
Chat	Choline acetyltransferase	45	36*	15**§
Chrm1	Cholinergic receptor, muscarinic 1	38	29*	16**§
Chrm2	Cholinergic receptor, muscarinic 2	35	29*	17**§
Chrm3	Cholinergic receptor, muscarinic 3	42	23*	15**§
Chrm4	Cholinergic receptor, muscarinic 4	40	30	17*§
Chrm5	Cholinergic receptor, muscarinic 5	46	24	12*§
Chrna3	Cholinergic receptor, nicotinic, $\alpha 3$	76	75	45**
Chrna4	Cholinergic receptor, nicotinic, $\alpha 4$	70	68	36*
Chrna5	Cholinergic receptor, nicotinic, $\alpha 5$	58	48*	25**
Chrna6	Cholinergic receptor, nicotinic, $\alpha 6$	52	42*	22*
Chrna7	Cholinergic receptor, nicotinic, $\alpha 7$	44	30*	14*§
Chrnb1	Cholinergic receptor, nicotinic, $\beta 1$	43	35	15*§
Chrnb2	Cholinergic receptor, nicotinic, $\beta 2$	37	31*	16**§
Chrnb3	Cholinergic receptor, nicotinic, $\beta 3$	39	24*	15**§
Chrnb4	Cholinergic receptor, nicotinic, $\beta 4$	39	36	19**§
	Monamine Receptors			
Comt	Catechol-O-methyltransferase	98	71	36**
Drd1a	Dopamine receptor D1A	82	69	35*
Drd2	Dopamine receptor 2	75	71	37*
Drd3	Dopamine receptor 3	62	44*	20*
Drd4	Dopamine receptor 4	29*	45	30*
Drd5	Dopamine receptor 5	43	30*	15**§
	GABA receptors			
Gabra1	GABA-A receptor, $\alpha 1$	38	42	25*
Gabra2	GABA-A receptor, $\alpha 2$	41	22*	13**§
Gabra3	GABA-A receptor, $\alpha 3$	40	26*	15**§
Gabra4	GABA-A receptor, $\alpha 4$	43	26	16**§
Gabra5	GABA-A receptor, $\alpha 5$	50	32	23*
Gabrb3	GABA-A receptor, $\beta 3$	73	62*	34*
Gabrd	GABA-A receptor, δ	57	62	31*
Gabrg1	GABA-A receptor, $\gamma 1$	48	43*	21**
Gabrg2	GABA-A receptor, $\gamma 2$	43	34*	23*
Gabrq	GABA-A receptor, θ	36	26*	13**
Gabrr1	GABA-A receptor, $\rho 1$	39	23*	16*§
Gabrr2	GABA-A receptor, $\rho 2$	40	23*	21*
Gad1	Glutamic acid decarboxylase 1	42	25	16**§
	Glycine Receptors			
Glra1	Glycine receptor, $\alpha 1$ subunit	80	55	28**†
Glra3	Glycine receptor, $\alpha 3$ subunit	45	33**	18**§
Glra4	Glycine receptor, $\alpha 4$ subunit	39	27*	14*§
Glrb	Glycine receptor, β subunit	39	35*	23*§

Table 3.2: Adolescent alcohol binge robustly alters neurotransmitter gene expression across development. Mice received either water or ethanol (5g/kg) once a day for 10 days during adolescence (P28-37). The expression of 84 neurotransmitter receptor genes was assessed in whole brain either 24 hours after treatment (P38) or in adulthood (P88) using an RT2 Profiler Neurotransmitter Receptor and Regulator SuperarrayTM. Gene expression levels are given as the percent of P38 control. Genes that changed in at least one treatment group are presented. A 2-way ANOVA with bonferroni post-tests to account for multiple comparisons was used to determine statistical significance of individual genes (§ $p<0.05$). Student t-tests were also performed in order to gain insight, however t-test analysis may produce type II errors. (t-test versus P38 control: * $p<0.05$, ** $p<0.01$; t-test versus P88 control: †$p<0.05$)

ANOVA: $p<0.0001$, F=109.8). Using *t*-tests, 11 genes showed continuing developmental reductions, mostly peptide receptors, muscarinic cholinergic receptors and $GABA_A$ subunits (Table 3.3, Figure 3.2B; *t*-test *$p<0.05$), with four genes reaching statistical significance following Bonferroni post-tests: GABAR α4, GAD1, Galantin receptor 1, Prokineticin receptor 2, and Neuropeptide FF receptor 2 (Table 3.3). Linear plots of gene expression show different patterns of gene expression across all the genes in the array during the two different developmental time periods (Figure 3.2A and 3.2B). Following adolescent control treatment, adolescent maturation (P38-P88) shows a dark band of many genes with reductions greater than 60% (Figure 3.2A; overall average reduction of 56%), whereas young adult maturation (P98-P148) shows less robust declines (Figure 3.2B; overall average reduction of 33%). Thus, there are developmental declines in neurotransmitter-specific gene expression that continue from adolescent P38 to P88 young adults and continuing to P148 young adulthood.

Table 3.3 The effect of adult binge ethanol on neurotransmitter receptor and regulator gene expression.

Symbol	Description	P98 Ethanol	P148 Control	P148 Ethanol
Peptide receptors				
Cckar	Cholecystokinin α receptor	108	66	44*
Galr1	Galanin receptor 1	45	33*	43
Galr2	Galanin receptor 2	79	111	45*
Npffr2	Neuropeptide FF receptor 2	70	21*§	36
Npy2r	Neuropeptide Y receptor Y2	94	33*	65
Npy5r	Neuropeptide Y receptor Y5	89	39*	80
Prokr2	Prokineticin receptor 2	87	24*§	47
Tacr3	Tachykinin receptor 3	54	31*	51
Cholinergic receptors				
Chrm3	Cholinergic receptor, muscarinic 3	88	33*	57
Chrm4	Cholinergic receptor, muscarinic 4	83	38*	79
Chrm5	Cholinergic receptor, muscarinic 5	81	31*	58
GABA receptors				
Gabra4	GABA-A receptor, α4	71	25*§	60
Gabrr2	GABA-A receptor, ρ2	111	65	87
Gad1	Glutamic acid decarboxylase 1	70	21*§	51

Table 3.3: Adult alcohol binge slightly alters neurotransmitter gene expression across development. Mice received either water or ethanol (5g/kg) once a day for 10 days during adulthood (P88-97). The expression of 84 neurotransmitter receptor genes was assessed in whole brain either 24 hours after treatment (P98) or in adulthood (P148) using an RT2 Profiler Neurotransmitter Receptor and Regulator SuperarrayTM. Gene expression levels are given as the percent of P88 control. Genes that changed in at least one treatment group are presented. A 2-way ANOVA with bonferroni post-tests to account for multiple comparisons was used to determine statistical significance of individual genes (§ $p<0.05$). Student t-tests were also performed in order to gain insight into other genes that might be changing, however t-test analysis may produce type II errors. (t-test versus P88 control: * $p<0.05$)

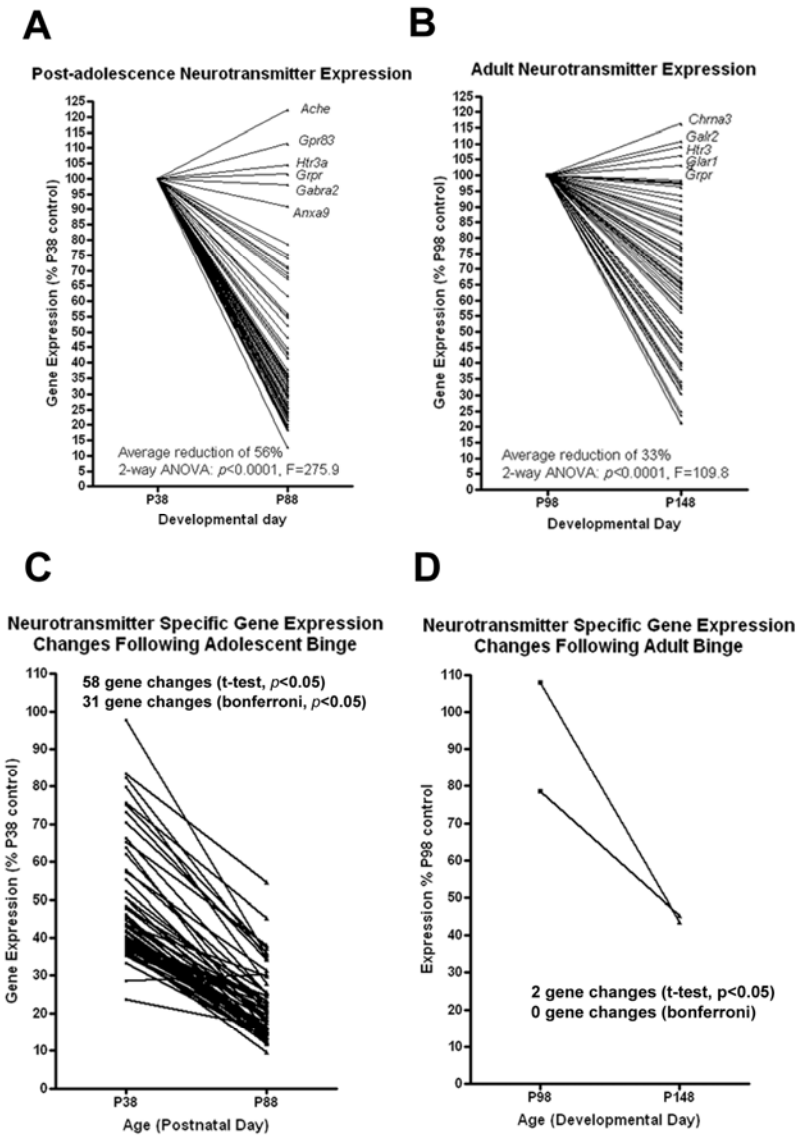

Figure 3.2 Binge ethanol treatment during adolescence but not during adulthood robustly alters the developmental trajectory of neurotransmitter specific gene expression. Mice received water or ethanol (5g/kg, i.g.) once a day for ten days during either adolescence (P28-37) or adulthood (P88-97). Neurotransmitter specific gene expression was assessed using a gene SuperArray either 24 hours (P38 or P88) or 50 days (P88 or P148) after the last alcohol treatment. Expression for each gene is compared to control expression levels 24 hours after treatment (P38 or P88). (A) Developmental changes in gene expression in young control mice. A developmental reduction in neurotransmitter receptor and regulator gene expression was observed across the entire array (Average of 56% reduction, 2-way ANOVA, ***p<0.001) with 36 genes reaching a p<0.05. Genes that showed either a potential increase in expression or no reduction at all are labeled. (B) Developmental changes in gene expression in adult control mice. A developmental reduction in neurotransmitter receptor and regulator gene expression was observed across all the genes tested (2-way ANOVA, ***p<0.0001) that was on average less than controls (33% average reduction) with 11 genes having a p<0.05. (C) Adolescent binge ethanol treatment potentiates the developmental reduction in gene expression, causing significant reductions in 59 genes (p<0.05, t-test of normalized ?Ct values vs P38 control) with 31 genes maintaining statistical significance following bonferroni adjusted post-tests. (D) Adult binge ethanol resulted in only two genes showing reductions from P98 to P148 that reached a p<0.05, with zero changes following bonferroni adjusted post-tests.

Neurotransmitter-specific gene expression allows for a global assessment of the impact of ethanol on brain. The impact of the ethanol binge drinking procedure was assessed in both adolescent and young adult groups one day after treatment and 50 days later. Adolescent ethanol binge treatment (P28-37, Fig. 3.1A) caused reduction in neurotransmitter-specific mRNA notable 24 hours after treatment on P38 (Table 3.2, Fig. 3.2C; average reduction of 57% across all genes, 2-Way ANOVA: $p<0.0001$, F=161.2). Young adult ethanol binge treatment (P88-97, Fig. 3.1B) did not induce a global change in neurotransmitter-specific mRNA 24 hours after treatment (Table 3.3; average fold change in expression: 0.98, 2-Way ANOVA: $p = 0.39$, F=0.74). The combination of adolescent binge ethanol treatment and developmental maturation resulted in large decreases in neurotransmitter gene expression (Table 3.2; average reduction of 73%, 2-Way ANOVA: $p<0.0001$, F=67.71, §$p<0.05$ Bonferroni post-test; *$p<0.05$, *t*-test of normalized ΔCt values, P38 control vs P88 ethanol). Adolescent binge ethanol treatment tended to exaggerate the developmental decrease in neurotransmitter-specific gene expression. Among the 73 neurotransmitter-specific genes measured in the array, 58 were persistently reduced by binge ethanol treatment at P88 as shown by *t*-tests, and 31 with Bonferroni post-tests (Fig. 3.2C, Table 3.2). Among 15 cholinergic genes, expression in young adults (P88) averaged 37% (range 23-75%) of control adolescent (P38) levels with no single gene significantly decreased (Table 3.2; 2 way ANOVA-Bonferroni post-test). Cholinergic gene expression in young adults (P88) following adolescent binge ethanol treatment averaged 20% (range 14-45%) of control P38 levels, with 11 of the 15 cholinergic genes being significantly lower, e.g. $p<0.05$; 2-way ANOVA with Bonferroni post-tests (Table 3.2). Young adults (P148) 50 days following younger adult binge ethanol treatment (P88-P97, Fig. 3.1) also had exaggerated

developmental decreases in neurotransmitter expression across the entire array as determined by ANOVA (Table 3.3; $p<0.0001$, F=40.18), although the reduction was less than that found in the adolescent binge treated group (average reduction of 37%). However, only two individual genes were suppressed persistently at P148 following young adult binge ethanol treatment (P88-P97): cholecystokinin (CCK) α and Galantin receptor 2 (*t*-test 56% reduction and 55% reduction respectively, at P148) and none following Bonferroni post-tests (Figure 3.2D, Table 3.3). These findings indicate that adolescent binge ethanol treatment causes more pronounced and persistent decreases in brain neurotransmitter-specific gene expression than young adult binge ethanol treatment.

Expression levels of most neurotransmitter-specific genes declined during adolescent brain development, i.e., P38-P88. Adolescent binge ethanol treatment resulted in significant persistent decreases in adult neurotransmitter-specific gene expression (2-Way ANOVA: $p<0.0001$, F=55.5, P88 control vs P88 ethanol). However, multiple developmental trajectory patterns of expression altered by binge ethanol suggest responses unique to each gene (Fig. 3.3, Fig. 3.4). Dopamine receptor-4 (D4DR) mRNA was decreased about 71% on P38 following adolescent binge treatment (Fig. 3.3, Table 3.2, $*p<0.05$, t-test of normalized ΔCt values). Interestingly, D4DR underwent a 70% developmental decline between P38 and P88, whereas binge ethanol treated animals showed no developmental change, i.e., expression on P38 and P88 following binge ethanol treatment were both 70% below P38 control levels (Table 3.2, Fig. 3.3). Since dopamine circuitry continues to develop during adolescence in frontal cortex we used immunohistochemistry (IHC) to assess D4DR expression. The orbitofrontal cortex (OFC) of adolescent rats showed strong punctate D4DR+IR that was 44% less in the OFC of P38 binge ethanol treated mice compared to P38 adolescent control

mice (Figure 3.3B, *p<0.05). Since the developmental decrease in D4DR mRNA mimicked the adolescent binge ethanol-induced decrease and no developmental change occurred in ethanol treated animals, D4DR gene expression was similar in P88 controls and P88 ethanol treated animals (Fig. 3.3A). Both punctate and somatic D4DR+IR staining were observed in adults, suggesting developmental regulation of D4DR subcellular localization (not shown). There was no effect of adult ethanol binge treatment (P88-P97) on D4DR gene expression either immediately (P98) or after 50 days (P148). Decreases in D4DR expression following adolescent binge ethanol treatment in adolescent brain P38 were longer apparent in the adult brain P88. In other words, D4DR development is disrupted by adolescent binge ethanol treatment, although expression levels in adults appear normal.

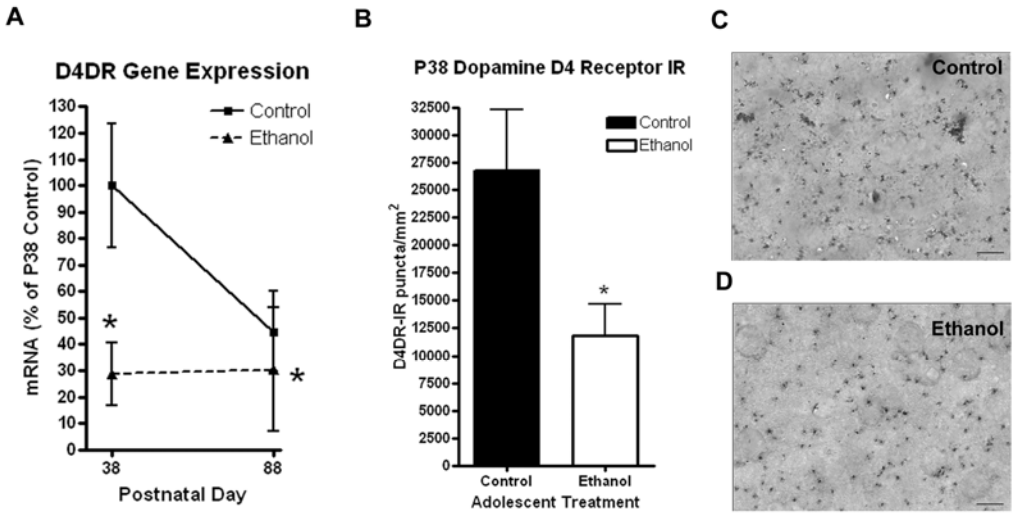

Figure 3.3: Binge ethanol reduced dopamine D4 receptor (D4DR) gene and protein expression in adolescent mice (P38). Adolescent mice received either water or binge ethanol (5g/kg once daily, i.g.) for ten days during adolescence (P28-37). Mice were sacrificed 24 hours after the last treatment for RT-PCR and immunohistochemistry. Immunohistochemistry for the D4DR was performed on sections from the orbitofrontal cortex. (A) Adolescent ethanol binge caused a 71% reduction in D4DR gene expression in whole brain 24 hours after treatment at P38 that remained reduced at P88. Control mice underwent a 55% developmental reduction in D4DR gene expression that did not reach statistical significance (*p<0.05 vs P38 controls) (B) Quantification of D4DR immunoreactivity (IR) in the orbitofrontal cortex in adolescent mice (P38). Adolescent mice that received binge ethanol had 44% less D4DR-IR in the orbitofrontal cortex than controls (Controls: 26800 ± 5500 D4DR-IR puncta/mm2, N=3; Ethanol: 11790 ± 2900 D4DR-IR puncta/mm2, N=4; *p<0.05, t-test.) (C) High powered image of punctuate D4DR-IR staining in a control animal (120X). Punctuate D4DR-IR staining in an ethanol treated mouse shows reduced D4DR-IR staining than control. Scale bar: 20 micron

Other patterns of adolescent binge ethanol neurotransmitter-specific gene responses involve persistent changes in adulthood, but varied adolescent brain responses (Fig. 3.4, Table 3.2). Although binge ethanol decreased expression in general, gene specific reductions in expression levels were often not statistically significant. Following ethanol treatment, most genes followed a decreasing developmental trajectory similar to that found in controls (Fig. 3.4A and B). This pattern is shown in Figure 3.4A for ChAT. Binge ethanol treatment (P28-37) reduced ChAT expression at P38 (55%, p=0.098), which continued to decline during development. At P88, ChAT expression was reduced 64% in control mice (*p<0.05 t-test vs P38 control) and 85% ethanol treated mice (§ p<0.05 Bonferroni post-test, **p<0.01 t-test vs P38 control, Fig. 3.4A). Gastrin releasing peptide

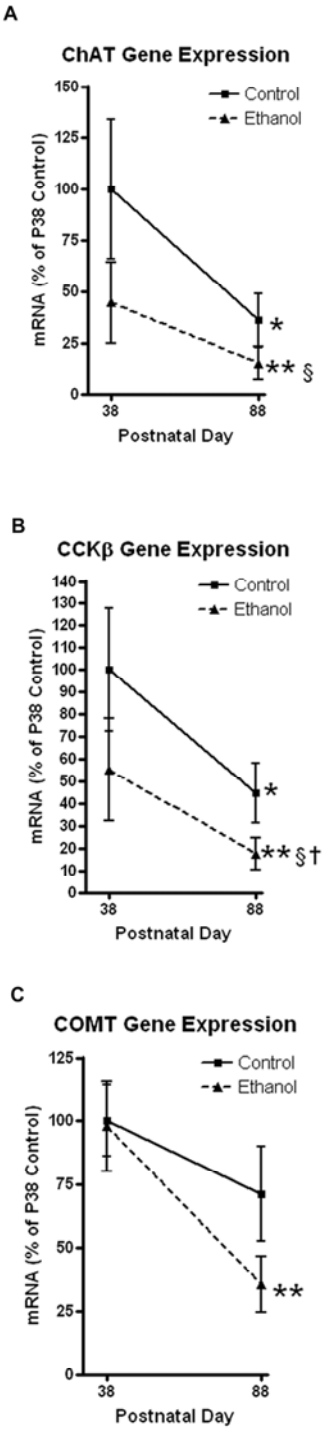

Figure 3.4: Adolescent alcohol binge differentially alters developmental trajectory of neurotransmitter receptor and regulator gene expression. Three different patterns of altered developmental gene expression trajectory displayed. Whole brain was mRNA levels were assessed either 24 hours (P38) or 50 days (P88) after adolescent treatment. RT-PCR was performed using an RT2 Profiler PCR Array for neurotransmitter receptor and regulator genes. mRNA levels are presented as percent of P38 control to demonstrate the effects across development (A) Cholineacetyltransferase (ChAT) mRNA levels changed significantly across development from P38 (100%) to P88 (64% reduction, *p < 0.05) in control animals. ChAT gene expression was showed a trend toward a significant reduction 24 hours following adolescent ethanol binge (P38, 55% reduction, p = 0.098). Fifty days after the adolescent ethanol binge ChAT mRNA levels were reduced 85% (**p<0.01 vs P38 control) (B) Cholecystokinin ? (CCK?) receptor expression. CCK? receptor gene expression reduced significantly across development from P38 (100%) to P88 (55% of P38 control, *p<0.05). Following adolescent ethanol binge a non-significant reduction in the level of CCK? mRNA was observed 24 hours after the last treatment (64% of control, p = 0.22). In adulthood, 50 days after the last alcohol treatment, CCK? mRNA expression were significantly reduced 82% from the P38 control level (**p<0.01, vs P38 control) and 39% from P88 control (†p<0.05, vs P88 control). (C) Catechol-O-methyltransferase (COMT) gene expression trajectory. No significant reduction in COMT gene expression was observed from P38 to P88 in control animals (29% reduction, p=0.24). Adolescent binge ethanol resulted in a significant reduction in COMT gene expression in P88 adults (74% reduction, p<0.01 vs P38 controls).

receptor, Grpr, was unique among the transmitter genes studied, in that it did not change expression during development or adulthood from P38-P148 (Fig. 3.2, Table 3.2), 24 hours following adolescent binge ethanol, or at all (24h or 50 days) following adult binge ethanol treatment. However, in adults (P88) 50 days after adolescent binge treatment, Grpr expression was 55% of P88 controls (†$p<0.05$, *t*-test, P88 control vs P88 ethanol group), suggesting a unique adolescent-specific ethanol effect. Other mRNAs that were not markedly altered in adolescence by binge treatment that reached statistically significant reductions after development are cholecystokinin α and β (CCKα and CCKβ), and the glycine receptor α1 subunit (†$p<0.05$, *t*-test of normalized ΔCt values, P88 control vs P88 ethanol group). The developmental trajectory for these genes is illustrated by the peptide receptor CCKβ (Figure 3.4B). Adolescent binge ethanol caused a 45% decrease in CCKβR mRNA 24 hours after the end of the binge, control animals underwent a 55% reduction in CCKβR mRNA from P38 to P88 (*$p<0.05$) while, ethanol treated animals underwent an additional 37% reduction in gene expression from P38 to P88, resulting in an overall 82% significant reduction from P38 control levels (§ $p<0.05$ Bonferroni post-test vs P38 control, †$p<0.05$ *t*-test vs P88 control). Catechol-O-methyltransferase (COMT) showed a particularly interesting pattern of altered developmental trajectory (Figure 3.4C). Adolescent binge ethanol did not cause any change COMT gene expression at P38. Although there was a nonsignificant developmental reduction in controls (29% reduction, $p=0.24$), adolescent binge treatment resulted in a 64% decrease in COMT mRNA expression in P88 adults (Table 3.2, Fig 3.4C **$p<0.01$ *t*-test). Similar developmental effects were observed with two other genes associated with the dopaminergic system, dopamine receptors D1a and D2. Thus, although alcohol showed no immediate effect on COMT, dopamine D1a or D2 expression,

the developmental trajectories were altered resulting in persistent reduced expression in adults. Therefore, adolescent binge ethanol treatment alters neurotransmitter-specific gene developmental trajectories, contributing to persistent changes in adult neurotransmitter gene expression.

Young Adult Behavior Following Adolescent Binge Ethanol Treatment: Reversal Learning Deficit.

To investigate global behaviors in adults following adolescent binge ethanol treatment (P28-37), we assessed young adult mice (P63-P72; Figure 3.1) for locomotor open field activity, Morris Water Maze acquisition and reversal learning, as well as prepulse inhibition and anxiety-like behavior in the elevated plus maze. In the water maze, mice from both groups easily learned with a visual cue on the platform (Figure 3.5A, <10 seconds). Similarly, in the hidden platform task, both groups learned in parallel over four days of testing, as indicated by reduced time to find the hidden platform (Figure 3.5B). Results from a probe trial also supported equivalent learning ability in both groups, since both spent significantly more of their search time in the correct quadrant, and less than 20% in the incorrect quadrants, with no difference between the treatment groups (Figure 3.5C). Both groups of mice received 3 days of reversal learning training with the platform in the opposite quadrant, with both groups showing a modest reversal (Figure 3.5D).

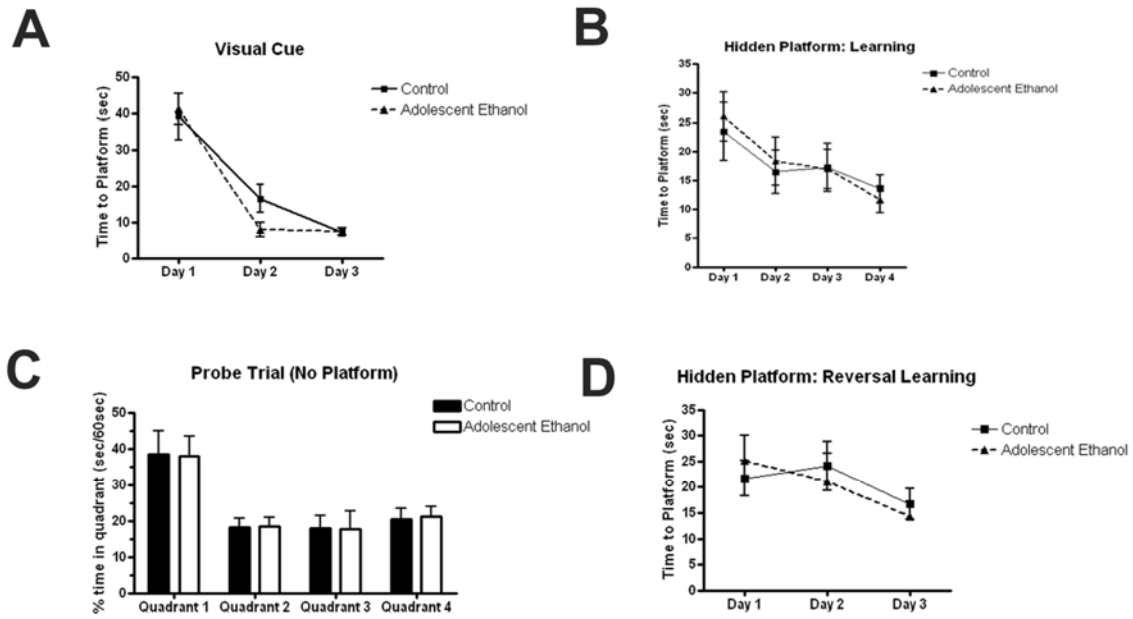

Figure 3.5: Morris Water Maze Learning. There were no differences in the ability of both groups of mice to learn the platform location. (A) Mice were first trained to locate the platform with a visual cue placed on the platform. There were no significant differences in learning acquisition between the two treatment groups on any testing day (Day 2, p=0.09 t test) or across days, however there was significant learning across treatment days in both groups (2-Way ANOVA: Day 62.6% total variation, p=0.0001; Treatment 0.31% total variation, p=0.6. N=10 Control, 8 Ethanol). (B) Initial Learning with the hidden platform location over four days. Both treatment groups significantly improved in learning of the location of the hidden platform across four days. There were no significant differences between treatment groups (2-Way ANOVA: Day 13.53% total variation, p=0.0006; Treatment 0.06% total variation, p=0.89. N=10 Control, 8 Ethanol) (C) Learning probe trial. Mice were placed in the tank for 60 seconds with no platform to measure which quadrant in the tank they preferred. Both groups of mice spent more time in Quadrant 1, where the platform was during the hidden platform trials. (2-Way ANOVA: Quadrant 32.64% total variation, p=0.0001; Treatment 0.00% total variation, p=0.99. N=10 Control, 8 Ethanol) (D) Reversal learning acquisition. The hidden platform was moved to Quadrant 3. Both groups of mice significantly improved in learning the new platform location over three days. There were no differences in learning between the two groups. (2-Way ANOVA: Day 9.25% total variation, p=0.029; Treatment 0.07% total variation, p=0.90. N=9 Control, 8 Ethanol).

The reversal learning probe trial indicated significant differences between young adult control and young adults following adolescent binge ethanol treatment (Figure 3.6). Following reversal training, the control mice no longer demonstrated a strong preference for the original platform location in quadrant 1, spending roughly an equal amount of time also searching quadrant 3, where the platform had been re-located during reversal. In contrast, the ethanol-treated mice significantly spent more than twice as much time in quadrant 1 (35.6%) than in the quadrant with the new platform location (15.5%), demonstrating a perseverative response pattern (Figure 3.6A; $^{**}p<0.01$). Further, the ethanol-treated group spent significantly less time than the control mice searching quadrant 3, where the platform had been re-located during reversal († $p<0.05$, compared to controls). These findings

demonstrate adolescent binge ethanol treatment of C57BL/6 mice does not cause young adult spatial learning deficits, but disrupts reversal learning.

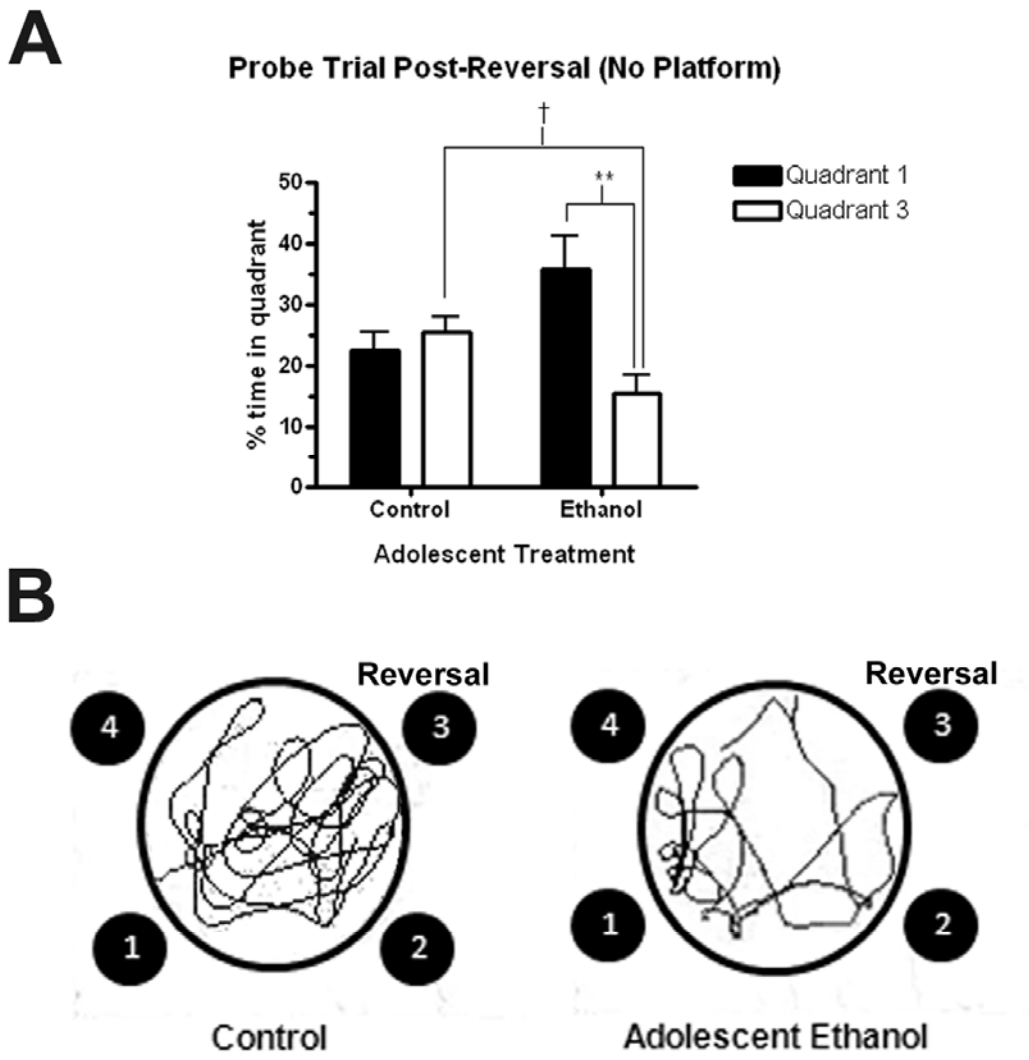

Figure 3.6: Mice that received ethanol binge during adolescence had a deficit in reversal learning as adults. Following acquisition of reversal learning, mice were tested in a 60 second probe trial in the absence of the hidden platform. (A) Control mice spent a nearly equal amount time in the initial learning quadrant (Quadrant 1, 22.4%±3.02) and the reversal learning quadrant (Quadrant 3, 25.5%±2.5). Adult mice were treated with ethanol during adolescence spent more than twice as much time in the quadrant where the platform was during initial learning (Quadrant 1, 35.6%±5.5) than where the platform was during reversal learning (Quadrant 3, 15.5%±7.7) (**,t test $p < 0.01$). Also, control mice spent significantly more time in the reversal quadrant (Quadrant 3, 25.5%±2.5) than the mice that received alcohol during adolescence (15.5%±7.7) (†, t test, $p<0.05$). N = 7 Control, 7 Ethanol. Data is presented as mean ± SEM. (B) Representative tracings of the reversal probe trial from one animal in each treatment group, depicting the increased time spent by control mice in the reversal learning quadrant (Quadrant 3) compared to adolescent ethanol treated mice, which spent more time in the initial learning quadrant (Quadrant 1).

We tested a spectrum of other behaviors to determine if adolescent binge ethanol caused other differences in adult mice. Behaviors associated with sensorimotor gating,

locomotor activity, and anxiety showed no significant differences between groups. Prepulse inhibition is a measure of sensorimotor gating. Adult mice that received alcohol during adolescence showed nonsignificant reductions in prepulse inhibition across all the prepulse decibels tested (Figure 3.7, 2-way ANOVA: p=0.11, F=2.931). Reductions at two of the prepulse decibels measured (78 and 90dB) reached statistical significance using a *t*-test (*p<0.05). Locomotor activity in the open field was the same in both groups across a one-hour period (Figure 3.7B, 2-way ANOVA: p =0.27, F=1.30). In the elevated plus maze, a measure of anxiety-like behavior, both groups spent similar amounts of time in the open arms (Figure 3.7C, control: 35.9 sec ± 8.3, ethanol 39.4 sec ± 4.5, p=0.73, *t* test) and the closed arms (control: 203.6 ± 16.1, ethanol 210.7 ± 7.1, p=0.72, *t* test). Center time in the open field, another measure of anxiety-like behavior and activity in a novel environment, was also unchanged between groups (Figure 3.7D, 2-way ANOVA: p=0.94, F=0.005). Thus, C57BL/6 mice are behaviorally resilient and adolescent binge drinking procedures do not alter global locomotor, spatial learning, sensorimotor gating or anxiety assessments in young adults. Only the reversal learning probe trial indicated persistent young adult dysfunction following adolescent binge drinking.

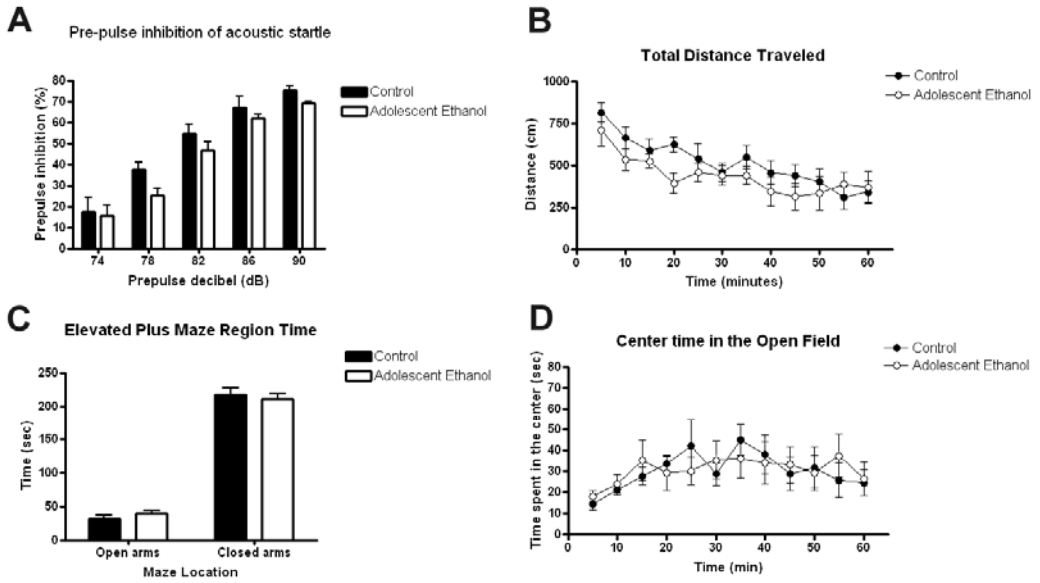

Figure 3.7 Adult behaviors that were unchanged by adolescent binge ethanol (A) There was a trend toward a significant reduction in pre-pulse inhibition, a measure of sensorimotor gating, in adult mice that received alcohol during adolescence (2-way ANOVA: Treatment 1.93% total variation, p=0.11) (B) Locomotor behavior. There were no differences between groups in total distance traveled across the 1 hour testing period (2-way ANOVA: Treatment 2.67% total variation, p =0.27) (C) Elevated Plus Maze. There were no differences in time spent in the open arms (control: 35.9 sec ± 8.3, ethanol 39.4 sec ± 4.5, p=0.73, t test) or closed arms (control: 203.6 ± 16.1, ethanol 210.7 ± 7.1, p=0.72, t test) of the elevated plus maze. (D) Center time in the open field, a measure of anxiety-like behavior showed no differences between the two groups (2-way ANOVA: Treatment 0.01% total variation, p=0.94)

Adolescent Binge Ethanol Reduces MRI Adult Basal Forebrain and Olfactory Bulb Brain Regional Volume.

To investigate adult brain structure following adolescent binge ethanol treatment, we performed MRI on postmortem adult mouse brains. Twenty brain regions were initially segmented in an automatic fashion to identify candidate regions for further manual segmentation. Although not statistically different, mean total brain volume and neocortex volume were 1-2% lower in adolescent ethanol treatment groups, being 441mm^3 vs 435 mm^3 and 152 mm^3 vs 148 mm^3 in young adult control and adolescent alcohol treated animals (both P79) respectively. Further segmentation of the frontal cortex (from the genu of the corpus callosum forward) found no differences in volume (not shown). Some brain regions

such as the globus pallidus and internal capsule tended to show increased mean volumes in adults following adolescent binge alcohol treatment that were not statistically significant. Four brain regions in adolescent binge treated young adults showed >4% decreases in mean volume, basal forebrain -4.4% ($p<0.02$), olfactory bulb -6.5% ($p<0.046$), anterior commissure -5.1% ($p<0.04$) and hippocampus -4.5% ($p=0.11$) (Table 3.4). These findings suggest that adolescent binge alcohol treatment has brain region specific effects.

Basal forebrain, olfactory bulb, anterior commissure, and hippocampus were manually segmented by blinded investigators to refine segmentation volumes. Manual segmentation reduced variation and mean differences

Table 3.4 Adult brain MRI volumes using automatic segmentation following adolescent binge ethanol.

Brain Region	Control (mm^3)	Ethanol (mm^3)	% Change	*p* value
Hippocampus	**24.6**	**23.5**	**- 4.5**	**0.11**
Corpus Callosum & External Capsule	13.2	13.2	0.0	0.95
Caudate & Putamen	22.3	22.1	- 0.9	0.69
Anterior Commissure	**1.2**	**1.1**	**- 5.1***	**0.04**
Globus Pallidus	2.4	2.6	6.6	0.39
Internal capsule	1.9	2.1	9.9	0.45
Thalamus	24.6	24.5	- 0.4	0.91
Cerebellum	53.0	54.1	2.1	0.42
Superior Colliculi	8.30	8.26	- 0.5	0.90
Ventricle	1.2	1.2	0.0	0.96
Hypothalamus	10.2	10.0	- 1.1	0.84
Inferior colliculi	5.1	5.2	2.8	0.52
Central Gray	4.0	3.9	- 2.0	0.63
Neocortex	151.5	147.5	- 2.6	0.23
Amygdala	12.6	12.7	0.4	0.91
Olfactory Bulb	**24.6**	**23.0**	**- 6.5***	**0.046**
Brain Stem	55.4	55.8	0.7	0.85
Rest of Midbrain	11.13	11.15	0.2	0.94
Basal Forebrain & Septum	**11.9**	**11.4**	**- 4.4***	**0.02**
Fimbria	1.8	1.9	4.9	0.55
Total Volume	440.9	435.2	- 1.3	0.37

Table 3.4: The effect of adolescent binge ethanol on adult regional brain volume using Magnetic Resonance Imaging (MRI). Postmortem brains were scanned using a 9.4T MRI scanner. Brain regions were segmented on the images using an automatic segmentation protocol. Volumes of the individual structures (mm3) in control and ethanol groups, percent change from control, and the p value (t-test) are shown. The anterior commissure, olfactory bulb, hippocampus and basal forebrain & septum (bold) showed changes that were investigated further with manual segmentation. Since this was an initial screening, a statistical correction for multiple comparisons was not performed, so that potential regions of interest would not be discarded prior to a more thorough manual segmentation. Therefore displayed p values may contain type II errors, resulting in false positives.

between groups. For example, control hippocampal automated segmentation volumes ranged from 22 to 27.5 mm^3 (coefficient of variation = 0.66) compared to manual hippocampal volumes that ranged from 24.5 to 28 mm^3 (coefficient of variation = 0.45), likely due to the difficulty in resolving the most anterior and ventral regions of the hippocampus. Both automated and blinded manual segmentation indicated adolescent ethanol treated animals have slightly smaller, but not significantly different hippocampal volumes (Figure 3.8A). Though automatic segmentation reported significantly smaller anterior commissure in mice that underwent adolescent binge, no significant difference was found when segmented manually (p=0.31), indicating that adolescent ethanol treated animals may have slightly smaller, but not significantly different anterior commissure volumes (Figure 3.8B).

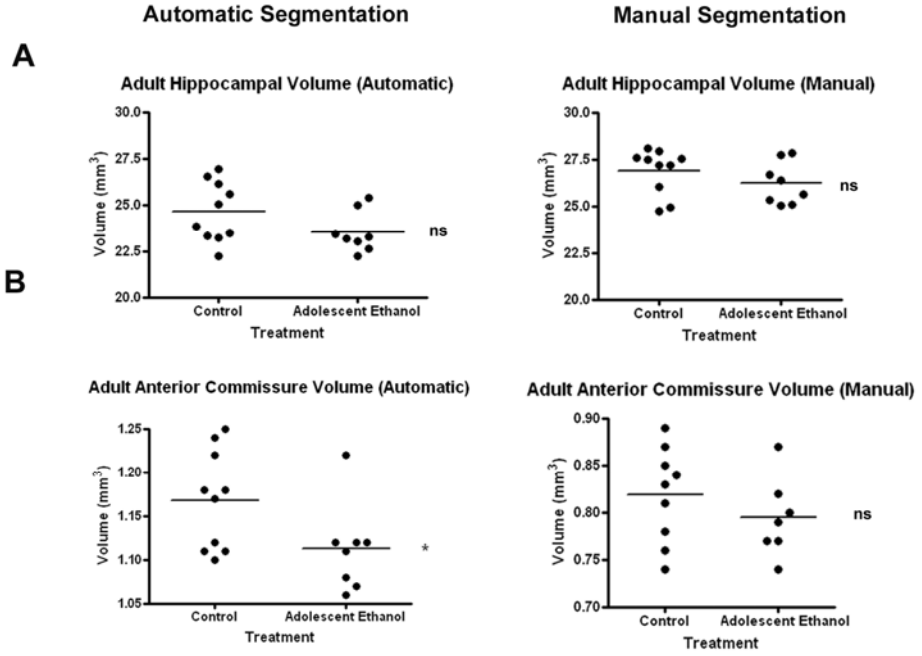

Figure 3.8: Comparison of automatic and manual assessments of anterior commissure, hippocampus and olfactory bulb volumes. Mice were treated with either water or alcohol (5g/kg) for ten days during adolescence (P28-37). Postmortem MRI was performed on adults (P79). Automatic segmentation of brain regions and volume analysis reported possible volume reductions in the hippocampus, anterior commissure and olfactory bulb. These changes not confirmed when the brain regions were manually segmented by blinded investigators using ITK-SNAP software. (A) Hippocampal volumes. Automatic segmentation showed a trend toward a reduction (4.5%) in adult mice that received ethanol during adolescence (Control: 24.64 ± 0.51mm3, N=10; Ethanol: 23.52 ± 0.39mm3, N=8, p=0.11). There was no significant reduction found following manual segmentation (Control: 26.87 ± 0.38 mm3, N=10; Ethanol: 26.22 ± 0.40 mm3, N=8, p = 0.26) (B) Anterior Commissure volume automatic segmentation showed a 5.1% reduction in adult mice that received ethanol during adolescence that reached significance (Control: 1.168 ± 0.018mm3, N=10; Ethanol: 1.113 ± 0.018mm3, N=8, * p<0.05). This was not confirmed by automatic segmentation (C) Olfactory Bulb volume automatic segmentation showed a 6.5% reduction that was not confirmed by automatic segmentation.

However, manual segmentation of the olfactory bulb (Fig. 3.9) and the basal forebrain/septum (Fig. 3.10) confirmed significant reductions in volume in adult mice that received adolescent binge ethanol treatment. The mouse olfactory bulb is a large frontal brain region representing over 5% of mouse brain volume that is embedded in the skull making automated skull striping and segmentation difficult. Olfactory bulb volume was reduced 6.5% by automated analysis (Table 3.4) and 7.8% (Figure 3.9, $^{**}p<0.005$) by manual segmentation. Overlays show overall olfactory bulb reductions (Fig. 3.9), consistent with binge ethanol treatment induced adolescent olfactory bulb and cortex necrosis (Crews et al., 2000a) and inhibition of adolescent frontal neurogenesis (Crews et al., 2006) found in rat studies.

The basal forebrain is a collection of structures located ventrally to the striatum. It is considered to be the major cholinergic output of the CNS. It includes a group of structures that lie near the bottom of the front of the brain, including the nucleus basalis, diagonal band of Broca, ventral pallidum and medial septal nuclei. These structures are important in the production of acetylcholine, which is then distributed widely throughout the brain. The adult basal forebrain/septum region volume was reduced in the adolescent ethanol treated young adults. Automated analysis found a -4.4% (Table 3.4; $p<0.03$) and manual analysis -4.5% decrease in forebrain/septal volume (Figure 3.10, $^{**}p<0.01$). Forebrain/septum includes the nucleus basalis, diagonal band of Broca, and medial septal nuclei. The basal forebrain, through widespread projections to cortex, particularly prefrontal cortex, plays an important role in the modulation of cortical activity in association with different behavioral states including sleep, learning and memory (Everitt and Robbins, 1997; Jones, 2004; Sarter et al., 2003; Weinberger, 2003).

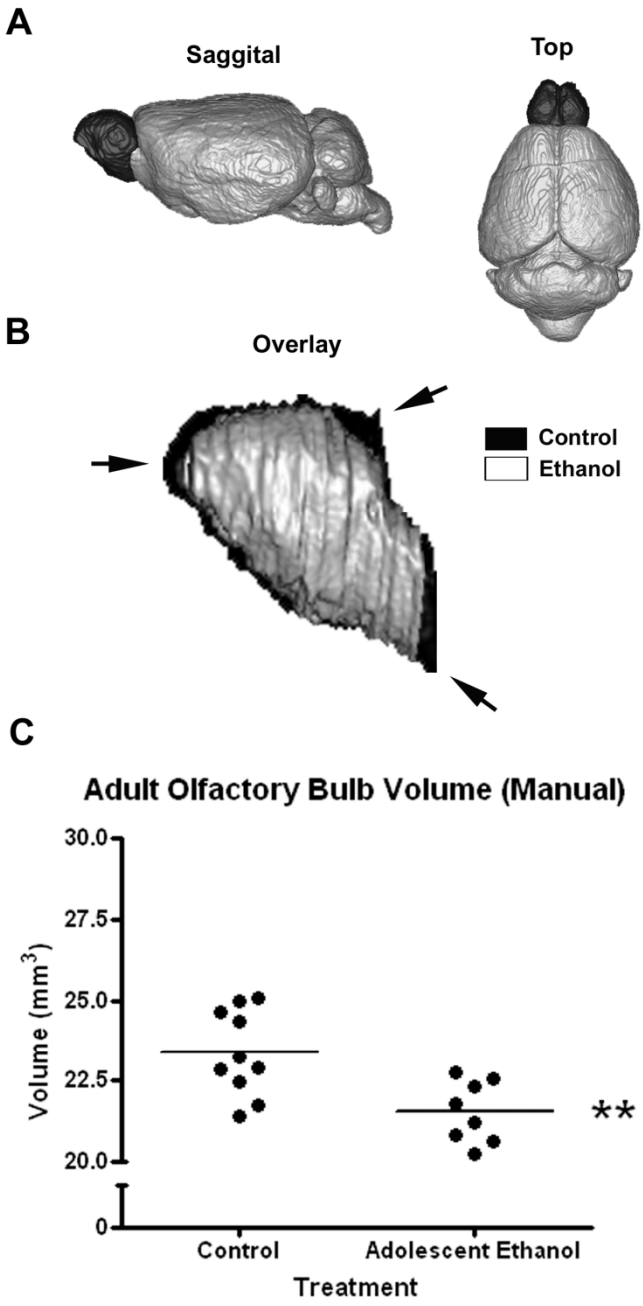

Figure 3.9: Adolescent ethanol binge causes a reduction in the volume of the olfactory bulb in adults. Adolescent mice received either water or ethanol (5g/kg) once a day for ten days (P28-37). Postmortem MRI was performed on adults (P79). Following automatic segmentation, manual segmentation of the olfactory was performed by blinded investigators. (A) 3D representation of the brain showing large relative size of the olfactory bulb in the rodent brain (darkened). (B) Overlay of 3D renderings of representative control and ethanol treated adult olfactory bulbs. Arrowheads highlight volume differences between control (black) and ethanol treated (white) groups (C) Adult olfactory bulb volume quantification following manual correction. Adult mice that received binge ethanol treatment during adolescence showed a 7.8% reduction in the olfactory bulb volume (Control: 23.37 ± 0.42 mm3, N=10; Ethanol: 21.54 ± 0.33 mm3, N=8; **p<0.005)

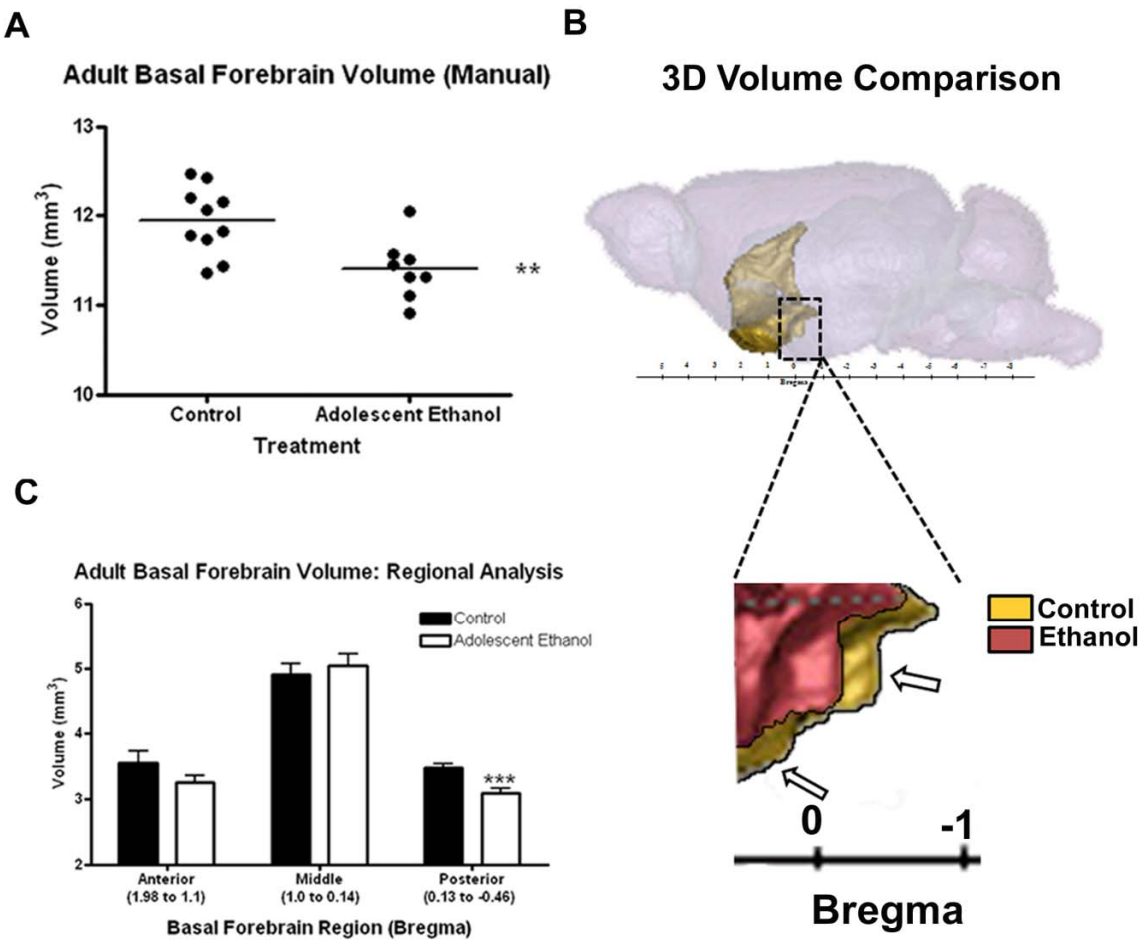

Figure 3.10: Adolescent ethanol binge causes a reduction in the volume of the basal forebrain/medial septum brain region in adults. Adolescent mice received either water or ethanol (5g/kg) once a day for ten days (P28-37). Postmortem MRI was performed on adults (P79), the basal forebrain region was manually segmented by blinded investigators, and its volume was measured. (A) 3D schematic of the location of the basal forebrain/medial septum region from the top, sagittal, and front/coronal perspectives. (B) Basal forebrain volumes from manual segmentation. Adult mice that previously received ethanol showed a 4.6% reduction in the volume of the basal forebrain/medial septum region (Control: 11.95 ± 0.12 mm3, N=10; Ethanol: 11.40 ± 0.12 mm3, N=8 **p<0.01). (C) A regional analysis of the basal forebrain volume shows that the majority of the volume reduction (11% reduced from controls) was to the posterior segment of the basal forebrain (bregma + 0.13 to -0.46), ***p<0.001 (D) sagittal 3D rendering of two representative cases showing volume reduction in adult mice that received adolescent binge ethanol.

By integrating images into a 3-dimensional rendering and overlaying forebrain (Fig. 3.10), we show that the posterior forebrain (bregma + 0.13 to -0.46) accounted for most (71%) of the regional volume loss (Figure 3.10C, 11% reduced from controls, ***p<0.001). To further investigate forebrain structure, histological sections were prepared and histochemistry used to determine cellular composition and forebrain/septum volume. Immunohistochemistry for GABA interneuron subtypes markers calretinin, calbindin, and

parvalbumin (PV) did not show visible changes in the density of these neurons. PV+IR neuron density is high in forebrain, allowing visualization of basal forebrain boundaries facilitating assessment of basal forebrain histology area. Area assessments of forebrain with PV+IR sections indicated adolescent binge alcohol treatment reduced basal forebrain area ($p<0.05$, 2-Way ANOVA, Figure 3.11). Dividing forebrain into bregma regions as done with MRI indicated histological forebrain area was reduced particularly in the more posterior regions of the basal forebrain from bregma + 0.02 to – 0.22 (Figure 3.11A, $*p<0.05$, *t*-test). Examples of two of the measured regions of interest in the posterior basal forebrain are shown (Figure 3.11B, C). Reduced histological basal forebrain area supports the observed MRI volume reduction in the posterior basal forebrain. Thus, adolescent binge ethanol treatment results in reduced volume of adult olfactory bulbs and basal forebrain.

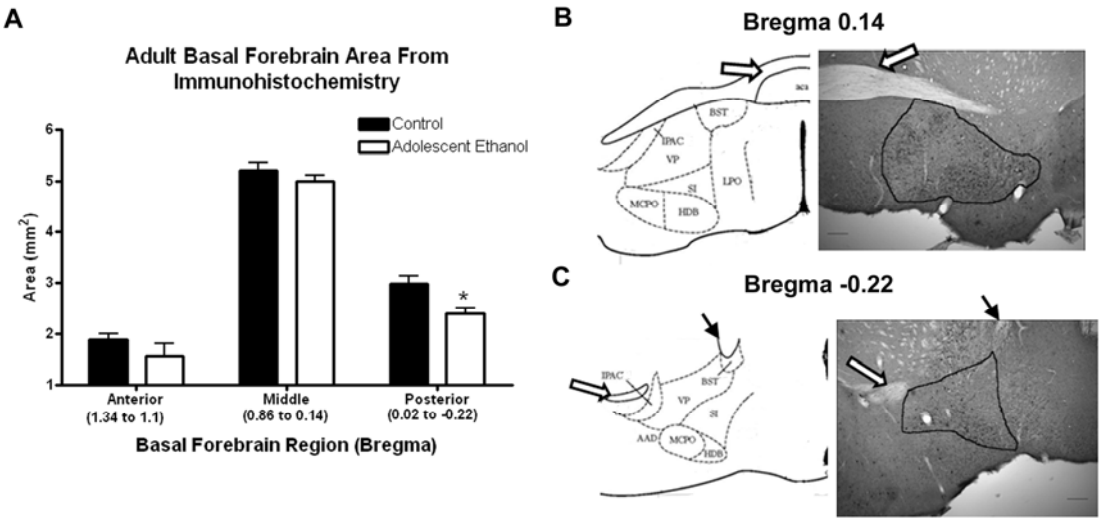

Figure 3.11: Basal forebrain nuclei area reduction in adults following adolescent ethanol treatment. In order to confirm volume reductions, the area of the basal forebrain region nuclei was measured microscopically using bioquant software on sections immunolabeled for parvalbumin. (A) The basal forebrain area was significantly reduced in the posterior bregma of the basal forebrain: 20% difference, 0.02 to -0.22 mm, * p<0.05. Basal forebrain areas measured at bregma 0.14mm (B) and -0.22mm (C) are shown from representative sections. The anterior commissure (open arrow) and internal capsule (closed arrow) were used as landmarks and are labeled on the atlas and image to help with orientation. Key: VP-ventral pallidum, SI-substantia innominata, HDB-horizontal diagonal band, MCPO-magnocellular preoptic nucleus, LPO-lateral preoptic area, IPAC-interstitial nucleus of the posterior limb of the anterior commissure, BST-bed nucleus of stria terminalis, AAD-anterior amygdaloid area dorsal, aca-anterior commissure anterior.

Adolescent Binge Ethanol Causes a Reduction in the Number of Cholinergic Neurons in the Adult Basal Forebrain.

Basal forebrain cellular composition was investigated using IHC. As mentioned above, histochemistry for GABA interneuron markers calretinin, calbindin, and parvalbumin found no marked changes after adolescent alcohol treatment. Similarly, astroglial marker glial fibrillary acidic protein was similar between groups (data not shown). The basal forebrain is rich in cholinergic neurons, critical for learning and memory, that project to multiple brain regions to integrate cortical activity. We used ChAT+IR to identify cholinergic neurons (Fig. 3.12). The density of ChAT+IR neurons was decreased 7.5% from 166 to 153 cells/mm^2 in the Ch4 region (see Methods) of the basal forebrain (Figure 3.12A, *p<0.05). This change is similar in magnitude to the observed volumetric reduction in these mice, suggesting that cholinergic neuron loss contributes to the reduction in basal forebrain volume. Thus, adolescent binge drinking reduced density of ChAT+IR neurons in the adult basal forebrain.

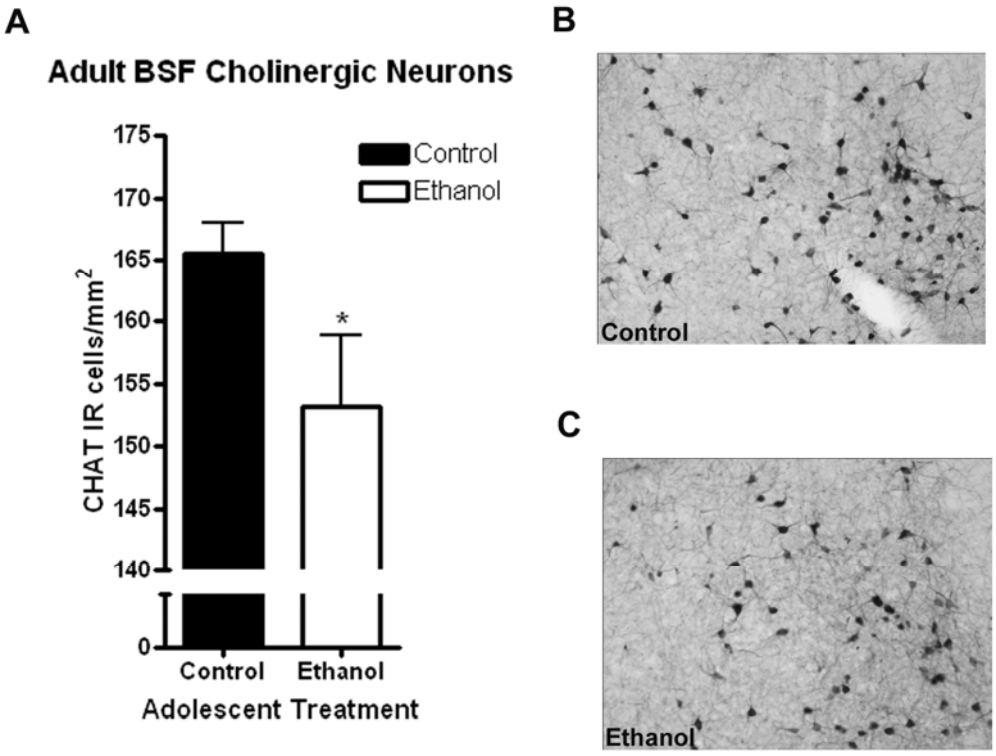

Figure 3.12 Acetylcholinergic neuron reductions in the basal forebrain. Acetylcholine neurons were identified by immunohistochemistry for choline acetyltransferase (ChAT). ChAT-immunoreactive neurons were counted in the posterior regions of the basal forebrain (bregma 0.14mm to -0.22mm), where the greatest volume changes were observed. This included the horizontal diagonal band, substantia inominata, ventral pallidum, and magnocellular preoptic nucleus. Significant reductions in the number of ChAT neurons per area were observed (7.5% reduction, *$p<0.05$). Representative images from an adult control (B) and ethanol (C) at the same bregma (0.14mm) showing differences in ChAT neuron density.

Discussion

Changes in adult neurotransmitter-specific gene expression, postmortem MRI brain region volumes, forebrain histological area, cholinergic neuron density and reversal learning converge to support the conclusion that adolescent binge drinking in mice persistently alters the adult brain. We found greater levels of neurotransmitter-specific gene expression in adolescent brain than adult brain, consistent with other studies finding that dopaminergic,

cholinergic and other key neurotransmitters peak during adolescence (Andersen et al., 2000; Crews et al., 2007a; Spear, 2000; Tarazi and Baldessarini, 2000). Adulthood changes in neurotransmitter gene expression over 50 days were not as large as adolescent maturational changes in neurotransmitter gene expression, but were statistically evident, suggesting neurotransmitter maturation continues into adulthood. Binge ethanol treatment in adolescence dramatically reduced expression of many neurotransmitter-specific genes early after treatment (P38, Fig. 3.2). None of the neurotransmitter-specific genes showed increased expression following ethanol treatment of adolescents. The greatest reductions were found with the combination of binge adolescent ethanol treatment followed by development to young adulthood, P88. The expression of several genes implicated in mental illnesses were decreased by adolescent binge ethanol treatment. Binge ethanol during adolescence, but not adulthood, decreased DA-D4R mRNA and orbital frontal cortical D4DR+IR in adolescence. D4 receptors bind atypical antipsychotics with higher affinity than other dopamine receptors (Van Tol et al., 1991), and are implicated in novelty seeking, substance abuse (Lusher et al., 2001; Munafo et al., 2008) and attention deficit with hyperactivity disorder (Bellgrove and Mattingley, 2008). Thus, adolescent binge drinking alters D4 dopamine receptors, particularly in the orbital frontal cortex.

GRPR (gastrin-releasing peptide receptor), COMT, dopamine receptors D1A, and D2 were not altered in adolescence immediately following binge treatment (P38), but after treatment, during young adulthood, mRNA expressions were about half as much as their age matched controls (Table 3.2, P88 Ethanol). Binge ethanol treatment of adolescent rats has been found to reduce D1 and D2 protein levels in frontal cortex and other brain regions (Pascual et al., 2009) and human alcoholics have fewer brain D2 receptors that are suggested

to be a predisposing factor due to persistently low levels in both early and late withdrawal (Volkow et al., 2002). Decreases in dopamine receptors could be associated with decreased motivation (Ernst et al., 2009). GRPR expression, a receptor for gastrin releasing peptide and bombesin, was stable across the ages studied, but adolescent binge treatment reduced adult expression 45% without altering adolescent expression. GRPR is enriched in amygdala and GRPR deficient mice show enhanced fear conditioning with normal spatial learning and no anxiety-like behavior in the water maze and elevated plus maze, respectively (Shumyatsky et al., 2002). Environmental enrichment during adolescence increases GRPR expression and reduces fearfulness (Qian et al., 2008), suggesting that environmental amygdala plasticity during adolescence is in part reflected in GRPR expression and lifelong sensitivity to amygdala fear conditioning. COMT polymorphisms have been implicated in many disorders including addiction (Enoch, 2006), schizophrenia (Tan et al., 2007), aggression (Volavka et al., 2004), and Alzheimer's disease (Serretti et al., 2007). These findings indicate that adolescent ethanol exposure alters expression of neurotransmitter genes in the young adult brain that are associated with psychopathology.

Heavy episodic drinking within the past 2 weeks is reported by 12% of 8th graders, 22% of 10th graders, 28% of 12th grade seniors and 44% of college students (Johnston et al., 2004; Masten et al., 2008; Wechsler et al., 1995; Windle et al., 2008). In our model of adolescent binge drinking in C57BL/6 mice the 5 gm/kg/day dose is less than mice from this strain drink by choice (>15 gm/kg/day) (Crews et al., 2004). The high peak blood ethanol levels (288 mg/dL) in this model are appropriate since alcohol dependent human adolescents report approximately 13 drinks per drinking episode (Deas et al., 2000), consistent with blood ethanol levels of 250-299 mg/dL, 50-65 mM (Jones and Holmgren, 2009). C57BL/6

mice metabolize ethanol approximately 3.5 times faster than humans (≈9.7mmole/kg/hr in mice vs ≈2.7mmole/kg/hr in humans), suggesting that elevated blood alcohol levels persist longer in humans than mice (Thurman et al., 1982; Bradford et al., 2007). Our adolescent binge ethanol treatment followed by assessments in young adults mimics the "young adult alcohol dependent subtype," the most common alcohol dependence subtype characterized by heavily drinking during adolescence -young adulthood, and maturation out of dependence (Jacob et al., 2005; Moss et al., 2007). Although it is of interest to distinguish adolescent from adult responses, since human adolescents represent the majority of binge drinkers, understanding the persistent effects of adolescent binge ethanol on the adult brain may be the most important for human health considerations. Therefore, though we compared the effects of binge ethanol during adolescence with that of adults on neurotransmitter receptor genes, we focused the remainder of our analyses on the persistent effects of the adolescent binge. Our model replicates rat models of binge drinking that did not demonstrate changes in locomotor activity (Slawecki et al., 2001), water maze spatial learning (Schulteis et al., 2008; White et al., 2002) or elevated plus maze performance (White et al., 2002). We found alterations in reversal learning in young adult mice after adolescent binge treatment, consistent with an adult rat binge drinking model (Obernier et al., 2002b). Reversal learning deficits have been observed in human alcoholics (C. B. Fortier et al., 2008), cocaine addicts (Fortier et al., 2008; Stalnaker et al., 2009) and neurodegenerative diseases (Freedman and Oscar-Berman, 1989; Oscar-Berman and Zola-Morgan, 1980). Frontal cortex, where we found altered adolescent D4DR expression, and marked rat adolescent binge brain damage (Crews et al., 2000a), is implicated in drug dependence and reversal learning deficits (Schoenbaum et al., 2009). Reversal learning deficits have also been observed in rats and

marmosets following lesions of the basal forebrain (Cabrera et al., 2006; Roberts et al., 1992; Tait and Brown, 2008). Our finding suggests that individuals who drink heavily during adolescence may be more likely to have reversal learning deficits, possibly mediated by chemical or structural changes in frontal cortex or basal forebrain.

Alcohol is known to have differential effects on adolescents than adults. Developing neurocircuitry in adolescents likely underlies the increased sensitivity to disruption of working memory and hippocampal function (White and Swartzwelder, 2004), reduced ethanol sedative response compared to adults (Silveri and Spear, 1998), increased neurotoxicity (Crews et al., 2000b) and exaggerated thrill seeking, social and motivational behaviors (Ernst et al., 2006). Human studies using *in vivo* brain imaging (Pfefferbaum et al., 2009) and postmortem histology (Harper, 2009) find alcoholics have brain volume reductions compared to age matched controls, including adolescents (De Bellis et al., 2005). Pre-existing conditions (Prescott and Kendler, 1999) and/or binge drinking induced pathology (Stephens and Duka, 2008) could contribute to differences between binge and non-binge drinkers.

To our knowledge, this is the first report of young adult mouse brain MRI following adolescent binge treatment. We found reduced olfactory bulb and basal forebrain volume. Alcoholics have persistent olfactory deficits (Kesslak et al., 1991; Rupp et al., 2003), associated with loss of brain volume and ventricular expansion (Shear et al., 1992). We found a 4-10% volume reduction across basal forebrain regions, comparable in magnitude to human MRI brain regional volume reductions in alcohol use disorder (Makris et al., 2008; Sullivan et al., 2005). Human MRI medial septal/diagonal band volume is negatively correlated with age in alcoholic individuals, with volume reductions being associated with

deficits in verbal working memory (Sullivan et al., 2005). Basal forebrain cholinergic neurons project to frontal cortex, hippocampus, and amygdala. These neurons modulate information processing, allowing contextual associated information to exist concurrently in memory with little interference to facilitate reversal plasticity. Proactive interference, previous learning disrupting later learning, is minimized by forebrain acetylcholine. Human fMRI shows basal forebrain activation during resolution of proactive interference tasks in normal individuals but not in alcoholics (De Rosa et al., 2004). Damage to the basal forebrain could alter an individual's ability to resolve proactive interference, altering reversal learning ability. These findings, taken together with our findings suggest persistent basal forebrain dysfunction following adolescent binge drinking that continues through life.

We found decreases in the expression of many cholinergic-specific genes including ChAT, as well as all 5 subtypes of the muscarinic cholinergic receptors measured in young adult mice following adolescent binge treatment. Postmortem brains from humans with alcohol use disorder have fewer muscarinic receptors and other cholinergic markers in hippocampus (Freund and Ballinger, 1989a; Nordberg et al., 1983) and cerebral cortex (Freund and Ballinger, 1989b). Adolescent binge treatment of rats has been shown to disrupt adult sleep and electrophysiology consistent with altered cholinergic systems (Ehlers and Criado, 2010). In adult rats, 28 weeks of alcohol treatment results in a progressive and persistent loss of 60-80% of multiple induces of forebrain cholinergic neurons (Arendt et al., 1995; Arendt et al., 1988b) that are associated with memory impairments (Arendt et al., 1988a). After 8 weeks of ethanol treatment in adult rats, full recovery of reductions in ChAT activity was observed in the basal forebrain during 4 weeks of abstinence (Arendt et al., 1989). We found reduced forebrain histological area and cholinergic neuron density in

young adult mice following adolescent binge treatment for only 10 days, with no evidence of recovery from gene array or immunohistochemistry.

In summary, adolescent binge ethanol treatment of mice reduces young adult neurotransmitter gene expression, particularly cholinergic genes, as well as forebrain MRI volume, histologic area, cholinergic neuron immunohistochemistry, and reversal learning performance.

Intermittent adolescent binge drinking causes adulthood anxiety and reversal learning deficits, and alters adult regional brain volumes.

Leon G. Coleman Jr., Ipek Oguz, Martin Styner, and Fulton T. Crews

Introduction

Alcohol is known to cause immediate neurotoxicity and disruption of behavioral functions during adolescence. Heavy episodic drinking is common among adolescents, and often occurs on the weekends, resulting in an 'on-off-on' intermittent temporal pattern of alcohol exposure (Del Boca et al., 2004). Adolescent drinkers participate in heavy and binge drinking (>5 drinks/episode) at substantially higher rates than adults (Jacob et al., 2005; Masten et al., 2008; SAMSA, 2007), with the rate of binge drinking peaking during adolescence (Masten et al., 2008). Though the age of first drink is associated with the prevalence is developing an alcohol use disorder in adulthood (Grant and Dawson, 1997), the majority of adolescent alcohol abusers then 'age out', becoming either light drinkers or abstinent as adults (Jacob et al., 2005; Moss et al., 2008). However, the adolescent period is a developmental time window where functional modification of circuitry associated with cognitive ability, personality and executive function is thought to solidify to establish the adult phenotype (Crews et al., 2007a; Spear, 2000). Several neural systems are undergoing structural and functional changes that are vulnerable to disruption by ethanol (Crews et al., 2007a; Spear, 2000). Therefore, heavy episodic drinking during adolescence may have long-term effects on brain structure and behavior. Using an adolescent intermittent ethanol (AIE)

treatment followed by a prolonged withdrawal period extending into adulthood, we have modeled these key features and hazards of adolescent binge drinking.

Developing brain regions are particularly sensitive to ethanol toxicity. For example, the frontal cortex is developing in adolescence and models of binge drinking in rats find greater neurotoxicity in adolescent frontal regions than adults (Crews et al., 2000a). Several studies have shown structural and cognitive deficits in human adolescent alcohol abusers (De Bellis et al., 2005; Medina et al., 2008; Nagel et al., 2005). However, the long-term effects of adolescent binge ethanol are not known. Since the developmental time frame for many cognitive and emotional functions occurs during adolescence, adolescent binge drinking might cause persistent alterations in brain structure with associated behavioral dysfunction.

Human brain imaging studies have found that several brain regions undergo volumetric changes during adolescence. Cortical gray matter volumes and thickness follow an inverted U-shaped curve with an increase during childhood, a peak during late childhood/early adolescence in most cortical regions, followed by a decline to adult sizes (Giedd, 2004; Giedd et al., 1999; Gogtay et al., 2004; Lenroot and Giedd, 2006; Shaw et al., 2006). White matter volume in both cortical and cerebellar regions, however, increases linearly into adulthood (Giedd, 2004; Ostby et al., 2009). Alcohol may disrupt these developmental changes. Male human adolescents with alcohol use disorder have larger ventral lateral prefrontal cortical volumes (which includes the orbitofrontal cortex) associated with increased white matter (Medina et al., 2008).

Frontal networks responsible for cognitive abilities continue to develop during adolescence (Luna et al., 2004). Alcohol is known to disrupt some of these functions. Adolescent binge drinkers have spatial, verbal, and nonverbal memory deficits (Brown and

Tapert, 2004; Sher et al., 1997; Townshend and Duka, 2005). Reversal learning deficits, (i.e., the inability to replace previous learning) are found in chronic alcoholics (Fortier et al., 2008) and are thought to be an underlying aspect of the pathogenesis of addiction (Crews et al., 2007a; Schoenbaum and Shaham, 2008). Orbitofrontal circuitry is important for reversal learning function and is refined during adolescence (Gogtay et al., 2004; Schoenbaum et al., 2007). A binge in adult rats (Obernier et al., 2002b) as well as a continuous adolescent exposure (Coleman et al 2010) induce long-lasting reversal learning deficits in the Morris water maze (12 days and 4 weeks after treatment respectively). However, the persistent effects of adolescent intermittent ethanol binges on reversal learning are unknown. Anxiety and depression are also common comorbidities of adolescent alcohol abuse (Deas and Brown, 2006). Since human adolescents typically binge drink in an intermittent fashion, we have investigated the long-term effects of AIE on adult reversal learning, anxiety and depression.

Human studies do not allow for the differentiation between pre-existing morphology associated with a predisposition for alcohol abuse and pathology caused by alcohol abuse. We have modeled human adolescent binge drinking using the AIE exposure in mice. In these mice ethanol was administered over a 10 day period during adolescence followed by a prolonged abstinence until adulthood. Adult regional brain volumetric differences were measured using postmortem structural MRI. Behavioral measures for adulthood reversal learning deficits, anxiety-like behavior, and depressive behavior were also performed. AIE resulted in changes in adult mice that are similar to those found in some human studies. A larger adult orbitofrontal cortex (observed in human adolescent binge-drinkers), reversal learning deficits (seen in alcoholics and cocaine abusers) and heightened anxiety-like

behavior (seen in alcoholics) were found in adult mice that underwent AIE. This suggests that human adolescent binge-drinkers may be at risk of brain structural and behavioral deficits that can persist for years after alcohol cessation.

We report that an adolescent intermittent ethanol binge model results in specific brain structural volume differences and a reversal learning deficit as well as reduced time spent in the center of the open field which suggests anxiety-like behavior in adulthood.

Methods

Animal treatment

Male C57BL/6 mice were ordered from Charles River Labs (Raleigh, NC), and were allowed to acclimate to the animal facilities for seven days in our animal facility prior to treatment. Adolescent mice were requested with the stipulation that all mice were the same weight in order to reduce potential variability in brain size. Mice were given either water or ethanol (5g/kg, i.g. 25% ethanol w/v) once a day during adolescence (P28-37) in an intermittent fashion (Figure 4.1).

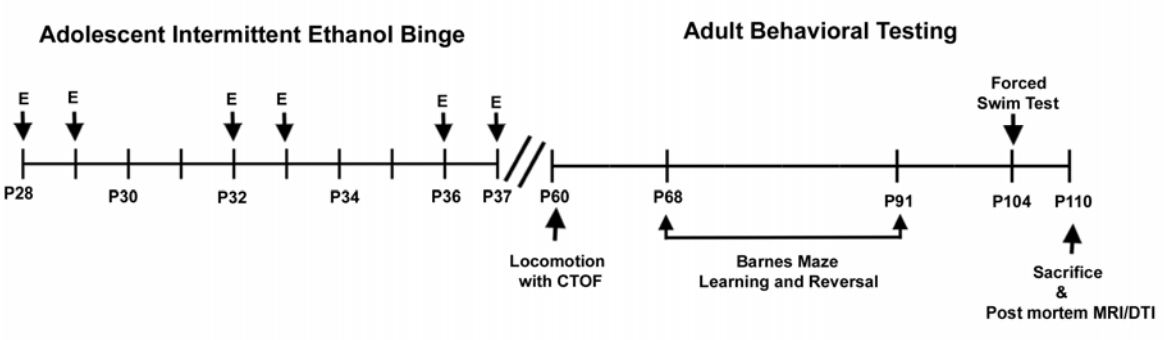

Figure 4.1: Adolescent intermittent ethanol (IE) binge and adult behavioral testing schedules. Mice were given either water or ethanol (5g/kg, i.g. 25% ethanol w/v) once a day during adolescence (P28-37) in an intermittent fashion. Water or ethanol was administered on days P28, P29, P32, P33, P36, and P37. Behavioral testing began in young adulthood on P60 with locomotor activity and center time in the open field. Spatial initial learning and reversal learning were measured using the Barnes maze from P68-91. Depressive behavior was assessed using the forced swim test on P104. Mice were sacrificed by perfusion on P110 for postmortem brain diffusion tensor imaging (DTI).

Specifically, water or ethanol was administered on days P28, P29, P32, P33, P36, and P37. In our lab this concentration of ethanol given to adolescent mice results in average blood alcohol levels of 310 mg/dL ± 93.7 (mean±SEM) measured 1 hour after the last ethanol administration. This blood alcohol level is similar to predicted levels in alcohol-dependent adolescents who report approximately 13 drinks per episode (Deas et al., 2000), which is estimated to result in average blood alcohol levels of approximately 250-299 mg/dL, 50-65 mM (Jones and Holmgren, 2009). There were no differences in weight between the two groups during the ethanol treatment (not shown). All protocols were approved by the University of North Carolina Institutional Animal Care and Use Committee and were in accordance with the Congressional Animal Welfare Act.

Perfusion and brain tissue preparation for MRI and IHC

Mice were sacrificed by perfusion with contrast agent for postmortem brain imaging. Mice were perfused with 0.1M phosphate buffered saline (PBS) and the gadoteridol contrast agent Prohance (10:1, v:v, 37°C) (Bracco Diagnostics, Princeton NJ) followed by a mixture of 4% PFA and Prohance (10:1, 4°C), similar to a previous study (Badea et al., 2009). Mouse skulls with the brains intact were stored in a PBS/Prohance solution (100:1) until scanning.

Adult Behavior

Behavioral testing began in young adulthood on P60. The following tests were performed: open field locomotion with center time (P60), Barnes maze learning and reversal (P68-91), and forced swim test (P104). Mice were sacrificed by perfusion on P110 for postmortem brain diffusion tensor imaging (DTI). All behavioral testing was performed in the UNC

Neurodevelopmental Disorders Research Center Mouse Behavioral Phenotyping Core using previously published methods (Moy et al., 2007).

Locomotor activity: Mice spent two hours in the open field chamber (40 cm x 40 cm x 30 cm, VersaMax system, AccuScan Instruments) (Moy et al., 2007). Total locomotor activity and time spent in the center of the open field were measured.

Barnes Maze spatial learning with reversal: The Barnes maze is a large, brightly-lit, circular platform (diameter = 122 cm), elevated 96.5 cm from the floor, and positioned like a table with 40 holes (diameter = 5 cm) drilled along the perimeter (Figure 4.2C). An escape box was located under one of the holes, and mice learned which hole allowed for escape from the maze surface. Each mouse was given his own individual escape location, which remained constant across the learning days. Mice were given one trial per day, with up to five minutes per trial to find the escape. The experimenter was blinded to treatment condition. Once criterion for initial learning was achieved (>20 second average latency to escape across all subjects), mice were given four days to rest prior to reversal learning trials. For reversal learning, each mouse's escape location was relocated to the hole that was exactly 180 degrees from the initial location. Mice were then given one 5 minute trial per day until the 20 second average latency was achieved across all subjects.

Forced swim test: This test was used to assess depressive-like behavior. Mice were placed in a clear beaker filled with 12-15 cm of tap water (23-26 ^{o}C) for 6 minutes. The amount of time a mouse spent immobile during the final 4 minutes was measured.

Postmortem MRI volume using semi-automatic segmentation

Whole mouse skulls with brain intact were scanned individually at the UNC Biomedical Research Imaging Center (BRIC) on a 9.4 Tesla Bruker BioSpec spectrometer (Bruker Biospin Inc., Billerica, MA). Total scan time was 15 hours 18min per animal. MRI images (0.12mm x 0.12mm x 0.12mm) were acquired using the following diffusion weighted 3D RARE sequence: TR=0.7s, TE_{eff} =23.749ms, Rare Factor = 3, RARE echo spacing = 11.3067ms, diffusion gradient time *d* =6ms, diffusion gradient separation D = 12.422, b value – 1600s/mm^2, matrix size = 200x125x80, FOV=24.0mm x 15mm x 9.6mm. Mean diffusivity images, computed from the reconstructed diffusion tensor data, were aligned and brain structures were segmented using an automatic segmentation protocol developed at the UNC Neuro Image Research and Analysis Laboratory (NIRAL) (Lee et al., 2009b). Following automatic segmentation, blinded investigators manually segmented selected regions of interest identified from the automatic segmentation, as well as measuring region volume and fractional anisotropy using ITK-SNAP^{TM} software version 1.8. Brain region boundaries were determined using the Brookhaven National Library 3-D MRI Digital Atlas Database of the adult C57BL/6 mouse (www.bnl.gov/medical/RCIBI/mouse) and the mouse brain atlas (Franklin and Paxinos, 2001).

Immunohistochemistry

Immunohistochemistry was performed as described previously (Coleman et al., 2009; Crews et al., 2004). Briefly, three to six sections (40μm) were incubated with 0.6% H_2O_2 to remove

endogenous peroxidase activity. Primary antibody incubation was performed overnight at 4°C (choline acetyl transferase 1:500, Millipore; GFAP 1:500 DAKO; Iba-1 1:1000 WAKO). Secondary antibody (1 hr, 1:200), ABC incubation (1hr) and DAB activation were performed at room temperature on the following day. The Bioquant Nova Advanced Image Analysis System™ was used to assess histological area and neuron using as described previously (Coleman et al., 2009; Crews et al., 2004). We have shown previously that this method results in nearly identical percent changes between treatment and control groups as other unbiased stereological techniques (Crews et al., 2004).

Structural volume statistics: For brain structural volume data, Student *t*-tests were performed to identify candidate regions for further manual segmentation ($p<0.05$ for significance). Since performing multiple comparisons can result in the reporting of false positives, the false discovery rate (FDR) was employed to calculate the number of false positives expected from the *p*-value distribution of the data set. The FDR method reports a *q*-value, which is used to calculate the number of false positives expected. The *q* values were calculated using the bootstrap method using the *Q-value* module in the *R for Windows Software* © (R Development Core Team 1995-2009). The following formula was then used to determine the number of false positives: # false positives = q_{target} x (# of regions with $q_{calculated} \leq q_{target}$). The threshold for significance was set such that the likelihood of a false positive would be less than 0.025. For this data set, this corresponded to a *q*-value < 0.09. The Grubb's Test was employed to identify outliers. The formula for the Z score for each data point was: Z=|mean-value|/standard deviation. $Z_{critical}$ was obtained from a Grubb's table of Z scores. No more than one outlier per data set was permitted to be removed. One outlier was detected

in the orbitofrontal cortex volume using the Grubb's test for outliers in the AIE treated group ($3.78mm^3$, $Z=2.26$, $Z_{critical} = 2.13$).

Behavioral and Immunohistochemistry statistics: A 2-way repeated measures ANOVA was performed for learning studies in the Barnes maze as well as for locomotor activity, followed by a Bonferroni post-test to evaluate significance at individual time points.

Results

Intermittent ethanol binge during adolescence causes a reversal learning deficit in adulthood without affecting initial learning

Reversal learning deficits have been observed in human alcoholics (Fortier et al., 2008), cocaine addicts (Fortier et al., 2008; Stalnaker et al., 2009), and in neurodegenerative disorders (Freedman and Oscar-Berman, 1989; Oscar-Berman and Zola-Morgan, 1980). This inability to replace a previously learned behavior with a new response was assessed using the Barnes maze. Mice received either water or binge ethanol during adolescence (P28-37) as described previously (Figure 4.1). Adult mice (P68) were tested first for their ability to learn the initial escape location. Each mouse was assigned its own specific escape location that remained constant for the initial learning days (e.g. Figure 4.2C). Both groups of mice successfully learned to find the escape, reaching criterion by the sixth day of testing. There was no significant main effect of adolescent treatment on adult escape latency during initial learning (Figure 4.2A; 2-way repeated measures ANOVA: $p=0.15$, $F=2.33$). Neither was there an effect of adolescent treatment on the number of errors during initial learning trials (Figure 4.2B; $p=0.26$, $F=1.37$). After initial learning acquisition, the escape location

for each mouse was changed to the hole located directly across from the initial learning location. The ability of mice to 'unlearn' the previous location and learn the new escape location was then assessed (P81).

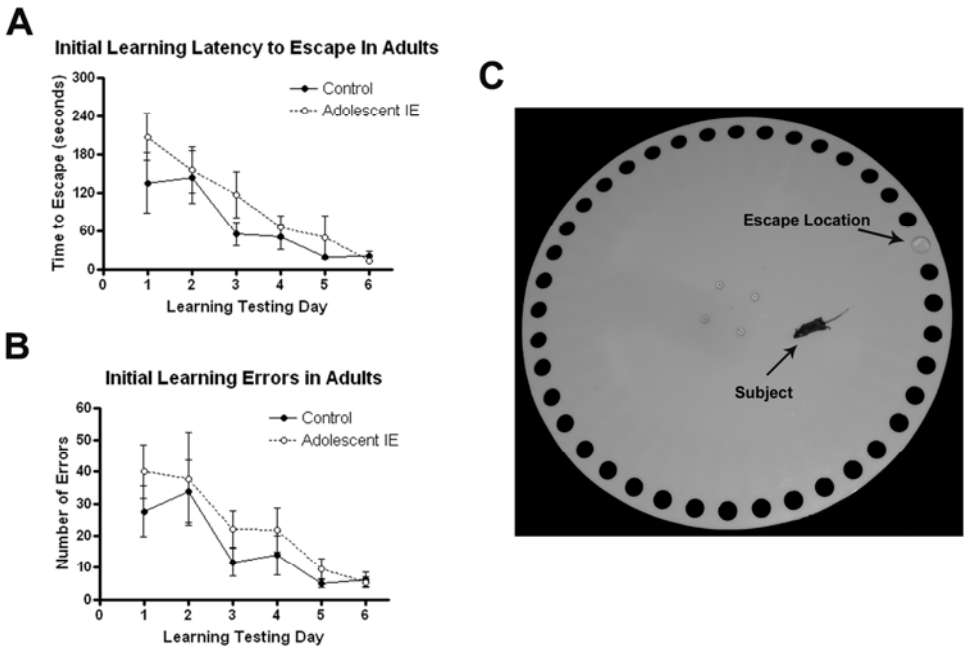

Figure 4.2: Intermittent adolescent binge ethanol does not alter initial learning in adult mice in the Barnes maze. Mice were given either water or ethanol (5g/kg, i.g.) in intermittent fashion (IE) during adolescence (P28-37). Spatial learning was assessed using the Barnes maze for six days in adulthood (P68-73). (A) Latency to escape. There was no significant main effect of adolescent treatment on latency to find the escape location during initial learning days (2-way repeated measures ANOVA: p=0.15, F=2.33). (B) Errors during initial learning. There was no significant main effect of adolescent treatment on the number of errors made during initial learning (p=0.26, F=1.37). (C) A photograph of a mouse on the Barnes maze. The subject and its assigned escape location are identified. N= 7 Control, 8 IE mice.

Mice that received intermittent ethanol binge during adolescence showed a clear deficit in reversal learning (Figure 4.3). IE mice were significantly slower than controls to learn the new escape location (Figure 4.3A; 2-way repeated measures ANOVA *p<0.03, F=6.22). IE mice also made more errors than controls (Figure 4.3B; *p<0.02, F=8.011). On the first day of reversal testing, IE adult mice spent nearly three times longer searching for the new escape location (control: 55.2s vs ethanol: 149.7s, **p<0.01 Bonferroni post-test), while making twice as many errors than controls (Figure 4.3B; control: 22.3 errors vs ethanol: 46.1 errors, **p<0.05 Bonferroni post-test). By the third day of testing, IE mice were closer to controls in the time needed to escape and the number of errors made. However, the distance travelled

in search of the escape remained elevated in IE mice through the fifth day of testing, during which IE mice traveled more than six times farther than controls ($p<0.05$, Bonferroni post-test). On average, IE mice traveled 3.4 times farther than controls searching for the escape across the six days of reversal testing ($p<0.01$, F=9.137). This demonstrates that the AIE binge caused deficits in reversal learning that were detectable over six weeks (44 days) after the adolescent treatment.

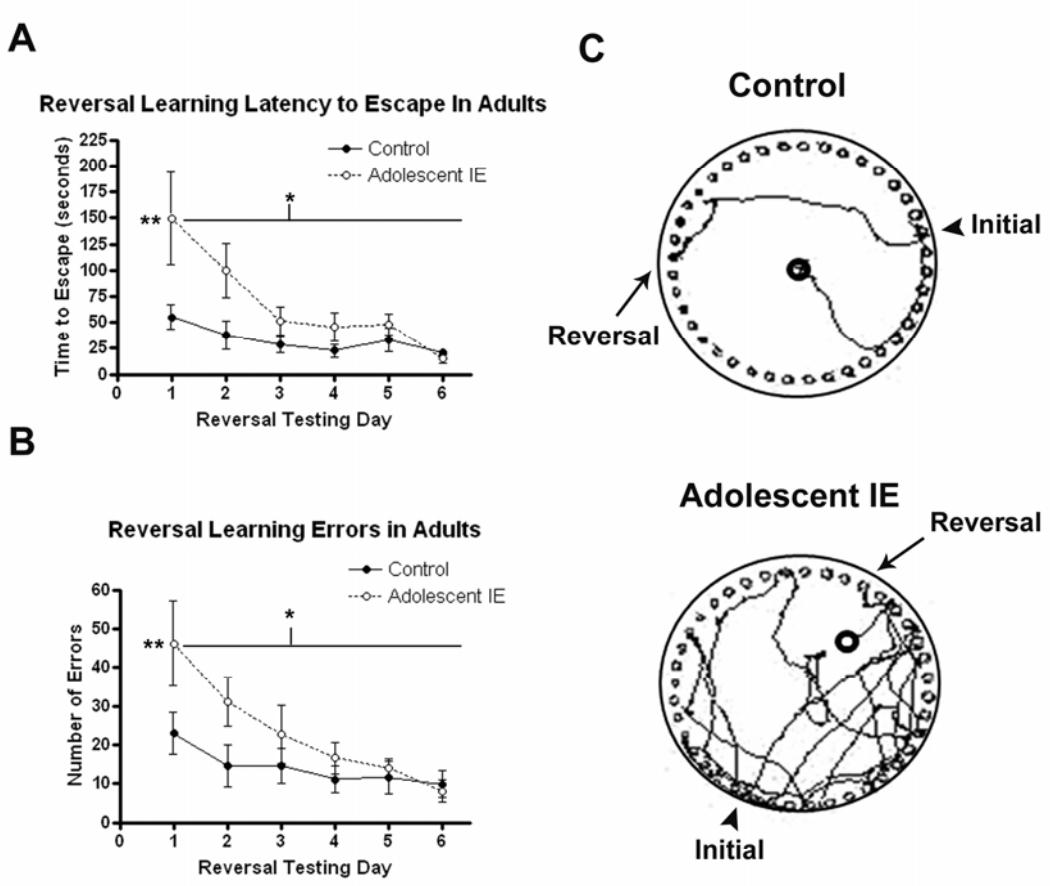

Figure 4.3: Intermittent adolescent binge ethanol causes a reversal learning impairment in adult mice in the Barnes maze. Mice were given either water or ethanol (5g/kg, i.g.) in an intermittent fashion (IE) during adolescence (P28-37). Reversal learning using the Barnes maze was assessed beginning on P81 for six days after initial learning was acquired. (A) Latency to escape. IE mice were slower to learn the new escape location than controls (2-way repeated measures ANOVA: p<0.03, F=6.22). IE mice spent nearly three times longer searching for the new escape on the first day of reversal testing than controls (p<0.01, Bonferroni post-test). (B) Errors during reversal learning. IE mice made significantly more errors than controls across the reversal learning period (p<0.02, F=8.011), making twice as many errors than controls on the first day (p<0.05, Bonferroni post-test). (C) Drawings of the paths taken by one control and one IE mouse in search of the escape on reversal day 1. Note how both mice revisited the initial learning location, though the IE mouse searched more at the former and traveled substantial more around the entire maze than the control mouse.

AIE causes anxiety-like behavior in adulthood

Heightened anxiety is common in human alcoholics (Deas and Brown, 2006). Non-conditioned anxiety-like behavior was assessed during adulthood by measuring time spent in the center of the open field. There were no significant differences in total locomotion during the two hours of testing in the open field (Figure 4.4A. p=0.22, F=1.698). Both groups showed the characteristic pattern of high initial levels of locomotion followed by a reduction in activity during habituation to the chamber. When the time spent in the center was measured, a clear deficit was observed. Adult mice that received IE binge spent less than 57% as much time as controls exploring the center of the open field box (Figure 4.4B, $^{**}p<0.005$). Controls spent 18.4 minutes (15.4% of the 2h period) exploring the center, while mice in the IE group spent 10.5 minutes (8.7% of the 2h) in the center. This robust reduction in center exploratory behavior is associated with anxiety-like behavior. The forced swim test was used to assess depressive behavior in adults. There were no differences in float time between treatment groups (not shown; t-test, p=0.76) suggesting no differences in depression-like behavior as measured by the forced swim test. These studies demonstrate that the adolescent IE binge resulted in persistent heightened non-conditioned anxiety-like behavior in adults.

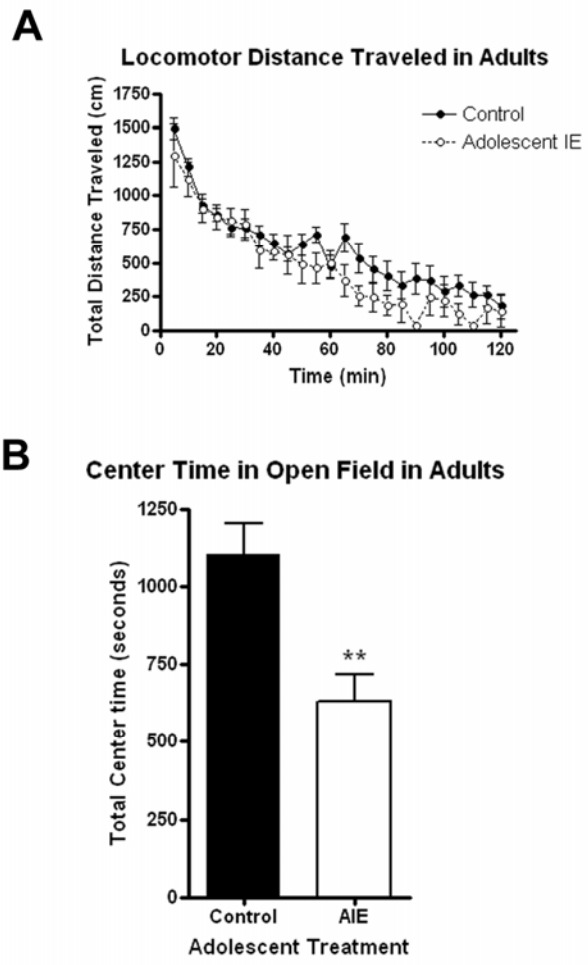

Figure 4.4: Intermittent adolescent binge ethanol causes anxiety-like behavior in adults without altering total locomotor activity measured in the open field test. Mice were given either water or ethanol (5g/kg, i.g.) in an intermittent fashion (IE) during adolescence (P28-37). Total locomotor activity and time spent in the center of the open field were assessed in young adults (P60). (A) Overall locomotor activity. Adolescent IE binge did not alter overall locomotor activity in adult mice across the two hour testing period ($p=0.22$, $F=1.698$). (B) Center time in the open field. Mice that underwent IE binge during adolescence spent less time in the center of the open field than controls consistent with anxiety-like behavior (57% of controls, $^{**}p<0.005$).

Regional brain volume differences in adult mice following adolescent IE binge

We examined the effect of adolescent IE binge on the volumes of multiple adult brain regions using structural brain imaging. There was no significant difference in total brain volume between groups (401.6 ± 4.25 vs 408.2 ± 2.64 mm^3, controls vs IE group mean ± SEM; p=0.20, t-test, P80). However, statistically significant differences were found in specific brain regions. Surprisingly, the internal capsule (+10.1%, $p<0.002$ t-test, q = 0.02 FDR), orbitofrontal cortex (+4.2%, $p<0.004$; $q = 0.028$), thalamus (+2.1%, $p<0.014$; $q = 0.071$), cerebellum (+4.5%, $p<0.019$, $q = 0.089$), and genu of the corpus callosum (+7.1%, $p<0.03$, $q = 0.089$) were larger in AIE treated animals (Table 4.1). There were no volume changes in the rest of the prefrontal cortex, including the medial prefrontal region (not

shown). The remainder of the corpus callosum and external capsule without the genu showed no significant differences (p=0.13, q=0.26). No changes were seen in astroglial activation (GFAP) or microglia structure (Iba-1) across multiple brain regions; neither was there a change in basal forebrain Ch4 region cholinergic neuron density as determined using immunohistochemistry (data not shown).

Table 4.1: Adult regional brain volume differences following adolescent intermittent ethanol binge

Brain Region	Control (mm^3)	Ethanol (mm^3)	% Difference	p value (*t*-test)	q values (FDR)
Internal Capsule	2.48	2.73	+ 10.1	0.0013 **	0.018 ***
Orbitofrontal Cortex	3.97	4.13	+ 4.2	0.0037 *	0.026 ***
Thalamus	25.4	26.0	+ 2.1	0.014 *	0.066 ***
Cerebellum	55.0	57.5	+ 4.5	0.027 *	0.082 ***
Genu of Corpus Callosum	0.07	0.08	+ 7.1	0.029	0.082
Basal Forebrain	11.3	11.9	+ 5.3	0.11	0.21
Rest of Neocortex	138.3	142.9	+ 3.3	0.11	0.21
Remainder of Corpus Callosum	8.60	8.90	+ 3.5	0.13	0.21
Rest of Midbrain	12.6	12.9	+ 2.4	0.15	0.21
Inferior Colliculi	5.70	5.90	- 3.5	0.15	0.21
Central Gray	4.30	4.40	+ 2.3	0.30	0.39
Ventricles	2.60	2.40	+ 7.7	0.34	0.40
Brain Stem	50.8	54.1	+ 6.5	0.37	0.40
Fimbria	2.26	2.32	- 2.7	0.40	0.40
Superior Colliculi	8.50	8.70	- 2.4	0.47	0.43
Olfactory bulb	19.0	18.7	+ 1.6	0.49	0.43
Hypothalamus	12.3	12.4	+ 0.8	0.62	0.49
Caudate & Putamen	25.8	26.1	- 1.2	0.63	0.49
Amygdala	12.8	12.9	+ 0.8	0.75	0.56
Globus Pallidus	3.13	3.13	+ 0.0	0.94	0.63
Hippocampus	25.3	25.7	- 1.6	0.95	0.63
Anterior Commissure	0.94	0.94	0.0	0.98	0.63

Table 4.1: Adult regional brain volume differences following adolescent intermittent ethanol. Mice were given either water or ethanol (5g/kg, i.g.) in an intermittent fashion (IE) during adolescence (P28-37). Postmortem images (P110) were obtained using 21 directional diffusion tensor imaging (DTI) and analyzed for structural brain volume. Multiple brain regions were segmented in a semi-automatic fashion. Statistical significance was determined using t-tests followed by a false discovery rate (FDR) calculation to identify false positives. Five regions were significantly larger in adults following adolescent IE binge (*p<0.05, t-test with**q-value <0.09, false discovery rate to detect false positives). Larger volumes were found in the internal capsule (+10.1%), orbitofrontal cortex (+4.2%), thalamus (+2.1%), cerebellum (+4.5%), and genu of corpus callosum (+7.1%).

Discussion

Underage drinking is a major public health problem. Between 75-82% of high school seniors report previous alcohol use (Johnston et al., 2004; Johnston, 2006). Adolescents consume large quantities of alcohol, averaging 13 drinks per episode, consistent with blood alcohol levels around 300mg/dL (Deas et al., 2000; Jones and Holmgren, 2009). Thus, the blood alcohol levels following the AIE treatment were around 310mg/dL which is similar to

what is expected in binge drinking human adolescents. Following AIE treatment, we found persistent long-term behavioral and structural differences in adulthood.

We observed a deficit in reversal learning in the Barnes maze. Initial spatial learning was unaffected. This reversal learning deficit in the Barnes maze is consistent with our previous observation in the continuous adolescent ethanol using the Morris water maze (Coleman et al 2010). Our observation of normal initial learning is consistent with previous adolescent ethanol exposure studies in rodents, which showed either no alterations or mild persistent deficits in learning (Schulteis et al., 2008; Sircar and Sircar, 2005). Reversal learning deficits have been seen in abstinent chronic alcoholics (Fortier et al., 2008). Reversal learning deficits, with normal initial learning, have also been observed following either chronic cocaine administration or orbitofrontal lesions in rats (Boulougouris et al., 2007; Schoenbaum and Shaham, 2008). The orbitofrontal cortex is critical for reversal learning tasks (Dias et al., 1996; Schoenbaum et al., 2007). Normal human adults have been found to activate the orbitofrontal cortex during a reversal learning proactive-interference task (De Rosa et al., 2004). However, alcoholics showed a lack of orbitofrontal cortical activation during a reversal learning-like proactive interference task (De Rosa et al., 2004). We observed an enlargement of the orbitofrontal cortex in adult mice that received AIE. This observation is consistent with a previous observation in human male adolescents (15-17 y/o) with alcohol use disorder (AUD) who had larger ventrolateral prefrontal cortical volume (a region that includes the orbitofrontal cortex) than healthy controls (≈10%) (Medina et al., 2008). Frontal cortical regions undergo a developmental change in volume during adolescence, with cortical volumes peaking during early adolescence followed by a decline in volume to adult volumes (Giedd, 2004; Giedd et al., 1999; Gogtay et al., 2004; Lenroot

and Giedd, 2006; Shaw et al., 2006). AIE may disrupt this normal developmental process, resulting in a larger OFC volume, or AIE could affect white matter resulting in larger brain volumes. The observed volume enlargement of the orbitofrontal cortex in conjuction with the reversal learning deficit suggests that orbitofrontal circuitry may be altered and associated with the observed reversal learning deficit.

We also observed that adult mice that underwent AIE spent significantly less time in the center of the open field. The tendency to avoid the center of the open field, or thygmotaxis, is an index of non-conditioned anxiety-like behavior that is exacerbated by anxiogenic drugs and reduced by anxiolytics (Simon et al., 1994; Treit and Fundytus, 1988). Anxiety is a common feature of alcohol use disorders (Deas and Brown, 2006). Anxiety-like behavior has been observed previously following intermittent adolescent alcohol treatment in an intermittent vapor chamber model in rats (Slawecki et al., 2004). Adult rats (P93) that underwent an intermittent vapor chamber ethanol exposure during adolescence (P30-44; 12 hours per day) moved faster to the dark area in the light-dark box, demonstrating anxiety-like behavior (Slawecki et al., 2004). Other studies have observed reduced novel object exploration and increased defecation during a passive avoidance test which might also be related to heightened anxiety (Pascual et al., 2007; Popovic et al., 2004).

Four other regions in addition to the orbitofrontal cortex were had larger volumes in adults that underwent binge-ethanol during adolescence. This included: the internal capsule, genu of corpus callosum, thalamus and cerebellum. Larger regional brain volumes can be associated with cognitive dysfunction. Thalamic enlargement has been associated with negative affect including both depression and suicide in humans (Young et al., 2008; Young et al., 2007). Also, autistic children have larger brains during development. It is interesting

that the regions that showed larger volumes in AIE treated adults are either purely white matter tracts or contain substantial white matter tracts. White matter maturation in the cortex, cerebellum, limbic regions and internal capsule continues through adolescence into early adulthood (Giedd, 2004; Juraska and Markham, 2004; Ostby et al., 2009; Paus et al., 1999). The enlarged ventrolateral prefrontal cortical volume in males with AUD observed by Medina et al was associated with a 7% increase in white matter in this region. This work and our observation suggest that adolescent alcohol use in both humans and mice may alter white matter development. The effect of adolescent ethanol on white matter may be different from the effects of chronic alcohol during adulthood, which is typically associated with white matter reductions (Pfefferbaum et al., 2006; Pfefferbaum et al., 1996).

This study demonstrates that adolescent binge drinking has consequences on adult brain structure and behavior. These structural and behavioral deficits have also been observed in human studies. Individuals that participate in episodic binge drinking during a period of adolescence may be at risk for altered white matter development as well as reversal learning deficits and heightened anxiety. These behavioral dysfunctions could put individuals at risk for numerous difficulties in adult life, making adolescent binge drinking a risk factor for aberrant neurodevelopment.

Discussion

Developing brain systems are uniquely sensitive to ethanol neurotoxicity. The way in which brain regions are affected by ethanol seems to be dependent upon the nature of the developmental process that is occurring at the time of ethanol exposure. This was first demonstrated with transplacental *in utero* ethanol exposure. During the early *in utero* period, the cranium and face, as well as gross brain structure, are forming. Ethanol exposure during this time frame disrupts developmental neuronal migration (Miller, 1997) resulting in craniofacial deficits and severe mental dysfunction resulting in the FAS (Jones and Smith, 1975; Jones et al., 1973; Sulik et al., 1981). P7 in rodents is comparable to the third trimester in humans (Dobbing and Sands, 1979; Ikonomidou et al., 1999). By P7, craniofacial features have developed and cortical migration and lamination is complete. Thus, the development of these regions is not altered by P7 ethanol. However, physiological cell death (PCD) is an ongoing developmental process that is disrupted by ethanol during this time (Ishimaru et al., 1999).

Developing neurons have a heightened vulnerability to apoptosis through the first 2 weeks of postnatal life. Both ethanol and NMDA antagonists result in similar patterns of robust apoptotic neurodegeneration (Harris et al., 2003; Ikonomidou et al., 2000; Ikonomidou et al., 1999; Lema Tome et al., 2006). This has been attributed to the fact that ethanol has NMDA antagonistic properties (Ikonomidou et al., 2000). The timing of maximum degeneration varied across brain regions. P7 ethanol and MK801 induced cell death was greatest in the frontal, parietal, temporal, cingulate, and retrosplenial cortices. Damage in

these regions was almost undetectable following P14 ethanol treatment (Ikonomidou et al., 2000). Other regions, such as the thalamus and hippocampus, were vulnerable to ethanol toxicity earlier, showing maximum degeneration following E19 and P3 ethanol treatment respectively. The vulnerability to apoptotic neurodegeneration during the first two weeks of postnatal life is developmentally regulated. Downregulation of apoptotic proteins caspase-3 and APAF-1 (Yakovlev et al., 2001), as well as upregulation of calcium binding proteins (Lema Tome et al., 2006), are developmental hallmarks coinciding with the ending of the period of vulnerability.

We found that both P7 ethanol and NMDA antagonism by MK801 caused similar long-term alterations in brain structure. The specific cell types damaged by these treatments were previously unidentified. Using activated caspase-3 double immunohistochemistry, we found that P7 MK801 caused activation of apoptotic pathways in both GAD67 + GABA interneurons as well as other GAD67 (-) negative neurons, which we presumed to be excitatory pyramidal neurons. Consistent with this observation, we found a persistent reduction in parvalbumin positive interneurons and layer V pyramidal neurons in the adult prefrontal cortex. P7 ethanol caused a similar pattern of neuron loss in adult animals, with both parvalbumin interneurons and layer II pyramidal neurons lost in prefrontal cortical areas of adults. Thus, ethanol and MK801 have similar long-term effects on cortical neurons. This may be due to the fact that both ethanol (NMDA antagonist and GABA agonist properties) and MK801 (NMDA antagonist) result in an inhibitory neuro-environment, resulting in caspase-3 activation. Interestingly, P7 ethanol caused different effects on adult neurogenesis between males and females, suggesting that there may be gender differences in the response to ethanol. Thus, ethanol during early postnatal life, corresponding to the third trimester or

birth in humans can have long-term effects on adult brain structure and function. This has public health implications for FASD, as pregnant mothers might potentially consume alcohol during the third trimester. Interestingly, ethanol has also been shown to disrupt ocular dominance plasticity during the visual cortical critical period in ferrets (Medina et al., 2003; Medina and Ramoa, 2005), while treatment after the critical period did not have long-term effects on visual cortical plasticity (Medina et al., 2003). This developmental time period occurs during childhood in humans. Thus, ethanol during either late pregnancy or early childhood could have detrimental long-term effects on the adult brain. However, the public health issue of greater concern is that of the long-term effects of alcohol during adolescence.

Alcohol consumption is common in human adolescents. By the senior year of high school, 75-82% of individuals report previous alcohol use (Johnston et al., 2004; Johnston, 2006). Of the 30% of 16-17 year olds reporting current alcohol use, 20% reported participating in monthly binge drinking (>5 drinks on one occasion, at least once a month) (SAMSA, 2007). Rates of hazardous drinking patterns such as binge drinking (>5 drinks per occasion) and heavy drinking (>5 binge drinking episodes in the past month) begin increasing from age 13 and continue to rise steadily through adolescence, reaching a peak between the ages 19 and 25 (Masten et al., 2008). Heavy drinking increases among college students. Forty-four epercent report binge drinking every 2 weeks, and 19% report more than 3 binge drinking episodes per week (O'Malley et al., 1998; Wechsler et al., 1995). The immediate, harmful effects of inappropriate or excessive alcohol—such as reckless behavior, car crashes, and violence—are well known. However, several developmental changes are occurring during adolescence. Given the ability of alcohol to cause long-term deficits during

earlier developmental periods, it is likely that alcohol exposure during the adolescent developmental time period also has long-term persistent effects.

The risk of DSM-IV lifetime alcohol abuse and alcohol dependence in adults is increased in individuals who start regular drinking in adolescence (Grant and Dawson, 1997). However, the majority of heavy drinking adolescents 'age out' and become either low or moderate drinkers. In fact, the most common subtype of human alcohol dependence is adolescent alcohol dependence that is developmentally limited to heavy drinking during adolescence (Jacob et al., 2005; Moss et al., 2008). Alcohol use associated with adverse consequences during late adolescence (ages 16 & 18) was a predictor of major depressive disorder in young adulthood (age 22) (Mason et al., 2008). However, epidemiological studies have not investigated the effects of adolescent drinking on the psychiatric health of older adults. Thus, there is a gap in our understanding of the long-term effects of alcohol abuse that is limited to adolescence since this has not been previously thought to have long-term effects. However, alcohol is a teratogen that has its greatest effects on developing brain tissues. Developmental processes during adolescence may at first appear to be more 'subtle' than those seen during prenatal or early postnatal life. However, these processes are critical for the development of cognitive functions that enable an individual to lead a healthy and productive adult life.

In order to model the common human adolescent alcohol dependent subtype, we employed models of binge drinking during adolescence followed by a prolonged abstinence into adulthood. Adolescents often participate in episodic drinking which occurs on the weekends, resulting in an 'on-off-on' temporal pattern of alcohol exposure (Del Boca et al., 2004). Since the specific pattern of drinking (either episodic or continuous) is thought to be

related to an individual's outcome, we utilized two models of binge drinking—one continuous and one intermittent. Both the continuous and intermittent models of binge drinking resulted in persistent structural and behavioral deficits in adulthood. Our goal was not to directly compare the two treatments or determine which is more harmful. Rather, our goal was to simply make observations on the long term effects of both patterns of ethanol exposure, as they are both models of the heterogeneous human adolescent binge drinking phenomenon. There were interesting similarities and differences between the outcomes of these two treatments.

Several neurotransmitter systems undergo functional remodeling and receptor downregulation during adolescence (Benes et al., 2000; Tarazi and Baldessarini, 2000; Tarazi et al., 1998). Consistent with this, we observed that the continuous adolescent binge enhanced developmental downregulation of many neurotransmitter receptor genes (Chapter 3, e.g. GABA, dopamine, acetylcholine, peptide receptors). Across a similar time period in adulthood, fewer neurotransmitter receptor genes were changing developmentally. A continuous binge during that adult period did not as robustly alter neurotransmitter receptor gene expression, which is consistent with previous observations that ethanol exerts greater effects on developing processes.

Both continuous and intermittent treatment paradigms resulted in reversal learning deficits in adults that underwent the adolescent binge treatment. These deficits were found in two different treatments in two different learning mazes: the Morris water maze (continuous model) and the Barnes maze (intermittent model), which increases the validity of the observation. It is important to note that the reversal learning deficit was not detected during the relearning trials in the Morris water maze, but it was detected during the probe trial after

reversal learning (continuous model). The reversal learning deficit appeared more robust in the Barnes maze (intermittent model) as a difference was observed during the relearning trials. However, the Morris water maze is potentially more stressful than the Barnes since the mice are placed in water, which could be a potential confounder. In order to know exactly which treatment regimen caused greater reversal learning deficits, both treatment groups would need to be tested in the same mazes. The reversal learning deficit is directly relevant to addiction. Reversal learning deficits have been found in human alcoholics (C. B. Fortier et al., 2008), cocaine addicts (Fortier et al., 2008; Stalnaker et al., 2009), and neurodegenerative diseases (Freedman and Oscar-Berman, 1989; Oscar-Berman and Zola-Morgan, 1980). It has been hypothesized that human alcoholics are thought to have difficulty 'unlearning' alcoholic behavior, resulting in perseveration. Furthermore, this deficit may have implications regarding an individual's ability to respond to changes in life as an adult.

The two models of adolescent binge drinking showed differences in adult anxiety-like behavior. There was no change in anxiety-like behavior in adult mice following the continuous adolescent binge. However, adult mice that received the intermittent ethanol binge during adolescence showed an increase in anxiety-like behavior evidenced by spending reduced time in the center of the open field. This is consistent with findings by Slawecki et al using an intermittent vapor chamber exposure model (Slawecki et al., 2004). Breese et al have demonstrated that multiple cycles of ethanol exposure is more anxiogenic than a continuous regimen (Breese et al., 2005). This may be related to the time course of cytokine or stress hormone release after ethanol treatment and during withdrawal. Future experiments

comparing the effects of continuous and intermittent adolescent binge on serum and brain cytokines and stress hormones would add insight to this difference.

Interestingly, regarding the structural changes we investigated, we found different effects between the continuous and the intermittent adolescent binge treatments. The continuous adolescent binge treatment resulted in reduced volumes of the olfactory bulb and the basal forebrain region in adults. The basal forebrain region shows presymptomatic volume reductions in cognitive impairment and in Alzheimer's disease (Hall et al., 2008; Muth et al., 2009). The basal forebrain volume reduction was associated with at reduction in the density of cholinergic neurons in the Ch4 region of the basal forebrain. Basal forebrain cholinergic neurons in Ch4 undergo a developmental decline in density across adolescence. From P21 to P126 the density of ChAT+IR acetylcholinergic neurons in basal forebrain Ch4 nucleus basalis region declines by one half (Bentivoglio et al., 1994). Our observations suggest that continuous ethanol binge enhances this cell loss. The basal forebrain is undergoing additional functional modulations during adolescence. Serotonin synapses and fibers are also reaching characteristic adult patterns in this region during adolescence (Dinopoulos et al., 1997; Dori et al., 1998). The number of serotonergic varicosities forming synapses increased from 17% at P21 to 46% in adulthood. We measured the density of serotonergic fibers in the anterior cingulate of adult mice that underwent continuous adolescent binge using tryptophan hydroxylase immunohistochemistry. There was a trend toward a significant reduction ($p<0.09$, data not shown). Continuous adolescent ethanol exposure might alter the density of these serotonergic fibers and could be measured in future experiments.

It is interesting that the intermittent ethanol binge did not cause either a volume reduction of the basal forebrain or a loss of cholinergic neurons in the Ch4 region. It seems

that more days of ethanol treatment are needed to damage the neurons in this brain region (10 days in continuous model vs. 6 days in the intermittent model). It is possible that the mice in the intermittent treatment group were able to recover on the days without ethanol treatment, resulting in no changes in the volumes of the olfactory bulb and basal forebrain. Instead of volume reductions, specific brain regions showed larger volumes in adult mice that received the intermittent adolescent binge treatment.

Intermittent adolescent binge ethanol treatment resulted in larger volumes of the internal capsule, orbitofrontal cortex, thalamus, cerebellum, and genu of the corpus callosum. The enlargement of the orbitofrontal cortex is consistent with observations in humans showing increased volume of the ventrolateral prefrontal cortex (which includes the orbitofrontal cortex) in adolescent males with alcohol use disorder (Medina et al., 2008). The frontal regions of the adolescent brain undergo a developmental change in volume, resulting in an inverted U-shaped pattern of gray matter volume across adolescence (Giedd, 2004; Giedd et al., 1999; Gogtay et al., 2004; Lenroot and Giedd, 2006; Shaw et al., 2006). It is possible that the intermittent ethanol treatment blocked this functional adolescent refinement of brain volume, resulting in larger volumes in certain brain regions. Future studies that measure brain volumes prior to treatment (P14) after treatment (P38) and in adulthood (P80) are needed in order to test this hypothesis.

Ventrolateral (includes the OFC) prefrontal cortical enlargement in male adolescents with alcohol use disorder was associated with an increase in white matter volume (Medina et al., 2008). The regions where we observed larger volumes are white matter rich regions. Myelination continues linearly across adolescence (Giedd, 2004; Toga et al., 2006) at the same time as a functional reduction in axons occurs. This pattern has been demonstrated in

the splenium of the corpus callosum, where the total number of axons declined by 16% from P15 to P60; but the number of myelinated axons increased by over 6-fold. Thus, if the intermittent ethanol binge treatment interferes with the removal of axons or if in enhanced myelination, enlargements of white matter regions, such as the internal capsule, would be observed. Therefore, future studies are needed to elucidate the effects of adolescent intermittent binge on white matter. Another possibility is that adolescent intermittent ethanol alters the extracellular matrix proteins. The extracellular matrix undergoes functional remodeling from childhood to adulthood (Viapiano et al., 2003; Zimmermann and Dours-Zimmermann, 2008) and is thought to regulate synaptic plasticity. Different extracellular matrix proteins are deposited in response to injury and inflammation (Leonardo et al., 2008) and may be affected by ethanol. Future immohistochemical and western blot studies could be performed to measure the expression of extracellular matrix proteins including: hyaluronan binding protein, brevican, phosphocan, aggrecan (Carulli et al., 2006; Zimmermann and Dours-Zimmermann, 2008).

The continuous and intermittent ethanol binge models resulted in similar reversal learning deficits with different structural features. However, both treatments resulted in changes in regions that are known to regulate reversal learning (Figure D1). Both the basal forebrain (Cabrera et al., 2006; Roberts et al., 1992; Tait and Brown, 2008) and the orbitofrontal cortex are integral parts of the circuit that regulates reversal learning (Dias et al., 1996; McAlonan and Brown, 2003; Schoenbaum et al., 2007). Damage to either one of these regions can result in reversal learning deficits (Figure D1). Thus, though continuous and intermittent ethanol had different effects on structure, they both alter structures that are important for reversal learning and thus have a common behavioral output.

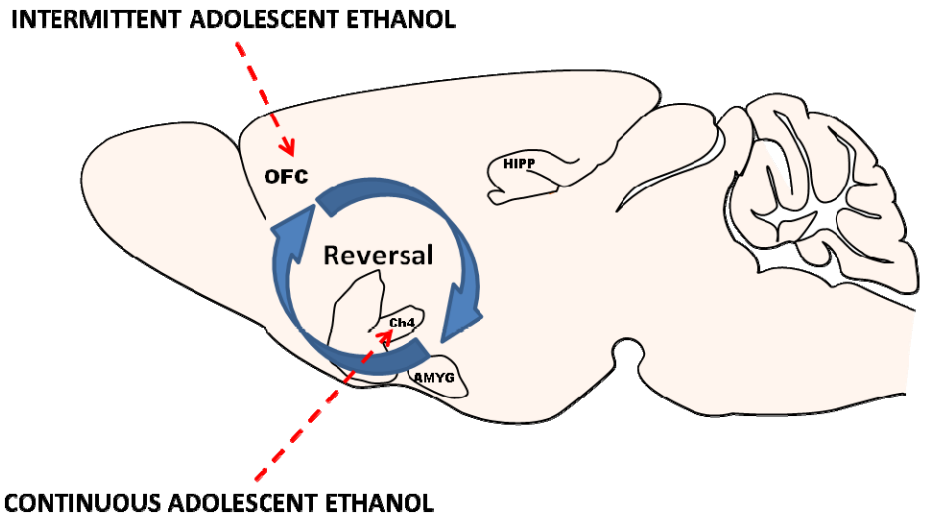

Figure D.1 Potential effects of adolescent binge models on reversal learning circuitry. Reversal learning circuitry involves projections from the amygdala (AMYG) and Ch4 region of the basal forebrain to the orbitofrontal cortex. Orbitofrontal projections to the striatum are also involved.

The multidisciplinary approach was very useful in this project. We used structural imaging and gene array results to guide our immunohistochemical investigations. This approach was not only useful in the process of discovery, but it increases the translational potential of these studies. Human studies of adolescent development are often limited to imaging. However the use of immunohistochemical studies to confirm imaging observations and identify the cellular aspects of the imaging lesion is a benefit of using rodents. Also, these long-term developmental findings can now be used to guide future epidemiological research. For instance, an important epidemiological question raised from our results is whether there is an association between adolescent binge drinking and Alzheimer's in late life. The association of current drinking and Alzheimer's disease has been investigated with light to moderate drinking showing a potential protective effect with no protection for heavy drinkers (Anstey et al., 2009; Panza et al., 2009). However, the effects of alcohol on the brain during the developmental window of adolescence are likely different than their effects

during late life. This research can be used as an intervention to educate adolescents regarding the long-term dangers of binge drinking as well as pregnant mothers regarding the dangers of drinking during the third trimester. Epidemiological studies show that perceived risk of harm is associated with reduced alcohol use in adolescents (Henry et al., 2005). If adolescents could perceive the potential long-term harm of binge drinking could have, it may reduce their likelihood to binge heavily.

Figure D.2 Hypothetical Effects of Developmental Ethanol Treatments on Brain Structural Measures

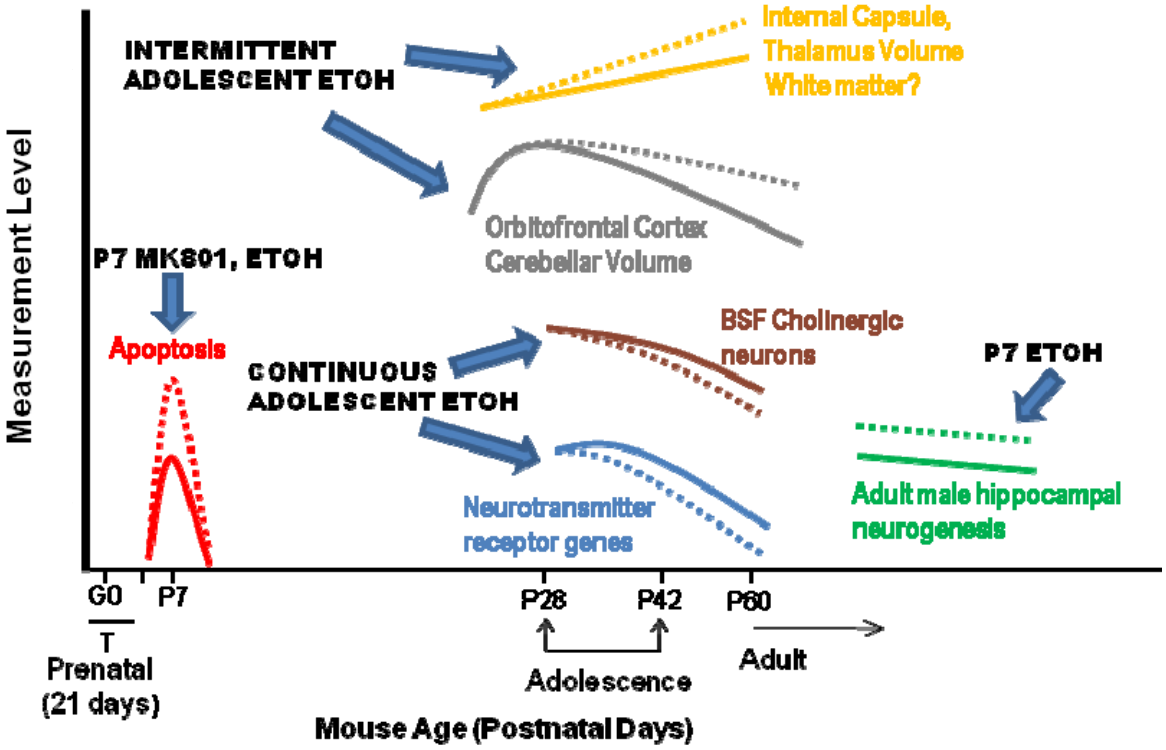

Key: dashed lines denote ethanol effect

Summary: Ethanol exposure during development was found to cause persistent deficits in the adult behaviors and brain structure. Postnatal day seven ethanol and MK801 both caused persistent losses of parvalbumin interneurons and layer V (P7 MK801) or layer II (P7

ethanol) pyramidal neurons. P7 MK801 also caused increased anxiety-like behavior. P7 ethanol differentially altered neurogenesis in adult males and females. Adult males that received P7 ethanol showed increased neurogenesis evidenced by increased dentate gyrus doublecortin and Ki67 immunohistochemistry. Adult females did not show any signs of increased neurogenesis. Adult females that received P7 ethanol showed a reduction in hippocampal volume, whereas males did not. This suggests that increases in neurogenesis in adult males may represent a compensatory response to maintain hippocampal volume. Adolescent ethanol treatment also caused persistent changes in adult brain structure and behavior. Both a continuous and an intermittent model of adolescent binge drinking caused reversal learning deficits in adults. The continuous model of adolescent binge drinking enhanced the developmental downregulation of several neurotransmitter receptor genes. The continuous treatment also caused a reduction in olfactory bulb and basal forebrain volumes in adulthood as measured by structural MRI. Basal forebrain volume reductions were associated with a reduction in cholinergic neurons in the Ch4 region of the basal forebrain. The intermittent adolescent binge model resulted in volume increases in the internal capsule, orbitofrontal cortex, thalamus, cerebellum, and genu of the corpus callosum in adulthood. The intermittent adolescent binge treatment also resulted in heightened anxiety-like behavior in adults. The observed and hypothesized effects of ethanol observed in this study are shown in Figure D2. The use of multiple techniques increases the validity and translational potential of these findings. This work could be used to inform future human epidemiological studies and be used to inform the general public about the dangers of adolescent binge drinking and maternal alcohol consumption during the third trimester.

REFERENCES

Anastasio NC, Johnson KM (2008) Atypical anti-schizophrenic drugs prevent changes in cortical N-methyl-D-aspartate receptors and behavior following sub-chronic phencyclidine administration in developing rat pups. Pharmacol Biochem Behav 90(4):569-77.

Andersen SL, Thompson AT, Rutstein M, Hostetter JC, Teicher MH (2000) Dopamine receptor pruning in prefrontal cortex during the periadolescent period in rats. Synapse 37(2):167-9.

Anstey KJ, Mack HA, Cherbuin N (2009) Alcohol consumption as a risk factor for dementia and cognitive decline: meta-analysis of prospective studies. Am J Geriatr Psychiatry 17(7):542-55.

Arendt T, Allen Y, Marchbanks RM, Schugens MM, Sinden J, Lantos PL, Gray JA (1989) Cholinergic system and memory in the rat: Effects of chronic ethanol, embryonic basal forebrain projection system. Neuroscience 33(4):435-462.

Arendt T, Allen Y, Sinden J, Schugens MM, Marchbanks RM, Lantos PL, Gray JA (1988a) Cholinergic-rich brain transplants reverse alcohol-induced memory deficits. Nature 332(6163):448-50.

Arendt T, Bruckner MK, Magliusi S, Krell T (1995) Degeneration of rat cholinergic basal forebrain neurons and reactive changes in nerve growth factor expression after chronic neurotoxic injury-I. Degeneration and plastic response of basal forebrain neurons. Neuroscience 65(3):633-645.

Arendt T, Henning D, Gray JA, Marchbanks R (1988b) Loss of neurons in the rat basal forebrain cholinergic projection system after prolonged intake of ethanol. Brain Res Bull 21(4):563-9.

Badea A, Johnson GA, Williams RW (2009) Genetic dissection of the mouse brain using high-field magnetic resonance microscopy. Neuroimage 45(4):1067-79.

Baimbridge KG, Celio MR, Rogers JH (1992) Calcium-binding proteins in the nervous system. Trends Neurosci 15(8):303-8.

Barker JM, Galea LA (2008) Repeated estradiol administration alters different aspects of neurogenesis and cell death in the hippocampus of female, but not male, rats. Neuroscience 152(4):888-902.

Barr HM, Streissguth AP (2001) Identifying maternal self-reported alcohol use associated with fetal alcohol spectrum disorders. Alcohol Clin Exp Res 25(2):283-7.

Baviera M, Invernizzi RW, Carli M (2008) Haloperidol and clozapine have dissociable effects in a model of attentional performance deficits induced by blockade of NMDA receptors in the mPFC. Psychopharmacology (Berl) 196(2):269-80.

Beasley CL, Reynolds GP (1997) Parvalbumin-immunoreactive neurons are reduced in the prefrontal cortex of schizophrenics. Schizophr Res 24(3):349-55.

Bechara A (2005) Decision making, impulse control and loss of willpower to resist drugs: a neurocognitive perspective. Nat Neurosci 8(11):1458-63.

Bell SH, Stade B, Reynolds JN, Rasmussen C, Andrew G, Hwang PA, Carlen PL The Remarkably High Prevalence of Epilepsy and Seizure History in Fetal Alcohol Spectrum Disorders. Alcohol Clin Exp Res.

Bellgrove MA, Mattingley JB (2008) Molecular genetics of attention. Ann N Y Acad Sci 1129:200-12.

Belzung C, Griebel G (2001) Measuring normal and pathological anxiety-like behaviour in mice: a review. Behav Brain Res 125(1-2):141-9.

Benes FM, Taylor JB, Cunningham MC (2000) Convergence and plasticity of monoaminergic systems in the medial prefrontal cortex during the postnatal period: implications for the development of psychopathology. Cereb Cortex 10(10):1014-27.

Bentivoglio AR, Altavista MC, Granata R, Albanese A (1994) Genetically determined cholinergic deficiency in the forebrain of C57BL/6 mice. Brain Res 637(1-2):181-9.

Birrell JM, Brown VJ (2000) Medial frontal cortex mediates perceptual attentional set shifting in the rat. J Neurosci 20(11):4320-4.

Blackwell BN, Bucci TJ, Hart RW, Turturro A (1995) Longevity, body weight, and neoplasia in ad libitum-fed and diet-restricted C57BL6 mice fed NIH-31 open formula diet. Toxicol Pathol 23(5):570-82.

Blakemore SJ (2008) The social brain in adolescence. Nat Rev Neurosci 9(4):267-77.

Blakemore SJ, Choudhury S (2006) Development of the adolescent brain: implications for executive function and social cognition. J Child Psychol Psychiatry 47(3-4):296-312.

Boulougouris V, Dalley JW, Robbins TW (2007) Effects of orbitofrontal, infralimbic and prelimbic cortical lesions on serial spatial reversal learning in the rat. Behav Brain Res 179(2):219-28.

Bowen R, Chavira DA, Bailey K, Stein MT, Stein MB (2008) Nature of anxiety comorbid with attention deficit hyperactivity disorder in children from a pediatric primary care setting. Psychiatry Res 157(1-3):201-9.

Brady KT, Lydiard RB (1993) The association of alcoholism and anxiety. Psychiatr Q 64(2):135-49.

Braga RJ, Mendlowicz MV, Marrocos RP, Figueira IL (2005) Anxiety disorders in outpatients with schizophrenia: prevalence and impact on the subjective quality of life. J Psychiatr Res 39(4):409-14.

Breese GR, Overstreet DH, Knapp DJ (2005) Conceptual framework for the etiology of alcoholism: a "kindling"/stress hypothesis. Psychopharmacology (Berl) 178(4):367-80.

Broadbelt K, Jones LB (2008) Evidence of altered calmodulin immunoreactivity in areas 9 and 32 of schizophrenic prefrontal cortex. J Psychiatr Res 42(8):612-21.

Brown SA, Tapert SF (2004) Adolescence and the trajectory of alcohol use: basic to clinical studies. Ann N Y Acad Sci 1021:234-44.

Brown SA, Tapert SF, Granholm E, Delis DC (2000) Neurocognitive functioning of adolescents: effects of protracted alcohol use. Alcohol Clin Exp Res 24(2):164-71.

Cabrera SM, Chavez CM, Corley SR, Kitto MR, Butt AE (2006) Selective lesions of the nucleus basalis magnocellularis impair cognitive flexibility. Behav Neurosci 120(2):298-306.

Caine SB, Geyer MA, Swerdlow NR (1992) Hippocampal modulation of acoustic startle and prepulse inhibition in the rat. Pharmacol Biochem Behav 43(4):1201-8.

Carli M, Baviera M, Invernizzi RW, Balducci C (2006) Dissociable contribution of 5-HT1A and 5-HT2A receptors in the medial prefrontal cortex to different aspects of executive control such as impulsivity and compulsive perseveration in rats. Neuropsychopharmacology 31(4):757-67.

Carulli D, Rhodes KE, Brown DJ, Bonnert TP, Pollack SJ, Oliver K, Strata P, Fawcett JW (2006) Composition of perineuronal nets in the adult rat cerebellum and the cellular origin of their components. J Comp Neurol 494(4):559-77.

Coleman Jr LG, He J, Lee J, Styner M, Crews FT (2009) The effects of adolescent binge-drinking on adult behavior and brain structure in mice: Altered reversal learning and reduced basal forebrain volume. Journal of Neuroscience Society Abstracts 9042:157.17.

Coleman LG, Jr., Jarskog LF, Moy SS, Crews FT (2009) Deficits in adult prefrontal cortex neurons and behavior following early post-natal NMDA antagonist treatment. Pharmacol Biochem Behav 93(3):322-30.

Conde F, Lund JS, Jacobowitz DM, Baimbridge KG, Lewis DA (1994) Local circuit neurons immunoreactive for calretinin, calbindin D-28k or parvalbumin in monkey prefrontal cortex: distribution and morphology. J Comp Neurol 341(1):95-116.

Crawley JN (1999) Behavioral phenotyping of transgenic and knockout mice: experimental design and evaluation of general health, sensory functions, motor abilities, and specific behavioral tests. Brain Res 835(1):18-26.

Crews F, He J, Hodge C (2007a) Adolescent cortical development: a critical period of vulnerability for addiction. Pharmacol Biochem Behav 86(2):189-99.

Crews FT, Braun CJ, Hoplight B, Switzer RC, 3rd, Knapp DJ (2000a) Binge ethanol consumption causes differential brain damage in young adolescent rats compared with adult rats. Alcohol Clin Exp Res 24(11):1712-23.

Crews FT, Braun CJ, III RCS, Knapp DJ (2000b) Binge ethanol causes differential brain damage in young adolescent rats compared to adult rats. Alcoholism: Clinical and Experimental Research 24(11):1712-1723.

Crews FT, He J, Hodge C (2007b) Adolescent cortical development: a critical period of vulnerability for addiction. Pharmacol Biochem Behav 86(2):189-99.

Crews FT, Mdzinarishvili A, Kim D, He J, Nixon K (2006) Neurogenesis in adolescent brain is potently inhibited by ethanol. Neuroscience 137(2):437-45.

Crews FT, Nixon K, Wilkie ME (2004) Exercise reverses ethanol inhibition of neural stem cell proliferation. Alcohol 33(1):63-71.

Davidson RJ (2002) Anxiety and affective style: role of prefrontal cortex and amygdala. Biol Psychiatry 51(1):68-80.

Davis M, Gendelman DS, Tischler MD, Gendelman PM (1982) A primary acoustic startle circuit: lesion and stimulation studies. J Neurosci 2(6):791-805.

De Bellis MD, Narasimhan A, Thatcher DL, Keshavan MS, Soloff P, Clark DB (2005) Prefrontal cortex, thalamus, and cerebellar volumes in adolescents and young adults with adolescent-onset alcohol use disorders and comorbid mental disorders. Alcohol Clin Exp Res 29(9):1590-600.

De Rosa E, Desmond JE, Anderson AK, Pfefferbaum A, Sullivan EV (2004) The human basal forebrain integrates the old and the new. Neuron 41(5):825-37.

Deas D, Brown ES (2006) Adolescent substance abuse and psychiatric comorbidities. J Clin Psychiatry 67(7):e02.

Deas D, Riggs P, Langenbucher J, Goldman M, Brown S (2000) Adolescents are not adults: developmental considerations in alcohol users. Alcohol Clin Exp Res 24(2):232-7.

Del Boca FK, Darkes J, Greenbaum PE, Goldman MS (2004) Up close and personal: temporal variability in the drinking of individual college students during their first year. J Consult Clin Psychol 72(2):155-64.

Dias R, Robbins TW, Roberts AC (1996) Dissociation in prefrontal cortex of affective and attentional shifts. Nature 380(6569):69-72.

Dinopoulos A, Dori I, Parnavelas JG (1997) The serotonin innervation of the basal forebrain shows a transient phase during development. Brain Res Dev Brain Res 99(1):38-52.

Dobbing J, Sands J (1979) Comparative aspects of the brain growth spurt. Early Hum Dev 3(1):79-83.

Dong H, Csernansky CA, Goico B, Csernansky JG (2003) Hippocampal neurogenesis follows kainic acid-induced apoptosis in neonatal rats. J Neurosci 23(5):1742-9.

Dori IE, Dinopoulos A, Parnavelas JG (1998) The development of the synaptic organization of the serotonergic system differs in brain areas with different functions. Exp Neurol 154(1):113-25.

Ehlers CL, Criado JR (2010) Adolescent ethanol exposure: does it produce long-lasting electrophysiological effects? Alcohol 44(1):27-37.

Enoch MA (2006) Genetic and environmental influences on the development of alcoholism: resilience vs. risk. Ann N Y Acad Sci 1094:193-201.

Ernst M, Pine DS, Hardin M (2006) Triadic model of the neurobiology of motivated behavior in adolescence. Psychol Med 36(3):299-312.

Ernst M, Romeo RD, Andersen SL (2009) Neurobiology of the development of motivated behaviors in adolescence: a window into a neural systems model. Pharmacol Biochem Behav 93(3):199-211.

Everitt BJ, Robbins TW (1997) Central cholinergic systems and cognition. Annu Rev Psychol 48:649-84.

Fendt M, Li L, Yeomans JS (2001) Brain stem circuits mediating prepulse inhibition of the startle reflex. Psychopharmacology (Berl) 156(2-3):216-24.

Feng G, Mellor RH, Bernstein M, Keller-Peck C, Nguyen QT, Wallace M, Nerbonne JM, Lichtman JW, Sanes JR (2000) Imaging neuronal subsets in transgenic mice expressing multiple spectral variants of GFP. Neuron 28(1):41-51.

Finlay BL, Darlington RB (1995) Linked regularities in the development and evolution of mammalian brains. Science 268(5217):1578-84.

Fortier CB, Steffen EM, Lafleche G, Venne JR, Disterhoft JF, McGlinchey RE (2008) Delay discrimination and reversal eyeblink classical conditioning in abstinent chronic alcoholics. Neuropsychology 22(2):196-208.

Franklin, Paxinos (2001) The Mouse Brain in Stereotaxic Coordinates.

Freedman M, Oscar-Berman M (1989) Spatial and visual learning deficits in Alzheimer's and Parkinson's disease. Brain Cogn 11(1):114-26.

Freund G, Ballinger WE, Jr. (1989a) Loss of muscarinic and benzodiazepine neuroreceptors from hippocampus of alcohol abusers. Alcohol 6(1):23-31.

Freund G, Ballinger WE, Jr. (1989b) Loss of muscarinic cholinergic receptors from the temporal cortex of alcohol abusers. Metab Brain Dis 4(2):121-41.

Fuster JM (1997) *The Prefrontal Cortex: Anatomy, Physiology, and Neuropsychology of the Frontal Lobe.* Lippincott-Raven, Philadelphia.

Gabbott PL, Bacon SJ (1996) Local circuit neurons in the medial prefrontal cortex (areas 24a,b,c, 25 and 32) in the monkey: I. Cell morphology and morphometrics. J Comp Neurol 364(4):567-608.

Gabbott PL, Dickie BG, Vaid RR, Headlam AJ, Bacon SJ (1997) Local-circuit neurones in the medial prefrontal cortex (areas 25, 32 and 24b) in the rat: morphology and quantitative distribution. J Comp Neurol 377(4):465-99.

Gibbs RB (1999) Treatment with estrogen and progesterone affects relative levels of brain-derived neurotrophic factor mRNA and protein in different regions of the adult rat brain. Brain Res 844(1-2):20-7.

Giedd JN (2004) Structural magnetic resonance imaging of the adolescent brain. Ann N Y Acad Sci 1021:77-85.

Giedd JN, Blumenthal J, Jeffries NO, Castellanos FX, Liu H, Zijdenbos A, Paus T, Evans AC, Rapoport JL (1999) Brain development during childhood and adolescence: a longitudinal MRI study. Nat Neurosci 2(10):861-3.

Giedd JN, Lenroot RK, Shaw P, Lalonde F, Celano M, White S, Tossell J, Addington A, Gogtay N (2008) Trajectories of anatomic brain development as a phenotype. Novartis Found Symp 289:101-12; discussion 112-8, 193-5.

Gogtay N, Giedd JN, Lusk L, Hayashi KM, Greenstein D, Vaituzis AC, Nugent TF, 3rd, Herman DH, Clasen LS, Toga AW, Rapoport JL, Thompson PM (2004) Dynamic

mapping of human cortical development during childhood through early adulthood. Proc Natl Acad Sci U S A 101(21):8174-9.

Gould E, Woolf NJ, Butcher LL (1991) Postnatal development of cholinergic neurons in the rat: I. Forebrain. Brain Res Bull 27(6):767-89.

Grant BF, Dawson DA (1997) Age of onset of alcohol use and its association with DSM-IV alcohol abuse and dependence: results from the National Longitudinal Alcohol Epidemiologic Survey. Journal of Substance Abuse 9:103-110.

Grobin AC, Heenan EJ, Lieberman JA, Morrow AL (2003) Perinatal neurosteroid levels influence GABAergic interneuron localization in adult rat prefrontal cortex. J Neurosci 23(5):1832-9.

Hall AM, Moore RY, Lopez OL, Kuller L, Becker JT (2008) Basal forebrain atrophy is a presymptomatic marker for Alzheimer's disease. Alzheimers Dement 4(4):271-9.

Harper C (2009) The neuropathology of alcohol-related brain damage. Alcohol Alcohol 44(2):136-40.

Harris LW, Sharp T, Gartlon J, Jones DN, Harrison PJ (2003) Long-term behavioural, molecular and morphological effects of neonatal NMDA receptor antagonism. Eur J Neurosci 18(6):1706-10.

Harris NG, Jones HC, Williams SC (1992) MR imaging for measurements of ventricles and cerebral cortex in postnatal rats (H-Tx strain) with progressive inherited hydrocephalus. Exp Neurol 118(1):1-6.

Hattox AM, Nelson SB (2007) Layer V neurons in mouse cortex projecting to different targets have distinct physiological properties. J Neurophysiol 98(6):3330-40.

He J, Crews F (2006) Neurogenesis Decreases during Brain Maturation from Adolescence to Adulthood. Pharmacol Biochem Behav Submitted June 2006.

He J, Nixon K, Shetty AK, Crews FT (2005) Chronic alcohol exposure reduces hippocampal neurogenesis and dendritic growth of newborn neurons. Eur J Neurosci 21(10):2711-20.

Heisler LK, Chu HM, Brennan TJ, Danao JA, Bajwa P, Parsons LH, Tecott LH (1998) Elevated anxiety and antidepressant-like responses in serotonin 5-HT1A receptor mutant mice. Proc Natl Acad Sci U S A 95(25):15049-54.

Henry KL, Slater MD, Oetting ER (2005) Alcohol use in early adolescence: the effect of changes in risk taking, perceived harm and friends' alcohol use. J Stud Alcohol 66(2):275-83.

Hoplight BJ, Vincow ES, Neumaier JF (2005) The effects of SB 224289 on anxiety and cocaine-related behaviors in a novel object task. Physiol Behav 84(5):707-14.

Ieraci A, Herrera DG (2007) Single alcohol exposure in early life damages hippocampal stem/progenitor cells and reduces adult neurogenesis. Neurobiol Dis 26(3):597-605.

Ikonomidou C, Bittigau P, Ishimaru MJ, Wozniak DF, Koch C, Genz K, Price MT, Stefovska V, Horster F, Tenkova T, Dikranian K, Olney JW (2000) Ethanol-induced apoptotic neurodegeneration and fetal alcohol syndrome. Science 287(5455):1056-60.

Ikonomidou C, Bosch F, Miksa M, Bittigau P, Vockler J, Dikranian K, Tenkova TI, Stefovska V, Turski L, Olney JW (1999) Blockade of NMDA receptors and apoptotic neurodegeneration in the developing brain. Science 283(5398):70-4.

Insel TR, Miller LP, Gelhard RE (1990) The ontogeny of excitatory amino acid receptors in rat forebrain--I. N-methyl-D-aspartate and quisqualate receptors. Neuroscience 35(1):31-43.

Ishimaru MJ, Ikonomidou C, Dikranian K, Olney JW (1997) Physiological cell death (PCD), an example of apoptosis, occurs naturally in the developing central nervous system. In the fetal rat brain, with the exception of germinal matrix zones where apoptosis is frequent, apoptotic neurons are confined primarily to lower brain centers. In the early neonatal period (P1 to P5) apoptotic profiles become increasingly abundant throughout many non-germinal matrix regions of the midbrain and forebrain. By P7, PCD has largely run its course and apoptotic profiles are not found in high concentration in any forebrain region. Society of Neuroscience Abstract 23(895).

Ishimaru MJ, Ikonomidou C, Tenkova TI, Der TC, Dikranian K, Sesma MA, Olney JW (1999) Distinguishing excitotoxic from apoptotic neurodegeneration in the developing rat brain. J Comp Neurol 408(4):461-76.

Jacob T, Bucholz KK, Sartor CE, Howell DN, Wood PK (2005) Drinking trajectories from adolescence to the mid-forties among alcohol dependent males. J Stud Alcohol 66(6):745-55.

Jarskog LF, Gilmore JH, Glantz LA, Gable KL, German TT, Tong RI, Lieberman JA (2007) Caspase-3 activation in rat frontal cortex following treatment with typical and atypical antipsychotics. Neuropsychopharmacology 32(1):95-102.

Johnston LD, O'Malley PM, Bachman JG, Schulenberg JE (2004) Monitoring the Future, National Survey Results on Drug Use, 1975-2004. NIH Pub No. 05-5727 1 Secondary School Students.

Johnston LD, O'Malley, P.M., Bachman, J.G., and Schulenberg, J.E. (2006) Monitoring The Future: National Results on Adolescent Drug Use: Overview of Key Findings. NIH Publication No. 06-5882, Bethesda, MD: National Institue on Drug Abuse, 2006.

Jones AW, Holmgren A (2009) Age and gender differences in blood-alcohol concentration in apprehended drivers in relation to the amounts of alcohol consumed. Forensic Sci Int 188(1-3):40-5.

Jones BE (2004) Activity, modulation and role of basal forebrain cholinergic neurons innervating the cerebral cortex. Prog Brain Res 145:157-69.

Jones KL, Smith DW (1975) The fetal alcohol syndrome. Teratology 12(1):1-10.

Jones KL, Smith DW, Ulleland CN, Streissguth P (1973) Pattern of malformation in offspring of chronic alcoholic mothers. Lancet 1(7815):1267-71.

Juraska JM, Markham JA (2004) The cellular basis for volume changes in the rat cortex during puberty: white and gray matter. Ann N Y Acad Sci 1021:431-5.

Kalsbeek A, Voorn P, Buijs RM, Pool CW, Uylings HB (1988) Development of the dopaminergic innervation in the prefrontal cortex of the rat. J Comp Neurol 269(1):58-72.

Kesslak JP, Profitt BF, Criswell P (1991) Olfactory function in chronic alcoholics. Percept Mot Skills 73(2):551-4.

Kiser PJ, Cooper NG, Mower GD (1998) Expression of two forms of glutamic acid decarboxylase (GAD67 and GAD65) during postnatal development of rat somatosensory barrel cortex. J Comp Neurol 402(1):62-74.

Kodituwakku PW (2007) Defining the behavioral phenotype in children with fetal alcohol spectrum disorders: a review. Neurosci Biobehav Rev 31(2):192-201.

Kostovic I (1990) Structural and histochemical reorganization of the human prefrontal cortex during perinatal and postnatal life. Prog Brain Res 85:223-39; discussion 239-40.

Krajewska M, Wang HG, Krajewski S, Zapata JM, Shabaik A, Gascoyne R, Reed JC (1997) Immunohistochemical analysis of in vivo patterns of expression of CPP32 (Caspase-3), a cell death protease. Cancer Res 57(8):1605-13.

Kuroda M, Yokofujita J, Murakami K (1998) An ultrastructural study of the neural circuit between the prefrontal cortex and the mediodorsal nucleus of the thalamus. Prog Neurobiol 54(4):417-58.

Lee J, Jomier J, Aylward S, Tyszka M, Moy S, Lauder J, Styner M (2009a) Evaluation of atlas based mouse brain segmentation. SPIE Medical Imaging 2009 Image Processing 7259:137 - 146

Lee J, Jomier J, Aylward S, Tyszka M, Moy S, Lauder J, Styner M (2009b) Evaluation of atlas based mouse brain segmentation. SPIE Medical Imaging 2009 Image Processing 7259:137 - 146

Lee JK, McCoy MK, Harms AS, Ruhn KA, Gold SJ, Tansey MG (2008) Regulator of G-protein signaling 10 promotes dopaminergic neuron survival via regulation of the microglial inflammatory response. J Neurosci 28(34):8517-28.

Lema Tome CM, Bauer C, Nottingham C, Smith C, Blackstone K, Brown L, Hlavaty C, Nelson C, Daker R, Sola R, Miller R, Bryan R, Turner CP (2006) MK801-induced caspase-3 in the postnatal brain: inverse relationship with calcium binding proteins. Neuroscience 141(3):1351-63.

Lenroot RK, Giedd JN (2006) Brain development in children and adolescents: insights from anatomical magnetic resonance imaging. Neurosci Biobehav Rev 30(6):718-29.

Leonardo CC, Eakin AK, Ajmo JM, Gottschall PE (2008) Versican and brevican are expressed with distinct pathology in neonatal hypoxic-ischemic injury. J Neurosci Res 86(5):1106-14.

Levi MS, Brimble MA (2004) A review of neuroprotective agents. Curr Med Chem 11(18):2383-97.

Lewis DA (1997) Development of the prefrontal cortex during adolescence: insights into vulnerable neural circuits in schizophrenia. Neuropsychopharmacology 16(6):385-98.

Luna B, Garver KE, Urban TA, Lazar NA, Sweeney JA (2004) Maturation of cognitive processes from late childhood to adulthood. Child Dev 75(5):1357-72.

Lusher JM, Chandler C, Ball D (2001) Dopamine D4 receptor gene (DRD4) is associated with Novelty Seeking (NS) and substance abuse: the saga continues. Mol Psychiatry 6(5):497-9.

Lyck L, Kroigard T, Finsen B (2007) Unbiased cell quantification reveals a continued increase in the number of neocortical neurones during early post-natal development in mice. Eur J Neurosci 26(7):1749-64.

Makris N, Oscar-Berman M, Jaffin SK, Hodge SM, Kennedy DN, Caviness VS, Marinkovic K, Breiter HC, Gasic GP, Harris GJ (2008) Decreased volume of the brain reward system in alcoholism. Biol Psychiatry 64(3):192-202.

Markham JA, Morris JR, Juraska JM (2007) Neuron number decreases in the rat ventral, but not dorsal, medial prefrontal cortex between adolescence and adulthood. Neuroscience 144(3):961-8.

Markwiese BJ, Acheson SK, Levin ED, Wilson WA, Swartzwelder HS (1998) Differential effects of ethanol on memory in adolescent and adult rats. Alcohol Clin Exp Res 22(2):416-21.

Mason WA, Kosterman R, Haggerty KP, Hawkins JD, Redmond C, Spoth RL, Shin C (2008) Dimensions of adolescent alcohol involvement as predictors of young-adult major depression. J Stud Alcohol Drugs 69(2):275-85.

Masten AS, Faden VB, Zucker RA, Spear LP (2008) Underage drinking: a developmental framework. Pediatrics 121 Suppl 4:S235-51.

Mattson SN, Riley EP (1998) A review of the neurobehavioral deficits in children with fetal alcohol syndrome or prenatal exposure to alcohol. Alcohol Clin Exp Res 22(2):279-94.

Mattson SN, Riley EP, Gramling L, Delis DC, Jones KL (1997) Heavy prenatal alcohol exposure with or without physical features of fetal alcohol syndrome leads to IQ deficits. J Pediatr 131(5):718-21.

May PA, Gossage JP, Kalberg WO, Robinson LK, Buckley D, Manning M, Hoyme HE (2009) Prevalence and epidemiologic characteristics of FASD from various research methods with an emphasis on recent in-school studies. Dev Disabil Res Rev 15(3):176-92.

McAlonan K, Brown VJ (2003) Orbital prefrontal cortex mediates reversal learning and not attentional set shifting in the rat. Behav Brain Res 146(1-2):97-103.

Medina AE, Krahe TE, Coppola DM, Ramoa AS (2003) Neonatal alcohol exposure induces long-lasting impairment of visual cortical plasticity in ferrets. J Neurosci 23(31):10002-12.

Medina AE, Ramoa AS (2005) Early alcohol exposure impairs ocular dominance plasticity throughout the critical period. Brain Res Dev Brain Res 157(1):107-11.

Medina KL, McQueeny T, Nagel BJ, Hanson KL, Schweinsburg AD, Tapert SF (2008) Prefrontal cortex volumes in adolescents with alcohol use disorders: unique gender effects. Alcohol Clin Exp Res 32(3):386-94.

Miller MW (1997) Effects of prenatal exposure to ethanol on callosal projection neurons in rat somatosensory cortex. Brain Res 766(1-2):121-8.

Mirjana C, Baviera M, Invernizzi RW, Balducci C (2004) The serotonin 5-HT2A receptors antagonist M100907 prevents impairment in attentional performance by NMDA receptor blockade in the rat prefrontal cortex. Neuropsychopharmacology 29(9):1637-47.

Mohn AR, Gainetdinov RR, Caron MG, Koller BH (1999) Mice with reduced NMDA receptor expression display behaviors related to schizophrenia. Cell 98(4):427-36.

Molnar Z, Cheung AF (2006) Towards the classification of subpopulations of layer V pyramidal projection neurons. Neurosci Res 55(2):105-15.

Moss HB, Chen CM, Yi HY (2008) DSM-IV criteria endorsement patterns in alcohol dependence: relationship to severity. Alcohol Clin Exp Res 32(2):306-13.

Moy SS, Nadler JJ, Young NB, Perez A, Holloway LP, Barbaro RP, Barbaro JR, Wilson LM, Threadgill DW, Lauder JM, Magnuson TR, Crawley JN (2007) Mouse behavioral tasks relevant to autism: phenotypes of 10 inbred strains. Behav Brain Res 176(1):4-20.

Moy SS, Perez A, Koller BH, Duncan GE (2006) Amphetamine-induced disruption of prepulse inhibition in mice with reduced NMDA receptor function. Brain Res 1089(1):186-94.

Muir JL, Everitt BJ, Robbins TW (1996) The cerebral cortex of the rat and visual attentional function: dissociable effects of mediofrontal, cingulate, anterior dorsolateral, and parietal cortex lesions on a five-choice serial reaction time task. Cereb Cortex 6(3):470-81.

Munafo MR, Yalcin B, Willis-Owen SA, Flint J (2008) Association of the dopamine D4 receptor (DRD4) gene and approach-related personality traits: meta-analysis and new data. Biol Psychiatry 63(2):197-206.

Muth K, Schonmeyer R, Matura S, Haenschel C, Schroder J, Pantel J (2009) Mild Cognitive Impairment in the Elderly is Associated with Volume Loss of the Cholinergic Basal Forebrain Region. Biol Psychiatry.

Nagel BJ, Schweinsburg AD, Phan V, Tapert SF (2005) Reduced hippocampal volume among adolescents with alcohol use disorders without psychiatric comorbidity. Psychiatry Res 139(3):181-90.

Nixon K, Crews FT (2002) Binge ethanol exposure decreases neurogenesis in adult rat hippocampus. J Neurochem 83(5):1087-93.

Nixon K, Crews FT (2004) Temporally specific burst in cell proliferation increases hippocampal neurogenesis in protracted abstinence from alcohol. J Neurosci 24(43):9714-22.

Nordberg A, Larsson C, Perdahl E, Winblad B (1983) Changes in cholinergic activity in human hippocampus following chronic alcohol abuse. Pharmacology, Biochemistry and Behavior 18:397-400.

Norman AL, Crocker N, Mattson SN, Riley EP (2009) Neuroimaging and fetal alcohol spectrum disorders. Dev Disabil Res Rev 15(3):209-17.

O'Malley PM, Johnston LD, Bachman JG (1998) Alcohol use among adolescents. Alcohol Health and Research 22:85-93.

Obernier JA, Bouldin TW, Crews FT (2002a) Binge ethanol exposure in adult rats causes necrotic cell death. Alcohol Clin Exp Res 26(4):547-57.

Obernier JA, White AM, Swartzwelder HS, Crews FT (2002b) Cognitive deficits and CNS damage after a 4-day binge ethanol exposure in rats. Pharmacol Biochem Behav 72(3):521-32.

Olney J, Tenkova T, Dikranian K, Qin Y, Labruyere J, Ikonomidou C (2005) Ethanol-induced apoptotic neurodegeneration in the developing C57BL/6 mouse brain. Brain research. Developmental brain research 133(2):115-26.

Olney JW, Tenkova T, Dikranian K, Muglia LJ, Jermakowicz WJ, D'Sa C, Roth KA (2002a) Ethanol-induced caspase-3 activation in the in vivo developing mouse brain. Neurobiol Dis 9(2):205-19.

Olney JW, Tenkova T, Dikranian K, Qin YQ, Labruyere J, Ikonomidou C (2002b) Ethanol-induced apoptotic neurodegeneration in the developing C57BL/6 mouse brain. Brain Res Dev Brain Res 133(2):115-26.

Oscar-Berman M, Zola-Morgan SM (1980) Comparative neuropsychology and Korsakoff's syndrome. I.--Spatial and visual reversal learning. Neuropsychologia 18(4-5):499-512.

Ostby Y, Tamnes CK, Fjell AM, Westlye LT, Due-Tonnessen P, Walhovd KB (2009) Heterogeneity in subcortical brain development: A structural magnetic resonance imaging study of brain maturation from 8 to 30 years. J Neurosci 29(38):11772-82.

Panza F, Capurso C, D'Introno A, Colacicco AM, Frisardi V, Lorusso M, Santamato A, Seripa D, Pilotto A, Scafato E, Vendemiale G, Capurso A, Solfrizzi V (2009) Alcohol drinking, cognitive functions in older age, predementia, and dementia syndromes. J Alzheimers Dis 17(1):7-31.

Pascual M, Blanco AM, Cauli O, Minarro J, Guerri C (2007) Intermittent ethanol exposure induces inflammatory brain damage and causes long-term behavioural alterations in adolescent rats. Eur J Neurosci 25(2):541-50.

Pascual M, Boix J, Felipo V, Guerri C (2009) Repeated alcohol administration during adolescence causes changes in the mesolimbic dopaminergic and glutamatergic systems and promotes alcohol intake in the adult rat. J Neurochem 108(4):920-31.

Paus T, Zijdenbos A, Worsley K, Collins DL, Blumenthal J, Giedd JN, Rapoport JL, Evans AC (1999) Structural maturation of neural pathways in children and adolescents: in vivo study. Science 283(5409):1908-11.

Paylor R, Crawley JN (1997) Inbred strain differences in prepulse inhibition of the mouse startle response. Psychopharmacology (Berl) 132(2):169-80.

Pfefferbaum A, Adalsteinsson E, Sullivan EV (2006) Dysmorphology and microstructural degradation of the corpus callosum: Interaction of age and alcoholism. Neurobiol Aging 27(7):994-1009.

Pfefferbaum A, Lim KO, Desmond JE, Sullivan EV (1996) Thinning of the corpus callosum in older alcoholic men: A magnetic resonance imaging study. Alcoholism, Clinical and Experimental Research 20:752-757.

Pfefferbaum A, Rosenbloom M, Rohlfing T, Sullivan EV (2009) Degradation of association and projection white matter systems in alcoholism detected with quantitative fiber tracking. Biol Psychiatry 65(8):680-90.

Pierrot-Deseilligny C, Rivaud S, Gaymard B, Agid Y (1991) Cortical control of reflexive visually-guided saccades. Brain 114 (Pt 3):1473-85.

Popovic M, Caballero-Bleda M, Puelles L, Guerri C (2004) Multiple binge alcohol consumption during rat adolescence increases anxiety but does not impair retention in the passive avoidance task. Neurosci Lett 357(2):79-82.

Powell CM, Miyakawa T (2006) Schizophrenia-relevant behavioral testing in rodent models: a uniquely human disorder? Biol Psychiatry 59(12):1198-207.

Prescott CA, Kendler KS (1999) Age at first drink and risk for alcoholism: a noncausal association. Alcohol Clin Exp Res 23(1):101-7.

Qian J, Zhou D, Pan F, Liu CX, Wang YW (2008) Effect of environmental enrichment on fearful behavior and gastrin-releasing peptide receptor expression in the amygdala of prenatal stressed rats. J Neurosci Res 86(13):3011-7.

Qin L, He J, Hanes RN, Pluzarev O, Hong JS, Crews FT (2008) Increased systemic and brain cytokine production and neuroinflammation by endotoxin following ethanol treatment. J Neuroinflammation 5:10.

Qin L, Wu X, Block ML, Liu Y, Breese GR, Hong JS, Knapp DJ, Crews FT (2007) Systemic LPS causes chronic neuroinflammation and progressive neurodegeneration. Glia 55(5):453-62.

Rajkowska G, O'Dwyer G, Teleki Z, Stockmeier CA, Miguel-Hidalgo JJ (2007) GABAergic neurons immunoreactive for calcium binding proteins are reduced in the prefrontal cortex in major depression. Neuropsychopharmacology 32(2):471-82.

Roberts AC, Robbins TW, Everitt BJ, Muir JL (1992) A specific form of cognitive rigidity following excitotoxic lesions of the basal forebrain in marmosets. Neuroscience 47(2):251-64.

Rosenberg DR, Lewis DA (1994) Changes in the dopaminergic innervation of monkey prefrontal cortex during late postnatal development: a tyrosine hydroxylase immunohistochemical study. Biol Psychiatry 36(4):272-7.

Rotaru DC, Barrionuevo G, Sesack SR (2005) Mediodorsal thalamic afferents to layer III of the rat prefrontal cortex: synaptic relationships to subclasses of interneurons. J Comp Neurol 490(3):220-38.

Rupp CI, Kurz M, Kemmler G, Mair D, Hausmann A, Hinterhuber H, Fleischhacker WW (2003) Reduced olfactory sensitivity, discrimination, and identification in patients with alcohol dependence. Alcohol Clin Exp Res 27(3):432-9.

SAMSA (2007) Substance Abuse and Mental Health Services Administration. (2007). Results from the
2006 National Survey on Drug Use and Health: National Findings (Office of Applied Studies, NSDUH Series H-32, DHHS Publication No. SMA 07-4293). Rockville, MD.

Sarter M, Bruno JP, Givens B (2003) Attentional functions of cortical cholinergic inputs: what does it mean for learning and memory? Neurobiol Learn Mem 80(3):245-56.

Schatz DB, Rostain AL (2006) ADHD with comorbid anxiety: a review of the current literature. J Atten Disord 10(2):141-9.

Schoenbaum G, Roesch MR, Stalnaker TA, Takahashi YK (2009) A new perspective on the role of the orbitofrontal cortex in adaptive behaviour. Nat Rev Neurosci 10(12):885-92.

Schoenbaum G, Saddoris MP, Stalnaker TA (2007) Reconciling the roles of orbitofrontal cortex in reversal learning and the encoding of outcome expectancies. Ann N Y Acad Sci 1121:320-35.

Schoenbaum G, Shaham Y (2008) The role of orbitofrontal cortex in drug addiction: a review of preclinical studies. Biol Psychiatry 63(3):256-62.

Schulteis G, Archer C, Tapert SF, Frank LR (2008) Intermittent binge alcohol exposure during the periadolescent period induces spatial working memory deficits in young adult rats. Alcohol 42(6):459-67.

Schwabe K, Koch M (2004) Role of the medial prefrontal cortex in N-methyl-D-aspartate receptor antagonist induced sensorimotor gating deficit in rats. Neurosci Lett 355(1-2):5-8.

Schweinsburg AD, Nagel BJ, Tapert SF (2005) fMRI reveals alteration of spatial working memory networks across adolescence. J Int Neuropsychol Soc 11(5):631-44.

Serretti A, Olgiati P, De Ronchi D (2007) Genetics of Alzheimer's disease. A rapidly evolving field. J Alzheimers Dis 12(1):73-92.

Shaw P, Greenstein D, Lerch J, Clasen L, Lenroot R, Gogtay N, Evans A, Rapoport J, Giedd J (2006) Intellectual ability and cortical development in children and adolescents. Nature 440(7084):676-9.

Shear PK, Butters N, Jernigan TL, DiTraglia GM, Irwin M, Schuckit MA, Cermak LS (1992) Olfactory loss in alcoholics: correlations with cortical and subcortical MRI indices. Alcohol 9(3):247-255.

Sher KJ, Martin ED, Wood PK, Rutledge PC (1997) Alcohol use disorders and neuropsychological functioning in first-year undergraduates. Exp Clin Psychopharmacol 5(3):304-15.

Shumyatsky GP, Tsvetkov E, Malleret G, Vronskaya S, Hatton M, Hampton L, Battey JF, Dulac C, Kandel ER, Bolshakov VY (2002) Identification of a signaling network in lateral nucleus of amygdala important for inhibiting memory specifically related to learned fear. Cell 111(6):905-18.

Silveri MM, Spear LP (1998) Decreased sensitivity to the hypnotic effects of ethanol early in ontogeny. Alcohol Clin Exp Res 22(3):670-6.

Simon P, Dupuis R, Costentin J (1994) Thigmotaxis as an index of anxiety in mice. Influence of dopaminergic transmissions. Behav Brain Res 61(1):59-64.

Sircar R, Sircar D (2005) Adolescent rats exposed to repeated ethanol treatment show lingering behavioral impairments. Alcohol Clin Exp Res 29(8):1402-10.

Slawecki CJ, Betancourt M, Cole M, Ehlers CL (2001) Periadolescent alcohol exposure has lasting effects on adult neurophysiological function in rats. Brain Res Dev Brain Res 128(1):63-72.

Slawecki CJ, Thorsell A, Ehlers CL (2004) Long-term neurobehavioral effects of alcohol or nicotine exposure in adolescent animal models. Ann N Y Acad Sci 1021:448-52.

Sowell ER, Thompson PM, Holmes CJ, Jernigan TL, Toga AW (1999) In vivo evidence for post-adolescent brain maturation in frontal and striatal regions. Nat Neurosci 2(10):859-61.

Spear LP (2000) The adolescent brain and age-related behavioral manifestations. Neurosci Biobehav Rev 24(4):417-63.

Stalnaker TA, Takahashi Y, Roesch MR, Schoenbaum G (2009) Neural substrates of cognitive inflexibility after chronic cocaine exposure. Neuropharmacology 56 Suppl 1:63-72.

Stefani MR, Moghaddam B (2005) Transient N-methyl-D-aspartate receptor blockade in early development causes lasting cognitive deficits relevant to schizophrenia. Biol Psychiatry 57(4):433-6.

Stephens DN, Duka T (2008) Review. Cognitive and emotional consequences of binge drinking: role of amygdala and prefrontal cortex. Philos Trans R Soc Lond B Biol Sci 363(1507):3169-79.

Sulik KK, Johnston MC, Webb MA (1981) Fetal alcohol syndrome: embryogenesis in a mouse model. Science 214(4523):936-8.

Sullivan EV, Deshmukh A, De Rosa E, Rosenbloom MJ, Pfefferbaum A (2005) Striatal and forebrain nuclei volumes: contribution to motor function and working memory deficits in alcoholism. Biol Psychiatry 57(7):768-76.

Tait DS, Brown VJ (2008) Lesions of the basal forebrain impair reversal learning but not shifting of attentional set in rats. Behav Brain Res 187(1):100-8.

Tamamaki N, Yanagawa Y, Tomioka R, Miyazaki J, Obata K, Kaneko T (2003) Green fluorescent protein expression and colocalization with calretinin, parvalbumin, and somatostatin in the GAD67-GFP knock-in mouse. J Comp Neurol 467(1):60-79.

Tan HY, Callicott JH, Weinberger DR (2007) Dysfunctional and compensatory prefrontal cortical systems, genes and the pathogenesis of schizophrenia. Cereb Cortex 17 Suppl 1:i171-81.

Tarazi FI, Baldessarini RJ (2000) Comparative postnatal development of dopamine D(1), D(2) and D(4) receptors in rat forebrain. Int J Dev Neurosci 18(1):29-37.

Tarazi FI, Tomasini EC, Baldessarini RJ (1998) Postnatal development of dopamine D4-like receptors in rat forebrain regions: comparison with D2-like receptors. Brain Res Dev Brain Res 110(2):227-33.

Thiebot MH, Le Bihan C, Soubrie P, Simon P (1985) Benzodiazepines reduce the tolerance to reward delay in rats. Psychopharmacology (Berl) 86(1-2):147-52.

Toga AW, Thompson PM, Sowell ER (2006) Mapping brain maturation. Trends Neurosci 29(3):148-59.

Townshend JM, Duka T (2005) Binge drinking, cognitive performance and mood in a population of young social drinkers. Alcohol Clin Exp Res 29(3):317-25.

Treit D, Fundytus M (1988) Thigmotaxis as a test for anxiolytic activity in rats. Pharmacol Biochem Behav 31(4):959-62.

Uylings HB, Groenewegen HJ, Kolb B (2003) Do rats have a prefrontal cortex? Behav Brain Res 146(1-2):3-17.

Van Eden CG, Uylings HB (1985) Postnatal volumetric development of the prefrontal cortex in the rat. J Comp Neurol 241(3):268-74.

Van Tol HH, Bunzow JR, Guan HC, Sunahara RK, Seeman P, Niznik HB, Civelli O (1991) Cloning of the gene for a human dopamine D4 receptor with high affinity for the antipsychotic clozapine. Nature 350(6319):610-4.

Viapiano MS, Matthews RT, Hockfield S (2003) A novel membrane-associated glycovariant of BEHAB/brevican is up-regulated during rat brain development and in a rat model of invasive glioma. J Biol Chem 278(35):33239-47.

Volavka J, Bilder R, Nolan K (2004) Catecholamines and aggression: the role of COMT and MAO polymorphisms. Ann N Y Acad Sci 1036:393-8.

Volkow ND, Wang GJ, Maynard L, Fowler JS, Jayne B, Telang F, Logan J, Ding YS, Gatley SJ, Hitzemann R, Wong C, Pappas N (2002) Effects of alcohol detoxification on dopamine D2 receptors in alcoholics: a preliminary study. Psychiatry Res 116(3):163-72.

Wang C, McInnis J, Ross-Sanchez M, Shinnick-Gallagher P, Wiley JL, Johnson KM (2001) Long-term behavioral and neurodegenerative effects of perinatal phencyclidine administration: implications for schizophrenia. Neuroscience 107(4):535-50.

Wang CZ, Johnson KM (2007) The role of caspase-3 activation in phencyclidine-induced neuronal death in postnatal rats. Neuropsychopharmacology 32(5):1178-94.

Wang CZ, Yang SF, Xia Y, Johnson KM (2008) Postnatal phencyclidine administration selectively reduces adult cortical parvalbumin-containing interneurons. Neuropsychopharmacology 33(10):2442-55.

Wechsler H, Dowdall GW, Davenport A, Castillo S (1995) Correlates of college student binge drinking. Am J Public Health 85(7):921-6.

Wedzony K, Fijal K, Mackowiak M, Chocyk A, Zajaczkowski W (2008) Impact of postnatal blockade of N-methyl-d-aspartate receptors on rat behavior: A search for a new developmental model of schizophrenia. Neuroscience 153(4):1370-9.

Weinberger NM (2003) The nucleus basalis and memory codes: auditory cortical plasticity and the induction of specific, associative behavioral memory. Neurobiol Learn Mem 80(3):268-84.

White AM, Bae JG, Truesdale MC, Ahmad S, Wilson WA, Swartzwelder HS (2002) Chronic-intermittent ethanol exposure during adolescence prevents normal developmental changes in sensitivity to ethanol-induced motor impairments. Alcohol Clin Exp Res 26(7):960-8.

White AM, Swartzwelder HS (2004) Hippocampal function during adolescence: a unique target of ethanol effects. Ann N Y Acad Sci 1021:206-20.

Windle M, Spear LP, Fuligni AJ, Angold A, Brown JD, Pine D, Smith GT, Giedd J, Dahl RE (2008) Transitions into underage and problem drinking: developmental processes and mechanisms between 10 and 15 years of age. Pediatrics 121 Suppl 4:S273-89.

Yakovlev AG, Ota K, Wang G, Movsesyan V, Bao WL, Yoshihara K, Faden AI (2001) Differential expression of apoptotic protease-activating factor-1 and caspase-3 genes and susceptibility to apoptosis during brain development and after traumatic brain injury. J Neurosci 21(19):7439-46.

Yoon WJ, Won SJ, Ryu BR, Gwag BJ (2003) Blockade of ionotropic glutamate receptors produces neuronal apoptosis through the Bax-cytochrome C-caspase pathway: the causative role of Ca2+ deficiency. J Neurochem 85(2):525-33.

Young KA, Bonkale WL, Holcomb LA, Hicks PB, German DC (2008) Major depression, 5HTTLPR genotype, suicide and antidepressant influences on thalamic volume. Br J Psychiatry 192(4):285-9.

Young KA, Holcomb LA, Bonkale WL, Hicks PB, Yazdani U, German DC (2007) 5HTTLPR polymorphism and enlargement of the pulvinar: unlocking the backdoor to the limbic system. Biol Psychiatry 61(6):813-8.

Zimmermann DR, Dours-Zimmermann MT (2008) Extracellular matrix of the central nervous system: from neglect to challenge. Histochem Cell Biol 130(4):635-53.